A RHEOLOGICAL STUDY OF POLYMER AND MICROEMULSION IN POROUS MEDIA

APPROVED:

_____

_____

A RHEOLOGICAL STUDY OF POLYMER AND MICROEMULSION IN POROUS MEDIA

BY

MEI-KOU YUAN, B.S. in Chemistry, M.S. in Chemistry

THESIS

Presented to the Faculty of the Graduate School of

The University of Texas at Austin

in Partial Fulfillment

of the Requirements

for the Degree of

MASTER OF SCIENCE IN ENGINEERING

THE UNIVERSITY OF TEXAS AT AUSTIN

May, 1981

ACKNOWLEDGEMENT

The author wishes to express his sincere appreciation and gratitude to his supervising professor, Dr. Gary A. Pope, for his guidance and inspiration throughout this study.

Thanks and appreciation are also extended to:

Professor R. S. Schechter, for his valuable suggestions and advice;

Professor G. B. Thurston, whose special contributions are generously given and gratefully received;

Dr. Bruce Rouse, for his technical guidance and stimulating discussions;

To his parents, sincere thanks are also extended for their love, support and encouragement;

Special appreciation is expressed to my wife, Rebecca Yee for her understanding and encouragement, and to my son, Edward, for his cooperation.

Thanks are also expressed to Marathon Oil Company, Shell Development Company, Exxon Company, U. S. A., and the Department of Energy for financial support of this research, and to Dow Chemical, Tiorco, Kelco, and Witco for supplying samples of polymer and sulfonate.

Mei-Kou Yuan

The University of Texas at Austin
Austin, Texas 78712
December, 1980

ABSTRACT

The rheological properties of polymer used in mobility control and the micellar solutions used in chemical flooding have been studied under both static and dynamic flow conditions. The polymer solutions under investigation include Xanflood (a xanthan gum polysaccharide sold by Kelco) and Pusher 700(a hydrolyzed polyacrylamide sold by Dow) polymer solutions with different polymer concentrations and salinities. The micellar solutions studied consist of TRS 10-80 (a petroleum sulfonate sold by Witco), isobutanol, isooctane and sodium chloride. The effects of inertia, shear thinning viscosity and viscoelasticity are demonstrated. An effort was made to correlate the apparent viscosity of the polymer and micellar solutions while flowing in a porous medium. Similar studies were also extended to Water Cut 110 and Water Cut 160 polymers (a hydrolyzed polyacrylamide sold by Tiorco Inc.), with special attention to the studies of shear degradation.

Packed beds with spherical, uniform glass beads of different sizes were used and packed in either glass or stainless steel columns. In order to eliminate entrance and exit end effects, one of the stainless steel columns was especially designed at the inlet and outlet ends, and three pressure taps were drilled on the packed section to allow accurate measurements of the fully developed, steady state pressure gradient.

A Newtonian fluid, water, was used to study the effect of inertia. The Ergun equation was used to correlate these results. The correlation was excellent. Inertia contributes 1% to the pressure drop at a Reynolds number of 1.0, and increases to 12% at $N_{Re} = 10$.

For polymer solution, three types of rheological measurements were conducted. An ultra-sensitive couette viscometer which can be used under exceptional low shear stress conditions was employed to measure the steady state viscosity as a function of shear rate. The second type of measurement is pressure drop-flow rate data on the same fluids. The third, which was done by Professor Thurston, involves an unsteady-state complex viscosity measurement as a function of shear rate and frequency. For micellar solution, only the first and second type of measurements were conducted.

The viscosities of Xanflood polymer solutions, which are relatively insensitive to the effects of salt concentration, show flow resistance in porous media that can be correlated with their shear-thinning bulk viscosities. The apparent viscosities agree with those measured with the viscometer up to the highest shear rate measured by both techniques (1000 sec^{-1}). The dynamic measurement in the beadpacks extended up to 63,009 sec^{-1}. No shear degradation has been observed. A second Newtonian region was approached at the highest shear rates for all Xanflood polymer solutions.

Pusher 700 polymer solutions are much more sensitive to the effects of salt concentration. The higher the salt concentration, the lower the viscosity. Addition of salt shields the repulsive forces among the negatively charged functional groups in the polymer chain and therefore decreases the viscosity. The apparent viscosity of Pusher 700 polymer solution in the beadpacks was the same as that measured with the viscometer before the onset of the elastic response. As observed by others[4-7,12-15], the latter becomes significant at high shear rate and increases the flow resistance. Pack permeability, polymer concentration, and salt concentration all affect the viscoelastic response of the polymer solution. Under the conditions studied, this polymer shear degraded at flowing shear rates above 10,000 sec^{-1}, and lost about 5% of its original viscosity at 20,000 sec^{-1}.

The Water Cut 110 polymer and Water Cut 160 polymer, with both viscous and elastic characteristics, showed a similar behavior to those of Pusher 700 polymer under dynamic flow conditions. Efforts have been made to study the thermal and shear stabilities of these polymers. Results indicate that Water Cut 110 polymer, after heating in oven at $80^{o}C$ for 24 hours, lost about 50% of its viscosity, and the resulting solution showed a smalled viscoelastic response. Both Water 110 and Water Cut 160 showed a 4% viscosity loss due to shear degradation at flowing shear rates up to 30,000 sec^{-1}.

A single experiment was done using a microemulsion. This microemulsion consists of Witco TRS 10-80, iso-octane, isobutanol and salt. The steady and apparent viscosities showed excellent agreement up to the maximum shear rate reached. No viscoelastic response was evident for this microemulsion. Further study on the behavior of microemulsion in porous medium is currently being conducted.[60]

Permeability reduction was also observed. It was smaller for the more permeable packs. The polymer solutions flowed through packs already flushed with polymer solution experienced a further reduction in permeability, even though the previous polymer solution had been flushed out extensively with brine. The brine permeability following each polymer solution (or microemulsion) was used to correlate the apparent viscosity of the same polymer solution (or microemulsion). This worked very well for all the solutions. The method and all the results are discussed later.

TABLE OF CONTENTS

LIST OF TABLES

LIST OF TABLES(Continued)

LIST OF FIGURES

LIST OF FIGURES (Continued)

LIST OF FIGURES (Continued)

LIST OF SYMBOLS

A : cross sectional area, cm^2

D_p: diameter of glass beads, cm^2 or micron

$(D_p)_{eff}$: effective bead size, cm^2 or micron

H : coefficient in Blake-Kozeny model, $(cm/sec)^{1-n} \times cp$

K : permeability of packed bed, darcy

K_f: flushed permeability of packed bed, darcy

K_o: permeability of oil phase, darcy

K_w: permeability of water phase, darcy

L, ΔL : length of porous medium, cm

M : mobility ratio

m : power law coefficient

n : power law exponent

N_{Deb}: Deborah number

N_{Re}: Reynolds number

ΔP : pressure drop, psi or atm

P_1 : pressure drop calculated based on equation (2)

P_2 : pressure drop calculated from the second term of right hand side of equation (1)

P_{Ergun} : pressure drop calculated based on equation (1), and equal to P_1 plus P_2

q : volumetric flow rate, cc/sec

R_{eq} : an equivalent pore radius, cm

R_f : resistance factor

V : superficial velocity, cm/sec

γ : shear rate; sec^{-1}

θ : sphericity factor for glass beads

θ_f : relaxation time of fluid, sec

θ_p : relative time of process, sec

μ : viscosity, cp

μ_{app} : apparent viscosity, cp

μ_o : viscosity of oil phase, cp

μ_w : viscosity of water phase, cp

ρ : density of fluid, g/cm^3

τ : tortuosity factor

ϕ : porosity

λ_o : mobility of oil phase

λ_p : mobility of polymer solution

λ_w : mobility of water phase

CHAPTER I

INTRODUCTION

A. Statement of the Problem

In many scientific and engineering applications, such as in chemical flooding enhanced oil recovery, polymer solutions and micellar solutions are subjected to extremely widely varying velocities and the corresponding shear rates. The flow of polymer and micellar solutions in porous media is a complicated process for many reasons. The bulk properties of polymer and micellar solution are complex. Unlike a Newtonian fluid for which the relation between shear stress and shear rate is a simple proportionality, polymer and micellar solutions are non-Newtonian; i.e., fluid for which the relation between shear stress and shear rate is not a simple proportionality. The vast majority of these "non-linear" fluids show a shear-rate-dependent viscosity and, under certain conditions, exhibit significant elasticity. The salt concentration plays an important role on the rheological properties of ionic polymer solutions and micellar solutions. Polymer molecules are also vulnerable to mechanical, chemical and biological degradation. Further, the geometry of the porous media is also complex, and heterogeneities are the rule. Under such conditions, the usual form of Darcy's law is no longer valid to describe the behavior of the flow of the fluids. The non-Newtonian properties of the solutions result in complex fluid mechanics in permeable media. The adsorption and mechanical entrapment of polymer molecules and micellar solution

can cause a permeability reduction of the permeable media. The so-called inaccessible pore volume also affects the fluid propagation. Thus, a systematic laboratory study of the behavior of the polymer and micellar solutions is appropriate. A better understanding of these factors influencing the performance of the polymer and micellar solutions and the mechanisms involved should enable a better choice of the materials to be used under any given reservoir environment, and a more reliable and efficient design of the enhanced oil recovery projects.

B. Method of Attack

Initial studies of the characterization of polymer and micellar solutions will be restricted to a system which is as simple as possible.Every attempt will be made to emphasize the behavior of the fluids and not to allow the properties of the porous media to "mask" this behavior. Thus the present investigation will be restricted to a system with the following conditions:

1. Single phase flow-aqueous phase for polymer solutions and microemulsion phase for micellar solutions.
2. Unconsolidated porous media-glass bead packs.
3. Room temperature.

The variables involved in this study are:

1. Two types of polymer, one type of surfactant, alcohol and hydrocarbon.

2. Polymer concentration
3. Salinity
4. Permeability
5. Flow rate
6. Dimension of the packed bed

C. Literature Survey on Non-Newtonian Flow through Porous Media

Many investigators have studied the flow of fluids through porous media. Early investigators, such as Darcy, Kozeny and Ergun formulated equations for predicting pressure drop versus flow rate relationships for Newtonian fluids. In recent years, Christopher, Middleman and others[1,2,3] have modified Darcy's equation to account for flow of purely viscous, non-Newtonian fluids. Some workers have mentioned the effects of elasticity on flow through porous media.[4,5,6,7,8,9,10] Analyses of fluid flow through porous media under laminar flow conditions have almost universally been developed by coupling a specific model of the pore structure of the medium with a specific model of the rheological properties of the fluid being employed in the flow process. Most commonly the pore structure is modeled by means of the "cylindrical equivalent capillary": a cylindrical duct of length and diameter such that it exhibits the same resistance to flow as the actual interstices in the real porous medium. Thoughtful and clear descriptions of this model are

presented by Bird et al,[11] and in the comprehensive summary of the subject by Savins.[12] The review paper by Savins shows how a particular rheological model of the viscosity function of the fluid may be replaced with a generalized analysis similar to that employed in laminar and turbulent flows of non-Newtonian fluids through tubes.

A detailed analysis of factors influencing polymer solution properties on flow in porous media can be found in the research papers of Hirasaki and Pope,[13] and of Wang et al.[14] In Hirasaki and Pope's paper, it is mentioned that the rheological behavior of the flow of polymer solution through porous media could be Newtonian, pseudoplastic, and dilatant, depending on the flow rates. The pseudoplastic behavior is modeled with the Blake-Kozeny model for power low model fluids while the dilatant behavior is modeled with viscoelastic properties of the polymer solution. The reduction in permeability is postulated to be due to trapped or adsorbed polymer molecules that either plug or reduce the effective size of the pores. A dimensionless number was formulated to correlate the permeability reduction facor with the polymer, brine and rock properties. The dimensionless number represents the ratio of the size of the polymer molecular coil to an effctive pore radius of the porous medium. A model assumption was that the polymer is absorbed on the surface of the porous medium as a monolayer of molecular coils that have a segment density only slightly greater than the molecular coil in dilute solution.

Wang and his co-workers have studied the effect of inertia, shear-thinning viscosity, viscoelasticity, and molecule-wall interactions on the flow in porous media, and presented correlations of the appropriate dimensionless parameters. Power law parameters and the relaxation time of the solutions were determined from a cone and plate steady-shearing experiment. Polymers which are cellulose derivatives or fermentation polysaccharides show flow resistance in porous media that can be correlated simply with the the shear-thinning bulk viscosity while polymers with significant elastic properties such as polyacrylamides show flow resistance that may be larger by an order of magnitude than can be attributed to bulk viscosity alone. The permeability reduction associated with polymer adsorption is permanent, and the initial permeability can not be restored even with thorough flushing with a polymer-free solution.

D. Background Information on Polymer Solutions

The addition of certain polymers to injection water can significantly increase oil recovery by providing mobility control and by reducing channeling.[10,13,15-24] Polymers can be injected at different stages of enhanced recovery projects in order to improve the efficiency to oil recovery, and they can be injected in combination with other reactive chemicals for the purpose of restricting flow through high-permeability channels.

In order to obtain mobility control in a flood, it is necessary for the displacing phase to have a mobility equal to or lower than the mobility of the oil. This mobility relationship can be expressed as follows:

$$M = \frac{\lambda_w}{\lambda_o} = \frac{K_w/\mu_w}{K_o/\mu_o}$$

The addition of the selected polymers to water increases the viscosity, and in some cases the polymers reduce the permeability of reservoir rock to water. The total reduction in mobility is defined by Pye[17] as a "resistance factor". The resistance factor increases as the mobility of the water is reduced.

$$R_f = \frac{\lambda_w}{\lambda_p}$$

After the polymer solution has been displaced by water, a residual resistance to water flow remains, and residual resistance factor is defined as:

$$R_f(\text{Residual}) = \frac{\lambda_w\ (\text{initial})}{\lambda_w\ (\text{after polymer})}$$

Polymers can also be used to reduce mobility or to cause plugging in water channels by combining the pôlymers with other reactive chemicals. In these processes, the polymers can interact in the formation to form gels, or they can be used to reduce the mobility of one reactant so that a second reactant can catch up and

form a gel plug. The purpose of such uses of polymers is to improve sweep efficiency. All oil reservoirs are heterogeneous to various degrees; in some cases the high-permeability channels dominate the flow pattern, but these channels can be relatively small in cross section. In such cases, a successful plug in the small channel can greatly improve the sweep efficiency of a flood.

Several kinds of water-soluble polymers are used in polymer flooding or micellar/polymer flooding. These include hydrolyzed polyacrylamide (HPAM), xanthan gum (XG), polyethylene oxide (PEO), hydroxyethylcellulose (HEC) and various copolymers of acrylamide. In the current study, only two types of the various polymers will be investigated, namely, xanthan gum and hydrolyzed polyacrylamide.

Xanflood (XF), a commercial xanthan gum product of Kelco Company, is a high molecular wight polysaccharide produced in a pure culture fermentation process by the micro-organism xanthomonas compestris.[25-28] Three different monosaccharides are found in xanthan gum: mannose, glucose and glucuronic acid (as a mixed potassium, sodium, and calcium salt). The molecular weight of this polymer is probably on the order of 2 million but has been reported to as high as 13-50 million.[29] Pusher 700, a commercial product of Dow Chemical Co., is a hydrolyzed polyacrylamide (HPAM) with molecular weight of one to ten million.[8,10,15] The Water Cut 110 and Water Cut 160 polymers, sold by Tiorco Inc., are also hydrolyzed polyacrylamides.

Being non-Newtonian fluids , polymer solutions generally show a shear-rate-dependent viscosity and under certain conditions,

some exhibit significant elasticity. The stability of the polymer solution is of major importance since the polymers must function for a long period of time, frequently at elevated temperatures. The presence of salt can affect the rheological properties of ionic polymer solutions. Polymer molecules are also vulnerable to mechanical, thermal, chemical or biochemical degradations. XG polymer solution is highly tolerant to electrolytes and is less sensitive to shear degradation. HPAM polymer solution, however, is very sensitive to electrolyte and starts to shear degrade at a few thousand reciprocal seconds.[19,30] A number of papers[31-33] have addressed the problem of mechanical degradation during injection into oil reservoirs for secondary and/or tertiary recovery applications.

CHAPTER II

OBJECTIVE AND SCOPE

The immediate objective of this study is to establish an understanding of the flow behavior of polymer and micellar solutions in porous media. The ultimate goal is to apply this knowledge to chemical flooding methods in enhanced oil recovery because the characterization of the behavior of these fluids will enable a better understanding of the rheology of the materials used, a better selection of the materials to be used under any given reservoir environments, and more reliable and efficient design of the chemical flooding.

Polymer type and concentration, salt concentration, flow velocity, and grain size of the porous media were the main variables in this study. All the experiments were at room temperature. Three types of rheological measurements were conducted: The first consists of determining the steady state viscosity as a function of shear rate using an ultra-sensitive couette viscometer which can be used under the exceptionally low shear stress conditions encountered in these studies. This instrument is 100 to 1000 times more sensitive than the ones commonly used for such purposes. This sensitivity is necessary because of the very low shear rate(as low as 0.01 sec^{-1}) existing in some parts of oil reservoirs during chemical flooding operations. The second type of measurement is pressure drop versus flow rate data on the same fluids flowing through porous media.The third type consists of the complex viscosity as a function of shear rate and

...ing an ultra-sensitive instrument especially designed ... Thurston[47] to study fluids such as blood, and currently ... to study the fluids used for chemical flooding. These ... correlated using models of the porous media coupled with ...hanical models of the non-linear, non-Newtonian fluids. The ...eed for the basic rheological parameters, the relaxation times, ...rposes of explaining the flow of polymers through porous ... also been established.[13,48,49]

... the present study we will also look at the viscoelastic ...mon. Theoretical relationships are presented here which deal ... flow of viscous, Newtonian and non-Newtonian fluids through ... media. These theoretical equations related flow and pressure ... bed and fluid parameters. The relationships for viscous ... compared with the experimental data obtained in porous ... Deviations from the viscous flow theory are taken as an ...ation of viscoelasticity.

CHAPTER III

THEORETICAL MODELS

One of the basic correlations describing the relation between the pressure drop and fluid velocity for a Newtonian fluid is the Ergun equation.[50] For a packed bed composed of uniform particles:

$$\frac{\Delta P}{L} = \frac{150\,\mu V}{(\theta D_p)^2} \times \frac{(1-\phi)^2}{\phi^3} + \frac{1.75\rho V^2}{\theta D_p} \times \frac{(1-\phi)}{\phi^3} \qquad (1)$$

This equation applies in both the laminar region and in the transition and turbulent regions. The first term on the right hand side of equation (1), which applies to the laminar region only, is commonly known as the Blake-Kozeny correlation:[11,48,51]

$$\frac{\Delta P}{L} = \frac{150\mu V}{(\theta D_p)^2} \times \frac{(1-\phi)^2}{\phi^3} \qquad (2)$$

By rearranging the above equation, the superficial velocity is given by:

$$V = \frac{(\theta D_p)^2}{150\mu} \times \frac{\Delta P}{L} \times \frac{\phi^3}{(1-\phi)^2} \qquad (3)$$

Equation (3) is identical with the Darcy's law when the permeability is equal to :

$$K = \frac{(\theta D_p)^2}{150} \times \frac{\phi^3}{(1-\phi)^2} \qquad (4)$$

or :

$$K = \frac{(Dp)^2_{eff}}{150} \times \frac{\phi^3}{(1-\phi)^2} \qquad (5)$$

The Blake-Kozeny model represents the porous medium as a bundle of capillary tubes with a length that is greater than the length of the porous medium by a tortuosity factor, τ. The equivalent radius of the capillary tubes can be related to the particle diameter of a packed bed from the hydraulic radius concept or to the permeability and porosity by comparison with Darcy's law for Newtonian fluids.

The modified Blake-Kozeny model[1] represents the flow of a power law fluid in the capillaries. The apparent viscosity can be related to the pack permeability and porosity through the following relationships[13]:

$$\mu_{app} = HV^{n-1} \tag{6}$$

where:

$$\mu_{app} = \frac{K_f A}{q} \frac{\Delta P}{L} \tag{7}$$

$$H = \frac{m}{12} \left(\frac{9n + 3}{n} \right) (150\, K\phi)^{\frac{1-n}{2}} \tag{8}$$

The coefficient: m , (cp sec^{n-1}) and the exponent, n, are the power low parameters determined from viscometric data.

$$\mu = m\gamma^{n-1} \tag{9}$$

The superficial velocity, V is determined by :

$$V = \frac{q}{A} \tag{10}$$

The coefficient, H, determined from equation (8) and power-law parameters: m, n, can be used to compute the apparent viscosity from equation (6).

Equation(6)can be expressed in terms of an equivalent shear rate in the porous medium such that the viscosity can be determined directly from the viscosity-shear rate data from viscometric measurement :[13]

$$\mu_{app} = m\gamma_{pack}^{n-1} \tag{11}$$

$$\gamma_{pack} = \left(\frac{3n+1}{4n}\right)^{\frac{n}{n-1}} \times \frac{4V\tau}{\phi R_{eq}} \tag{12}$$

where

$$R_{eq} = \left(\frac{8\tau^2 K}{\phi}\right)^{\frac{1}{2}} \tag{13}$$

The shear rate then becomes:

$$\gamma_{pack} = \left(\frac{3n+1}{4n}\right)^{\frac{n}{n-1}} \times \frac{4\mathcal{U}}{(8K\phi)^{\frac{1}{2}}} \tag{14}$$

The Reynold's number, N_{Re}, which represents the ratio of inertial effect to viscous effect, can be expressed as:[49]

$$N_{Re} = \frac{\theta D_p \rho V}{\mu(1-\phi)} \tag{15}$$

The modified Blake-Kozeny model does not represent the dilatant behavior observed at high flow rates. We should not expect to see viscoelastic effects with this model as the power-law fluid model does not have a characteristic relaxation time and the flow field in a smooth bore capillary tube does not have a characteristic deformation time.

Marshall and Metzner[5] suggested that the fluid relaxation

time, θ_f, and the rate of elongation or contraction that occurs as the fluid flows through a channel or pore with varying cross-sectional area should be used to represent viscoelastic behavior. Thus, a dimensionless group such as the Deborah number should be used to represent the viscoelastic effect in a porous medium. The Deborah number for flow in a packed bed was expressed as:

$$N_{Deb} = \frac{\theta_f}{\theta_p} = \frac{\theta_f V}{(\theta D_p)\phi} \qquad (16)$$

Equation (16) represents a measure of the importance of elasticity. If N_{Deb} is small, viscous fluid-like behavior is implied. By contrast, elastic solid-like behavior is implied by large N_{Deb}.

CHAPTER IV

DESCRIPTION AND OPERATION OF EXPERIMENTAL APPARATUS

The experiments consisted of three major categories, namely, characterization of polymer solution properties, characterization of porous media, and flow experiments of the polymer solutions through the porous media. Bulk fluid property characterized is the viscosity as function of shear rate. Porous media parameters determined are the porosity and permeability. In the flow experiments, the pressure drop is measured as a function of flow rate or superficial velocity, V.

A. Rheometers:

Rheometer, or the viscometer, is the apparatus used to determine the bulk rheological property of the material. The Contraves Low-Shear 30 rheometer[52] is used in this study. It is a rotational rheometer based on the couette principle. The highly sensitive torque measuring system ensures rapid response to changes in torque value. Only a very small amount of sample (1 ml.) is needed for the LS-30 viscosity measurements.

The LS-30 has a broader range of shear rate (0.0174 - 128.5 sec^{-1} for #1 bob and cup) than the commonly used Brookfield viscometer (o.37 - 73.5 sec^{-1}) and is about 100 to 1000 times more sensitive. Consequently, very low shear stresses can be measured.

The temperature regulated, interchangable measuring cup is driven by a speed-controlled motor incorporated in the measuring head. The speed is controlled by the electronic module which

generates 30 fixed speeds in a geometric progression through the range 10^2 to 10^{-2} $minute^{-1}$. The measuring cup of the coaxial meansuring system, rotating at accurately defined speeds, exerts a torque on the measuring bob through the test substance. The interchangeable measuring bob is attached to a tilting system on which is fixed a multi-pole magnet arrangement and mirror. The complete tilting system is suspended on a torsion wire.

An arrangement of electro-magnetic coils, concentric to the pivoted magnet system, is rigidly mounted within the measuring head.

Using a photo-electric system, the angular postion of the bob is monitored by the mirror. When the pivoting system undergoes a deflection caused by a torque exerted on the bob, a regulating current is produced by the photo-electric system in conjuction with the compensation amplifier. This regulating current passes through the electro-magnetic coils, and produces an electro-magnetic torque on the multi-pole magnet which is in equilibrium with the mechanical moment. This regulating current is proportional to the torque prevailing at the bob and thus also to the viscosity. The torque is indicated digitally.

The operating procedure used is as follows:

1. Turn on the main power and the motor.
2. Put 1 ml. of the sample in the measuring cup. Insert the measuring bob into the cup. The measuring bob must hang concentrically in the measuring cup. Guide by hand if necessary.

Avoid formation of any air bubbles. To avoid the air current, a shield is installed around the cup.

3. Adjust the zero point by the zero adjustment screw, with the speed at zero, and the damping set at 1. Repeat as the range is varied from 5 to 1.
4. Take readings for each speed (from low speed to high speed), starting with range set at 1. As soon as the reading becomes over scale, a higher range should be used.
5. The reading can be converted to either shear stress or viscosity using conversion factors given for each bob and cup set.

B. Packed Columns

Three different types of columns were used in this study. The first type used is a Glenco series 3400 column[53] (1" inner diameter, 12" or 24" long), constructed of borosilicate glass with polypropylene collars and end pieces originally designed for high quality classical chromatographic separations with gravity flow to moderate pressure (rated for 80 psi). Each column is constructed with non-clogging bed supports which consist of a thin 10-micron membrane suspended over a woven grid. The upper end plate has side vent port which can be used to bleed air or to introduce fluid on top of the bed with a long needle. An advantage of this type of column is that the flowing process is visible since it is made of glass. The

disadvantages include the low pressure rating and the large pore volume (need more fluids).

The schematic diagram of this column is shown in Figure 1. The second type of column used is a Glenco series 3210 stainless steel colum (7/16" inner diameter, 12" long) designed originally for high pressure, high speed, high resolution liquid chromatography. The packing support at both ends are modified to be same as that of the first type. A snap ring is used to hold the screen in place. The maximum operating pressure of this column is 2500 psi, which is high enough for the purpose of this study, but it resulted in a significant column end effect, an excessive pressure drop at the inflow and outflow ends when high flow rates are run. Consequently, a third type of column was needed. It is designed, made and tested to have negligible end effect even for the polymer solutions. Figure2 is a schmatic diagram of this column.

The first two types of column are commercially available, but there are no built-in pressure taps between the inlet and outlet ends. The pressures are measured at the inlet and outlet ends which are located outside the packed section. They are subject to column end effect at high flow rates. The third type of column, however, is made up with 9/16" inner diameter stainless steel pipe. The column is composed of a piece of stainless steel pipe and two end caps. The end caps are drilled and threaded at both ends, with one end to fit the outside diameter of the pipe and the other end to fit a 1/2" fitting which terminates for connection of 1/8" tubings. There is an

empty space between inlet (and outlet) and the packed section with this design. The end effects (fluid entrance and exit effects) as the fluids flow through packed column are eliminated. Further, five pressure taps are located along the column length, with three on the packed section separated at equal distance and two at the inlet and outlet ends respectively. The multiple pressure taps are so installed to observe the fluid entrance and exit end effects and the pressure distribution to determine if a fully developed flow is present inside the packed column, and if any plugging is occuring in the column.

Holes are drilled on the pipe along the packed section, and pressure taps are soldered on the pipe with 1/8" stainless steel fittings connected with 1/8" tubing. Soldering is desired for high pressure drop measurements. Nylon cloth with 74 micron opening is inserted in the pressure taps on the packed section to hold the glass beads used for the packing. A schematic diagram of this column is shown in Figure 3.

Glass beads were selected as the porous medium for all the experiments because of their uniformity and cleanness. Two different sizes of glass beads are used in this study, namely, 100-110 micron beads and 250-300 micron beads.

In packing the column, the glass beads are loaded gradually and a hand-held vibrator is used vibrating continuously against the column at and below the level of glass beads until the column is fully filled. This is to make sure that each of the bead particle sits at its most stable position and avoid

segregation of beads of different sizes and therefore give us a uniform and good packing. The packed column is then evacuated and saturated with brine and is ready for experiments. The detailed procedure about this will be described in next chapter.

C. Packed Bed Flow System:

A constant-flow-rate-feed system is employed to conduct the flow experiments through the packed colums. The whole system consists of a Zenith laboratory metering unit as the driving force to control the flow rate, a solution reservoir, a packed column with uniform glass beads as the porous medium, a system of pressure transducer - carrier demodulater - chart recorder system for pressure drop measurements and a fraction collector to collect the effluent samples automatically. The assembly of this whole system is shown in Figure 4.

a. The Zenith Metering Unit:

The metering unit consists mainly a digital motor speed control power package and a motor driver assembly containing the pumps. The pump is a rotary gear metering pump of unique precision , originally designed to meet the stringent requirements of spinning synthetic textiles. A uniform, pulseless flow rate under varying conditions of pressure, temperature and viscosity is the primary feature of the pump. A detailed description of this

metering unit is available from the manufacturer's instruction mannual.[54]

Two different sizes of pumps are used in this study. Pump size A gives a flow rate of 0.160cc per revolution while pump size B gives 1.752cc per revolution. The speed range is from 3 to 180 revolutions per minute. Thus,within the operating speed range, flow rates from 0.48cc/min., (0.008cc/sec) to 28.8cc/min.(0.48cc/sec) can readily be achieved for pump A and 5.26cc/min. (0.0876cc/sec) to 318cc/min.(5.3cc/sec) for pump B. Flow rates smaller than 0.008cc/sec are also possible through the use of a differential metering arrangement of two pumps. In this arrangement, two pumps of equal size are placed in series with a T fitting between the discharge of the first pump and inlet of the second pump. The first pump is driven faster than the second by a slightly smaller pump drive gear. The slower speed of the second pump will not permit it to receive the fully delivery of the first pump, hence the differential delivery is metered through the T fitting. The metered fluid will then be the difference to displacement of the two pumps per revolution of the common pinion. By using different sized drive gears and varying the speed of the drive, a wide range of deliveries of extremely small amounts can be obtained.

The differential flow rates are computed in the following manner: Two size A pump (0.160cc/rev.) with 42 and 44 tooth

drive gears are driven by a common 42 tooth pinion, the differential flow is calculated as follows:

$$42/42 \times 0.160\text{cc/rev.} = 0.160\text{cc/rev.}$$

$$42/4 \times 0.160\text{cc/rev.} = 0.1527\ \text{cc/rev.}$$

The differential flow is the difference of the two pumps or 0.0073cc/rev. Thus if the speed is set at 5 rpm, the differential flow rate is 0.0365cc/min or 0.00061 cc/sec. If the speed is 40 rpm, the differential flow rate is 0.292cc/min or 0.0049cc/sec.

Obviously, the differential metering arrangement of two pumps is another feature of this metering unit and flow rate is also very stable.

b. Solution Reservoir:

Two kinds of container are employed here to serve as the solution reservoir. A Glenco chromatographic glass column (the same as the first type packed column) is used for low pressure and low flow rate system. The reason to use a glass column is that it is constructed of borosilicate glass with polypropylene collars and end pieces and therefore suitable for saline solutions. Also the upper and plate has a side vent port which can be used to bleed air, or to introduce fluids with a long needle if necessary. This container has a bulk volume of about 300cc and a pressure rating of 80 psi. When the discharging pressure in the system is expected to be high, or when high flow rates are needed, a pressure vessel madeup with stainless steel with a capacity of

about 3 liters is then used.

All the solutions are filtered and/or degassed before they are introduced into the solution reservoir. Brines are filtered through 0.45 micron Millipore filter paper under 40 psi, with a Fan Filter Press unit. Polymer solutions are filtered through 1.2 micron Millipore filter paper under the same condition.

C. The Packed Columns:

The packed columns have been described in section B of this chapter. The tubing and fittings used are either nylon/teflon or stainless steel to avoid rust gathering and solution metal interaction. This is especially important because we are working with saline solutions and about two weeks are required to finish a complete run. The packed column was kept in a horizontal position during operation and the experiments were conducted at room temperature.

d. The Pressure Transducer-Carrier Demodulator-Chart Recorder System

The pressure drop in the packed bed during fluid flow is measured with pressure transducers. The Validyne diaphragm type variable reluctance differential pressure transducers (model DP15) are used. Field-interchangeable diaphragms make possible a multiple range pressure transducer. A disphragm of magnetically permeable

material, supported between two symmetrical assemblies, completes a magnetic circuit with each "E" core, Diaphragm deflection with application of pressure increases the gap in the magnetic flux path of one core and decrease the gap equally in the other. The magnetic reluctance varies with the gap, determing the induction ratio. The inductance ratio is conveniently measured in an AC bridge circuit in which an output voltage proportional to pressure is obtained. Demodulation following the suppressed carrier bridge output is required for a DC signal.

The MC1 module case is multi-channel, housing up to 20 plug-in units and providing the necessary carrier and DC operating voltages for a broad line of plug-in units and associated transducers. The plug-in unit selected is the Validyne CD-19 carrier demodulator. It is a high gain, dual output plug-in module with a six-position gain switch and a ten-turn vernier gain potentiometer. The electrical output connected with a chart recorder. A potentiometric strip chart recorder manufactured by Texas Instruments Inc. is used. It is a multipoint, self balancing recorder for accurate recording of multiple DC signals.

The input signals are switched in sequence to the amplifier by means of a 24-position rotary switch mounted in the rear of the recorder case. This switch is driven by and synchronized with a motorized drive in the slideout chassis. The print head synchronizes with the input switch and prints a dot with identifying

channel number on the chart. A detailed description for the transducer, module and recorder system can be obtained from the manfacturers' instruction mannuals.[55,56]

All the pressure drop data during the flow experiments are measured with use of transducers. Transducers are calibrated against a specific demodulator at a specific channel on the chart recorder before the experiments start.

Tranducers with replaceable diaphragm of 0.1,1,10,100, 500 and 1000 psid full pressure meansurement are employed during the experiments. The attenuator on the chart recorder can also be used to amplify the gain to give a more precise reading when necessary.

A general calibration procedure is described as follows:

1. Set the recorder at stand-by for the specific channel used.
2. Set gain on the demodulator at mid range.
3. Go to full scale.
4. Adjust gain on the demodulator to read full scale on recorder.
5. Let off pressure.
6. Adjust R & C controls on demodulator to read zero output.
7. Go to full scale again and make minor adjustments if necessary
8. Check zero.
9. Check 3 points in between to verify accuracy.

e. Sample Collector:

Effluent samples were collected in two ways. For slow to medium flow rates, the effluent samples were collected by the

application of a fraction collector. For medium to high flow rates, the samples were collected manually with either a 50cc or 100cc graduate cylinder. A timer is used for the second case to count the length of time. The actual flow rate can then be calculated. For the first case, an Instrumentation Specialties Company's model 328 fraction collector[57] was used. A controller has already been built in the fraction collector. The fraction collector provides the unattended collection of discrete fractions of a flowing effluent stream. The size of these fractions may be controlled by time, volume, drops, external control signal or manually, depending on how the controller is set. Up to 190 fractions may be collected. In this study, fractions are always controlled by time. Graduate test tubes with capacity of 10cc and the readability of 0.1cc are used so that the actual flow rate can be easily calculated.

CHAPTER V

EXPERIMENTAL PROCEDURES

A. Packed-Bed Characterization:

The configurations of the packed columns have been presented previously. The column is packed with either 100-110 micron glass beads or 250-300 micron glass beads. The packing procedure and the characterization of packed bed including the measurements of porosity, permeability, and effective particle size are described as follows:

1. With the column vertical, the glass beads were loaded gradually.
2. A hand-held vibrator is vibrating against the wall of the column at and below the level of glass beads to get a uniform packing.
3. After the column is packed, connect the upper end to a vacuum pump. Close valves at lower end and at pressure taps. Evacuate the column for 30 minutes.
4. Prepare a burette and fill it with 1% brine.
5. Connect the lower end of the packed column to burette. After bubbles have been purged out, close the upper end valve, open the lower end valve. The pressure differential plus the hydraulic head in the burette will push the brine in and saturate the packed column.
6. The volumetric loss in the burette less the end volume in the packed column is thus the pore volume of that specific packed bed.

7. The end volume can be experimentally determined by saturating the column without beads. The bulk volume of the packed section can be calculated with the known values of the length and inner diameter of the column. The difference of these two is then the end volume.
8. The porosity of this specific packed column is determined from the ratio of the pore volume to the bulk volume of the column.

The permeability and the effective particle size of the packed column were determined by a Newtonian fluid (1% brine) flooding under Darcy conditions.

Darcy's equation is used to calculate the permeability of the packed bed to 1% NaCl and equation (5) is employed to determine the effective particle size. The detailed procedure for the Newtonian fluid floods is given below.

B. Newtonian Fluid Studies:

The only Newtonian fluid involved in this study was brine. It was used to determine the permeability of the packed bed, the effective particle size, the inertial effect, and the column end effect.

Brine with 1% NaCl concentration by weight is made and filtered through 0.45 micron Millipore filter paper with the

application of the Fann Filter Press under 40 psi pressure. It is then fed into the solution reservoir after degassing. After all the air bubbles in the tubing and fitting are purged out, the flow experiment is ready to start. Pressure drops were measured from pressure taps with pressure transducers and recorded on the chart recorder. Since there was no pressure tap built on the packed section for the first and second types of columns, only one value of the pressure drop for the full length was recorded for those cases. For the third type of column, three pressure drop values were read for each flow rate. These were for (1). the section from the inlet to the outlet, (2). from the inlet to the first pressure tap on the packed section, and (3). from the first pressure tap to the third pressure tap on the packed section. Flow rate was determined after steady flow was established, which can be justified by the stablized pressure drop value on the chart recorder. About 20 to 30 different flow rates were run for each flood, starting with a low flow rate and ending with a high rate, which covered a wide range of flow rate and therefore, a wide range of Reynolds number and shear rate. Consistency of experimental data indicate that the column-end effect has been completely eliminated in the especially designed column (the third type) and any significant decrease in permeability at a high Reynolds number would indicate the emergence of inertial effect.

C. Polymer Solution Studies:

Two types of water-soluble polymer were used to study the viscoelasticity and shear degradation in porous flow:

(1) Xanthan gum : Kelco's Xanflood, lot No. XFL 14630.

(2) Partially hydrolyzed polyacrylamide : Dow's Pusher 700, lot No. 0817S141, and Tiorco's Water Cut 110 and Water Cut 160, product sample (September, 1978).

The polymers are all in powder form and aqueous solutions were prepared in different ways depending upon the polymer.[59] Pusher 700, Water Cut 110 and Water Cut 160 polymer solutions were made directly at the desired polymer and salt concentrations with magnetic stirring. The rate of addition of polymer should be slow enough for the particles to separate in water without lump formation, but not so slow that the solution thickens appreciably before all the solid is added. From eight to twenty four hours are generally required for complet hydration.

The general mixing procedure used for Xanflood polymer solution is as follows:

1. Add distilled water to a Waring blender. Determine amount such that total weight of final solution is 500 grams.
2. Blend in electrolyte by weight.
3. Blend in enzyme by weight.
4. If Oxygen scavengers and anti-oxidants are to be used, add them at this point. Filter through 0.45 Millipore if final solution is to be used in filtration study.

5. Add gum, at low speed blender setting. Then increase blender speed and mix for 10 minutes. Dry gum in dessicator at low temperature (25^{o}-35^{o}C) before using.
6. Transfer to flask and heat in water bath for 30 minutes after reaching 50^{o}C. Swirl occasionally.
7. Add biocide.
8. Dilute desired amount to desired final polymer concentration. Save balance in closed container for any additional experiments. Dilute by stirrring for a few minutes with magnetic stirrer on "high" speed, or 1 or 2 minutes with blender on "low" speed (to avoid air entrainment).
9. Filter, if necessary.

Enzyme is used to metabolize the shell of xanthomonas campestris. Heating increases the metabolization rate. Since xanthan gum is biodegradable, biocide is needed to preserve the polymer solution.

An example of a 10,000 ppm Xanflood concentrate is shown in the following:

1. Put 493.88 grams of distilled water in blender.
2. Add 0.5 grams of sodium bicarbonate in the distilled water.
3. Mix 0.02 grams of alcalase P1.5 (Novo Laboratory Inc., Batch No. M45219) in the water with low stirring speed.
4. Add 5 grams of dry Xanflood slowly to the solution with stirring.
5. Switch to high speed of blending for 10 minutes.

6. Transfer this polymer solution to a volumetric flask, and leave it in 50°C water bath for 30 minutes with occasional stirring.
7. Add 0.6 grams of DowicideB(Dow Chemical, Lot No. MM0277A) in the polymer solution and stir by magnetic stirrer.

This Xanflood solution contains the following:

Xanflood = 10,000 ppm

$NaHCO_3$ = 1,000 ppm

Dowicide B = 1,200 ppm

Alcalase = 40 ppm

Brines were made separately and mixed with polymer solutions to desired concentrations. The saline polymer solutions were then filtered through 1.2 micron Millipore filter paper and the bulk viscosity measured with the Contraves LS-30.

To start the experiment, the packed column which has been flooded with 1% brine solution is first flushed with polymer solutions at a medium flow rate. The Flow rate arbitrarily selected was 1.7cc/min. The initial flush is conducted until a steady pressure drop is established and the viscosity of the effluent is measured to be the same within experimental error as the injected polymer solution. This ensures that the packed column is indeed fully saturated with the polymer solution. Flooding is then conducted from low rates to high rates, and the pressure drops and flow rates are measured. The effluents are collected and viscosities are measured to see whether shear degradation occurred during the flow. The time span for each

experiment is minimized to maintain the freshness of the solution.

After the polymer flood has been finished, the brine is run to obtain the "flushed permeability".[48] The brine is run at a relatively high flow rate (25cc/min) until a large number of pore volumes have been injected (20-30 pore volumes) and a steady pressure drop established. The flow rate is then changed from low to high and steady pressure drops are measured.

D. Micellar Solution Studies:

The micellar solution studied consists of Witco's TRS 10-80 Surfactant, iso-butanol, isooctane and salt. A specific composition of micellar solution is selected after a complete phase scanning and the viscosity of the microemulsion phase is measured. Efforts were made to obtain a system with a small excess upper oleic phase and a lower microemulsion phase at which the composition is very close to a system at which middle phase microemulsion will occur.

The specific micellar composition selected is as follows:

3.5% Witco TRS 10-80, by volume

4.4% Iso-butanol(IBA),by volume

20% Isooctane, by volume

0.4% NaCl, by weight

71.7% distilled water, by volume

A concentrate TRS 10-80 with IBA stock solution is made and filtered through 0.45 micron Millipore filter paper.

Isooctane is also filtered through a 0.45 micron filter paper while brine is filtered through 1.2 micron filterpaper, all with the use of Fann Filter Press under 40 psi. The stock solutions are then mixed together at proper amount to give the desired micellar solution. Several days were allowed to let the micellar solution to get a stable phase equilibrium. The micellar solution is then ready to be used, and the lower microemulsion phase is injected into the packed column (third type) which is pre-saturated and flushed with brine. The experiment is started. The experimental procedure is the same as that for polymer solutions.

CHAPTER VI

EXPERIMENTAL RESULTS AND DISCUSSION

Table 1 lists the packs and solutions used in this study. These will be discussed in the order listed.

For all the porous packs, an initial brine flood was conducted before any polymer solutions were run. The purposes of this were to determine the permeability of the packed beds to the brine, to measure the inertial effect at high Reynolds number, and to determine if any column end effect existed.

After the initial brine flood, polymer solutions were run through the packed columns to study the viscoelastic nature and shear degradation of the solutions. The apparent viscosity determined from the flow experiment and the one measured with the Contraves LS-30 are compared for each of the polymer solutions. The flushed permeabilities for the polymer solutions were obtained from the brine flood following the polymer or microemulsion flood. The permeability reduction is thus experimentally determined.

The effluent samples, especially those collected at high flow rates, are saved and the viscosities are measured with the LS-30 to see if the solution shear degraded or otherwise changed during the flood.

A. Experiment No. PF-1. Preliminary Studies for Pusher 700 Polymer Solution

The glass column (type 1) was employed and packed with 100-110 micron glass beads. The porosity of this packed bed was determined, 1% brine was then flushed through the packed column.

Only three medium flow rates were run to get the permeability of the packed bed to 1% NaCl solution. The flow rate reached is not high enough to study the inertial effect, and, since there is no pressure tap made on the packed section, we do not know whether there is a significant end effect. In experiment PF-1b, a Pusher 700 polymer solution (1000 ppm with 1% NaCl) was studied. The characteristics of the packed bed were listed in Table 1, and all the results were shown in Figure 5 through Figure 6, and Table 2 through Table 4.

Table 2 shows the results for the brine flood. The permeability of this packed bed was obtained by the employment of Darcy's law. The brine viscosity is measured to be 0.92 centipoise at room temperature (24^{o}C). The effective bead size is calculated from equation (5) and, the sphericity factor for beads, is then obtained from equation (4), and shown in Table 1.

Figure 5 shows the pressure drop-flow rate data for the polymer solution flowing in the bead pack. The non-linearity of the curve is due to the viscoelasticity of the polymer and the point where the pressure drop-flow rate curve turns up is also the point where the apparent viscosity increases, which is shown in Figure 6.

The apparent viscosity is calculated using Darcy's equation and the shear rate is calculated from equation (14). In equation (14), the flushed permeability is used. This value is obtained from the brine flood following the polymer flood, and the results are shown in Table 4. The residual resistance factor, which represents the

the ratio of the mobilities of the initial brine to that of the brine after polymer, is also determined. The apparent viscosity obtained from flow experiments, has a very good correlation with the viscosity measured with the viscometer up to a certain shear rate. After that critical shear rate, the apparent viscosity starts to increase. The deviation from viscous flow, the dilatant behavior, is due to the viscoelastic nature of the Pusher 700 polymer solution.

As it has been pointed out earlier, the pressure rating for the glass column is only 80 psi. Obviously, high flow rates can not be reached and the inertial effect and column-end effect can not be studied. Besides, we are not sure whether fluid entrance and exit end effects have contributed any to the measured pressure drop. For these reasons, a high-pressure-rated stainless steel column without any pressure taps on the packed section was then employed. Since viscoelastic fluids generally show large entrance and exit effects, it is desirable then to study fluids without viscoelasticity first. This is the reason that a Newtonian fluid (brine) is run next in experiment no. 2, followed with a Xanflood polymer flood.

B. Experiment No. PF-2. End Effect Studies for Brine and Xanflood Polymer Solution

Brine with 1% NaCl and Xanflood polymer were studied in this experiment to test for the feasibility to use a column of the second type as described in section B of Chapter IV. The porosity

100-110 micron bead pack was determined to be 39% and the permeability is determined to be 6.0 Darcies. Results are shown in Figure 7 through Figure 10, and in Table 5 through Table 7.

From Figure 8, we might come to the conclusion that there is a significant inertial effect in the beads at Reynolds numbers greater than 1 because of a significant drop in permeability. But Figure 9 tells us that the excess in the pressure drop is not due to inertial force. In fact, it comes mostly from fluid entrance and exit column-end effects. The Ergun equation, equation (1), describes the motion of Newtonian fluids both in the laminar region and in the transition and turbulent regions. We should expect the experimentally determined pressure drop data to coincide with those calculated based on the Ergun equation, and the ratio of them should be close to unity, even at a high Reynolds number. Any significant deviation from that is primarily due to the end effect for this case.

In Figure 10, the apparent viscosity of the Xanflood polymer can not be correlated with the steady viscosity at high shear rate. The deviation is pronounced. Since there is a tremendous amount of pressure drop which comes from the end effects at relatively high Reynolds number (high shear rate), this column can not be used to study the polymer flow behavior in porous medium. The third type of column was thus designed, made, and tested to be appropriate for the study of polymer flow.

Experiment No. PF-3: Xanflood Polymer Solution Studies

In this set of experiments, Kelco's Xanflood polymer was used. Three different concentrations of Xanflood Polymer/Salt solution, namely, 1000 ppm XF with 1% NaCl, 500 ppm XF with 1% NaCl and 1000 ppm XF with 0.1% NaCl were prepared and flowed through the packed column. The column is packed with 100-110 micron glass beads, saturated with 1% brine and flushed with the same brine from a very low flow rate up to a high flow rate. The same procedure is then repeated for the polymer flows. The characteristics of the packed bed are tabulated in Table 1.

The purpose of the brine-flood study has been described earlier in section B, Chapter V. The results are presented in Figure 11 through Figure 13, and in Table 8.

Figure 11 shows the pressure drop-flow rate data. Three different pressure drops are measured for each flow rate during the experiment. They correspond to a 12"-long section for the total length, a 6"-long section between two pressure taps on the packed section and a 3"-long section between the inlet and the first pressure tap on the packed section. Experimental results generally show consistent values even at a shear rate as high as 88500 sec^{-1} (N_{Re}=3.5), indicating that the column-end effects are successfully eliminated, at least for brine flow. Further results indicae that this is also true even for fluids such as hydrolyzed polyacrylamide solutions which are generally known to have large fluid entrance and exit end effects.

The pressure drop data used in Figure 11 are those measured

between two pressure taps (6" section). The flow rate changes from 0.00072 cc/sec up to 5 cc/sec, a range of 4 orders of magnitude. It is a linear plot throughout. The permeability of the packed bed to brine is calculated from the individual measurements. Except for the first few points which are scattered presumably due to the inaccurate measurements of low pressure drops (10^{-2}-10^{-1}psi) in Figure 12, the permeability, as it should be, is constant over a wide range of Reynolds number. The highest Reynolds number reached is about 3.5. Only a slight inertial effect (4%) is observed at that Reynolds number (Figure 13). The calculated pressure drop based on the Ergun equation is very close to that measured directly from experiment.

Reviews on flow at large Reynolds numbers have been presented by Bear[58], and many others. In the various explanations presented for deviation from Darcy's law, inertial forces play the primary role. These forces are always present, but they gradually become predominant (with respect to viscous forces) at large Reynolds numbers. Most experiments indicate that actual turbulence occurs at N_{Re} values at least one order of magnitude higher than the N_{Re} at which deviation from Darcy's law is observed.

After the design of the column and the method to measure pressure drop had been shown to be appropriate, three Xanflood polymer solutions were studied. They are prepared and mixed with the use of a blender, as described in section C, Chapter V. The rheological

properties for these filtered poltmer solutions were determined with the LS-30 viscometer. They are shown in Figure 14.

The viscosity versus shear rate curves are typical for polymer solutions, showing a Newtonian region at low shear rate and a pseudoplastic region at moderate to high shear rate. In other words, the viscosity is constant in the low shear region. As the shear rate increases to a certain value, the viscosity starts to decrease. The higher the concentration, the lower shear rate at which this pseudoplastic behavior starts to occur, as can be seen in Figure 14. Results also show that salt has little effect on the rheological properties of Xanflood polymer solutions. The viscosities for 1000 ppm XF in 1% NaCl and in 0.1% NaCl are about the same. The latter is slightly lower than the former.

The very same polymer solutions are then flooded through the packed column. The packed column is first saturated with 1000 ppm XF in 1% NaCl solution by flushing the polymer solution through the packed bed until a stablized pressure drop is reached and the viscosity of the effluent sample is measured to be the same (within experimental accuracy) as that of the injected solution, then the polymer flood starts. Again three different pressure drops are recorded for each flow rate and they generally show consistent values indicating no fluid entrance and exit end effects have been observed during the experiment. The pressure drop data used for calculations are those obtained between a pair of pressure taps 6" apart. The flushed permeability is determined after polymer run with brine flowing. A relatively high flow rate, about 25 cc/min, is arbitrarily chosen

through the column to remove all polymer which is
rapped. Brine flow took place until 10 to 20
been flushed. Again, the amount of brine needed can
establishment of a steady state pressure drop.
sure drop and flow rate data were collected and the
ability obtained by use of Darcy's equation.
procedure is repeated for the other two Xanflood
. All the flow results are shown in Figure 15
shows pressure drop versus flow rate data for the
utions. Flushed permeabilities are determined as
. Figure 16 is a plot of the pressure gradient
throughput for the 500 ppm XF in 1% NaCl solution.
the three pressure drops obtained for each flow rate
ifferent lengths and sections generally give the same gradient
flow rate of 3.5 cc/sec, which corresponds to a shear rate
sec , indicating that the end effect is insignificant for
apparent viscosities, obtained by using Darcy's
are compared to the viscosities measured from the viscometer
and 18. Results indicate that the apparent viscosities
dynamic flow experiments are almost identical to those
viscometer. The curves also show the presence of the
plain region in the very high shear rate range.
ther characteristic which can be seen from Figure 17 and

is that up to shear rate of 63,009 sec^{-1}, the Xanflood polymer does not show any elasticity. Furthermore, no shear degradation has been observed up to the highest shear rate for all cases. Figure 19 shows a plot of the ratio of the viscosity of the effluent samples to the viscosity of the injected solution as a function of shear rate.

Figure 20 shows the flushed permeabilities after the three polymer floods. The original permeability of the pack to brine was 4.3 darcies. After the first polymer flood took place, the residual resistance factor was 1.075. After the second flood, the residual resistance factor was 1.044, and after the third polymer flood, 1.11.

One thing which needs to be pointed out is that the flushed permeability of the packed bed will be reduced further if the bed has already been flushed with polymer solution. As the results shown in Figure 20, the permeability for the first polymer flood was 4.0 darcies and reduced further to 3.83 and 3.45 darcies for the second and the third flood respectively.

D. Experiment No. PF-4: Unsheared Xanflood Polymer Solution Studies (Magnetic Stirring)

In preparing the Xanflood polymer solutions for EXP. NO. PF-3, the polymer had been sheared to some extent with the use of a Waring blender operating at full voltage (125V). To evaluate the effect of shear, Xanflood polymer solution was made with the use of magnetic stirring with all the other conditions the same. This will

referred to as unsheared polymer. The mixing for polymer took place for 60 to 90 minutes. This length of time is long enough to give a solution which appears homogeneous and has a viscosity even higher than the sheared solution (Figure 21) when unfiltered There was very little difference after filtration, however. Polymer solutions made with different degrees of shearing (rheostat settings at 20, 40, 60, 80, 100, and 125V on the blender)are compared in Figure 21 through 24. The viscosities were all measured after the solutions had been filtered unless otherwise indicated.

Polymer solution prepared at 20 volts exhibits the lowest viscosity. Presumably, this is due the fact that ten-minute mixing at 20 volts is not long enough to dissolve all the polymer. Some undisslved or gelled polymer is removed during the filtration process and therefore results in a lower viscosity. The solution mixed at 40 volts has the highest viscosity after filtration. Presumably this is because ten-minute mixing at 40 volts is long enough to give good mixing, yet not too long to cause any significant shear degradation of the polymer molecules. Solutions made at 60V, 80V, 100V and full voltage had almost the same viscosity.

A new column was prepared and packed with 100-110 micron glass beads to study the behavior of the "unsheared" polymer solution. As before, the packed column was saturated with 1% NaCl and a brine flood conducted, then the polymer floods. Filtered polymer was used. Table 15 through Table 17, and Table 25 through 29 show the results.

Generally speaking, this unsheared Xanflood polymer solution

behaves just like the one made in EXP. NO. PF-3. The apparent viscosity of this polymer solution is again about the same as that measured with the LS-30 viscometer. A second Newtonian region also emerges at about the same high shear rates as before. Also as before, no viscoelasticity is apparent, and no shear degradation was observed up to a shear rate of 56800 sec^{-1}.

E. Experiment No. PF-5,PF-6,PF-7: Pusher 700 Polymer Solution Studies

Partially hydrolyzed polyacrylamide polymer solutions are generally believed to show viscoelastic characteristics while flowing in porous media. Pusher 700 polymer, a Dow Chemical product, was selected, and the effects of polymer concentration, salinity and bead size studied. Figure 30 through Figure 36, and Table 18 through Table 25 present the results for experiments PF-5 and PF-6.

We can observe from Table 18 that, up to the maximum Reynolds number of 2.6, no significant inertial effect (3.6%) exists. This agrees with other experiments and the Ergun equation within experimental error.

The viscosity for the three Pusher 700 polymer in brine solutions are shown in Figure 30. The unfiltered polymer solutions had higher viscosities than the filtered solutions, and the difference is more pronounced at low shear rate. The usual pronounced decrease in viscosity is observed and explained by the polyelectrolyte nature of this polymer.

The pressure drop-flow rate data (Figure 31) show a linear trend at low flow rate. A very significant change in trend occurs in the order of 0.01 cc/sec. Eventually,another almost linear trend develops, but at a much higher slope. The two experiments in 1% NaCl (PF-5b and PF-6b) show almost the same slope, while the one experiment in 0.1% NaCl (PF-6d) show a lower slope at high rate even though its viscosity is considerably higher. The reason for this is not known.

From the plots of apparent viscosity versus shear rate (Figure 32), the critical shear rate at which viscoelasticity becomes noticeable can be seen. For experiments PF-5b and PF-6b, this shear rate is about 110 sec^{-1}, while for PF-6d it is only 10 sec^{-1}. The latter shear rate is very low, corresponding to the value in many reservoir floods even at considerable distances from the wells.This depends on the injection rate, rock properties, fluid saturation, and so forth, of course.

The agreement between steady viscosity and apparent viscosity below the onset of the elastic effect is , as with the Xanflood experiments, good. This is especially so for PF-5b. The data taken by Dr. G.B. Thurston is also shown for comparison with the viscosity of the solution used in PF-5b (1000 ppm Pusher, 1% NaCl). His data correspond to the real component of the complex viscosity (call this η), measured with his oscillatory instrument.[47] This is the viscous component and is shown only at 2 Hz. frequency. Other frequencies and the elastic component have been measured,but are not shown. This value of η at 2 Hz should agree with the steady viscosity

measured in our couette viscometer (the LS-30) at high shear rates, which it does. At low shear rates, the viscosity at 2 Hz. attains its Newtonian plateau at a higher shear rate than steady state viscosity. The two measurements of viscosity coincide even at low shear rates in the limit of zero frequency, i.e., at steady state. The quality of the agreement of the three values of viscosity at intermediate shear rates is remarkable. Recall that for the beadpack data, the shear rate must be calculated (from Equation 14) and is done so without any empirical adjustment. Of course, the permeability of this pack (4.2D) is high enough that permeability reduction is negligible . This was as intended, so that the viscoelestic effect could be isolated as much as possible.

Another way to analyze these data is to plot the ratio of apparent viscosity to viscosity versus Deborah number (Figures 33 and 34). The relaxation times used in these plots were determined by Thurston from the oscillatory data on the same solutions. He fit all of his data with a generalized Maxwell model using three relaxation times. The value of θ_f used in the calculations of Deborah number was the shortest of the three in each case. This was done because the elastic response is at high shear rates and frequencies. An alternative would be to determine an effective relaxation time as a function of both shear rate and frequency. This would require a model giving an equivalent frequency as a function of flow rate in the pack, much as is already done for shear rate.

Thurston and Pope are working on such a model now (1980).

Comparing PF-5b and PF-6d (Figure 33), we see that the results are not in very good agreement at high Deborah number. Had the same θ_f been used, the results would have been close at high Deborah number, but the onset of elasticity (when μ_{app}/μ first exceeds 1.0) would have not been at the same value (about 0.02 as shown). As expected, using a single θ_f is not satisfactory. The most striking disagreement, however, is between the hydrolyzed polyacrylamide tests just discussed, and the earlier xanthan gum test (PF-3b). The maximum value of μ_{app}/μ for the latter is 1.3, and this value would not increase much, if any, all the way up to a Deborah number of 7.4 (not shown, but from Table 9, the value corresponding to the maximum flow rate). Thus, more than an order of magnitude discrepancy exists at the high flow rates. Clearly, the xanthan gum is not very elastic despite the fact its smallest θ_f is as high as that for the Pusher 700 in 1% NaCl. Any general theory must somehow be able to reconcile these data.

The effect of bead size is evaluated by comparing experiment PF-5b (nominal 100 μm beads) with another Pusher 700 experiment (PF-7b, numerical 250 μm beads) discussed below and shown in Figure 34. Here the Deborah number appears to account for bead size satisfactorially. The permeability contrast was eight fold.

One possible cause for discrepancy in any polymer flow test is the change in solution viscosity which may occur (effluent versus

injected). Some of the causes include shear degradation (at high rates), chemical degradation(with time), changes in composition (calcium ion pickup, for example), plugging, and so on. In these experiments, the ratio of viscosity of the effluent samples to the viscosity of the injected solution was almost exactly one (Figure 35 and 36). Evidently none of the above effects were occurring. In particular, shear degradation did not occur despite shear rates up to 9088 sec^{-1} (PF-7b). As shown below in experiment PF-8b, shear degradation does occur, as expected, but only after about 10000 sec^{-1}.

Other results for PF-7 are shown in Figures 37 to 42. The pressure drop-flow rate (Figure 40) and apparent viscosity-shear rate (Figure 42) data are similar to previous Pusher 700 results. Especially noteworthy are the comparisons of pressure gradient for the polymer flood shown in Figure 41. Clearly, no end effects were detected.

Another potential sourse of misleading results is the inertial effect. From Table 26 and Figure 39, the onset of this effect can be seen to occur for the brine flood at a Reynolds number on the order of 1.0. The Ergun equation nicely accounts for the effect up to the highest N_{Re} of 10.7. But the highest N_{Re} for the polymer flood (PF-7b) was only 0.1, so no inertial effect was likely to be significantly affecting these data.

F. Shear Degradation Studies on HPAM: Experiment No. PF-8

Since no shear degradation was observed at maximum pressure

drop of 534 psi, a shorter column (9/16"x4") was used in this experiment. The same end piece was used as before starting with PF-3. It was packed with 250-300 μm glass beads. The three polymers used were Pusher 700, Water Cut 110 and Water Cut 160.The latter two are polyacrylamides sold by Tiorco. Water Cut 110 is anionic and Water Cut 160 is cationic.

The results are given in Table 29 through 37 and Figure 43 through 49. The Pusher 700 started degrading (Figure 43) at about 10000 sec^{-1} and had degraded about 5% at 20000 sec^{-1} ,as measured by the effluent viscosity at 1 sec^{-1} . These relatively high values for the onset of degradation are due to the complete absence of calcium.

The Water Cut 110 viscosity both before and after heating to 80°C is shown in Figure 44. Since no protective additives were used, a loss in viscosity of about 50% occurred when heated to 80°C for 24 hours. The apparent viscosity is shown in Figure 45. The viscoelastic effect is large even for this low concentration, low viscosity solution. The chemically degraded solution has a much lower apparent viscosity at high shear rate, however.

Shear degradation was very slight (maximum 4% at 30000 sec^{-1}) for the Water Cut 110 polymer. This indication, just as its viscosity does, that it is a smaller molecule than Pusher 700. This could be due to a lower molecular weight, or to a charge difference(degree of hydrolysis), or perhaps other factors such as branching.

The viscosity (Figure 47), apparent viscosity (Figure 48)

and shear degradation (Figure 49) of Water Cut 160 polymer are similar to Water Cut 110, except for the much lower viscosity. It is interesting that this cationic polyacrylamide shows a pronounced elastic effect (Figure 48) just as the anionic did, and shear degrades at about the same shear rate at Water Cut 110.

Recall that no shear degradation occurred for the Xanflood even at the maximum shear rate attained (63000).

C. Microemulsion Experiment: Experiment No. MF-1

A single experiment was done using a microemulsion. This experiment was conducted with Mr. Kim Jones, who is continuing these experiments. The 9/16" x 12" stainless steel column and 100-110 micron glass beads were used. The microemulsion was made up by mixing 20% (volume) iso-octane, 3.5 % (volume) Witco TRS 10-80, 4.4 % (volume) iso-butyl alcohol (IBA), 0.4% (weight) NaCl , and 71.7 % (volume) distilled water. A phase volume fraction diagram at 24^{o}C for this overall composition, except with variable salinity, is shown in Figure 50. This diagram shows that the microemulsion was Type II(-) , or a lower phase microemulsion, at 0.4 % NaCl, and that the volume fraction of excess oil was very small, about 1.0%. Thus, the composition of the microemulsion was very nearly the same as the overall composition.

The steady viscosity and apparent viscosity versus shear rate (Figure 51) show excellent agreement up to the maximum shear rate measured. No viscoelastic effect was evident. However, the

aximum shear rate was not very high, but it will be increased
o higher values by Jones. The injected and produced viscosities
greed very well, indicating no significant changes in the micro-
mulsion.

CHAPTER VII

CONCLUSIONS

The viscosity and apparent viscosity for several polymer solutions have been measured and compared more accurately and over a wider range of shear rates than previously possible. This was possible primarily because of the availability of the Contraves LS-30 couette viscometer, starting in 1978. Also, care was taken to eliminate pack end effects,to verify the steady state flow in the beadpack used, to establish the effect of inertia, and to verify no polymer degradation had occurred. By using glass beads large enough to give high permeability packs (roughly 5 to 39 Darcies), no chemical or mechanical trapping effects were thought to be significant. All these factors contributed to the accurate comparison of the viscosities, probably less than 5 % error exists in either type of measurement, which is about the maximum difference between the two viscosities at low shear rates before the onset of viscoelasticity. This agreement between viscosities is dependent upon a calculated equivalent shear rate. This was down without empirical adjustment, using only measured quantities. Since the equivalent shear rate is based upon the very simple bundle of capillaries model, this agreement is quite remarkable.The maximum shear rate range was 3 to 85000 sec^{-1}. The low end of this range is low enough to see the viscosities approach , or in some cases attain their low shear Newtonian limit. The high end extends the range of the available apparent viscosity type of measurement, and corresponds to the highest shear rates expected to occur in polymer injection wells, even under extreme conditions (high injection rates, filled perforations of small diameter, and so on).

No effect of elasticity was observed for the xanthan gum polymer, [illegible] at the highest shear rate(63009 sec^{-1}). Nor did any shear degradation [illegible]r. This was true even when the polymer solution was carefully [illegible]pared with a magnetic stirrer to minimize shearing during preparation. [illegible] "unsheared" solution was filtered, however, which shears it more [illegible]an the magnetic stirring, but less than the Waring blender used [illegible]r all other xanthan gum solutions.

By contrast to the xanthan gum, the polyacrylamides tested [illegible]owed pronounced viscoelasticity at high shear rates. The apparent [illegible]scosity started increasing at shear rates as low as 10 sec^{-1}. In all [illegible]es it occurred far below the onset of shear degradation. The latter [illegible]d not start until 10,000 sec^{-1} or more. This clearly establishes [illegible]hat the elasticity effect can be significant without shear degra-[illegible]ation occurring. Also, since the bead size (permeability) was large, [illegible]ermeability reduction was very small, and in all probability adsorp-tion on the glass beads was also very small, the elasticity effect is clearly significant regardless of these other factors. All of these phenomena may be related, but apparently need not be simultaneously significant.

The viscoelastic behavior of these polymers could not be correlated with the Deborah number using a single relaxation time. The discrepancy between the behavior of the hydrolyzed polyacrylamide (Pusher 700) and xanthan gum (Xanflood) is very large. The Pusher 700 in 1% NaCl shows an increase in apparent viscosity of a factor of ten at Deborah number of 0.3, while the Xanflood shows an increase of

least a factor of 1.8 at Deborah number of 7.4 (this value is about times greater than previously reported [48]). Perhaps a variable relaxation time, depanding on shear rate and frequency, could correlate these and other similar data, but this has not been established. The need for additional theoretical development is clear.

The Deborah number would appear to account for the change in bead size. But these data are too limited in range to be definitive. Other data [13,14,48] also support this dependence on bead size, but are typically more limited in other ways, such as a more limited range of shear rate, more complicated porous media, etc. Therefore, it is recommended that additional data be taken over a wider range of bead size. However, this will not be without potential complications. As the bead size decreases much below 100 micron, permeability reduction will become significant and ultimately will be dominant. On the other hand, as the bead size increases, inertia will increase and ultimately will be dominant.

Many additional experiments will be necessary to fully explore the many relevant variables associated with polymer flow in porous media. Some of these variables are (1) electrolyte effects, especially that of calcium ; (2) porous media characteristics; (3) the presence of other phases and components, especially those associated with surfactant flooding and (4) the effect of crosslinking and gels or microgels.

The single experiment done with a micellar solution shows that it is possible, just as in the case of the polymer solutions, to

ive excellent correspondence between measured viscosity and apparent viscosity. These data need to be extended to higher shear rates. Also, other types of micellar solutions should be studied, and polymer included in some cases, where this is possible (at low salinity).

BIBLIOGRAPHY

1. Christopher, R. H. and Middleman, S. "Power Law Flow Through a Packed Tube", I and EC Fundamentals, Vol. 4, No. 4 (Nov.1965) 422-425.

2. Christopher, R. H. and Middleman, S. "Flow of Viscoelastic Fluids Through Porous Media", I and EC Fundamentals, Vol. 6, No. 1 (Feb. 1967) 145-146.

3. Mckinley, R. M., Jahns, H. O., and Harris, W. "Non-Newtonian Flow in Porous Media", AICHE Journal, Vol. 12, No. 1(Jan. 1966) 17-20.

4. Jones, W. M. and Maddock, J. L. "Flow of VIscoelastic Liquids", SPE Symposium, Houston, Texas (Dec. 1966).

5. Marshall, R. J. and Metzner, A. B. "Flow of Viscoelastic Fluids Through Porous Media", I and EC Fundamentals, Vol. 6, No. 3 (Aug. 1967) 393-400.

6. Gogarty, W. B. "Mobility Control With Polymer Solutions", SPE Journal, (June 1967).

7. Gogarty, W. B. "Rheological Properties of Pseudoplastic Fluids in Porous Media", SPE Journal (June 1967).

8. Dominguez, J. G. and Willhite, G. P. "Retention and Flow Characteristics of Polymer Solutions in Porous Media", SPE Journal, (April 1977) 111.

9. Sadowski, T. J. and Bird, R. B. "Non-Newtonian Flow through Porous Media", Trans. of Sci. Rheology, Vol. 9 No. 2 (1965).

10. Jennings, R. R., Rogers, J. H. , and West, T. J.,"Factors Influencing Mobility Control by Polymer Solution", J. Pet. Tech. 23, 391 (1971).

11. Bird, R. B., Steward, W. E., and lightfoot, E. N., "Transport Phenomena", Wiley, New Yor, (1960).

12. Savins, J. G., "Non-Newtonian Flow Through Porous Media", Ind. Eng. Chem., 61, No. 10, 18 (1969).

13. Hirasaki, G. J. and Pope, G. A., "Analysis of Facotrs Influencing Mobility and Adsorption in the Flow of Polymer Solution through Porous Media", SPE Journal, (Aug. 1974).

Wang, F. H. L., Duda, J. L., and Klaus, E. E., "Influences of Polymer Solution Properties on Flow in Porous Media", SPE 8418, SPE Symposium, Las Vegas, Nevada (Sept. 1979).

MacWilliams, O. C., Rogers, J. H., and West, T. J. "Water Soluble Polymers in Petroleum Recovery", Published in "Water-Soluble Polymers", Polymer Science and Tech., Vol 2, N. M. Bikales Editor, Plenum Press, 105-126 (1973).

Sandiford, B. B., "Flow of Polymers through Porous Media in Relation to Oil Displacement", Published in "Improved Oil Recovery by Surfactant and Polymer Flooding", D. O. Shah and R. S. Schechter Editors, Academic Press, 487-509 (1977).

17. Pye, D. J., "Improved Secondary Recovery by Control of Water Mobility". J. Pet. Tech. 911-916 (Aug. 1964).

18. Lipton, D. "Improved Injectivity of Biopolymer Solutions". SPE 5099 (Oct. 1974).

19. Maerker, J. M.,"Shear Degradation of Polyacrylamide Solutions", SPE 5101 (Oct. 1974).

20. Szabo, M. T., "Factors Influencing Oil Recovery and Polymer Retention during Polymer Floods", SPE 4668 (Sept. 1973).

21. Szabo, M. T., "Laboratory Investigations of Factors Influencing Polymer Flood Performance", SPE 4669 (Sept. 1973).

22. Szabo, M. T., "A Comparative Evaluation of Polymers for Oil-Recovery-Rheological Properties", SPE 6601 (June 1977).

23. Foshee, W. C., Jennings, R. R. and West, T. J.,"Preparation and Testing of Partially Hydrolyzed Polyacrylamide Solutions", SPE 6202 (Oct. 1976).

24. Sandvik, E. I.and Maerker, J. M., "Application of Xanthan Gum for Enhanced Oil Recovery", Published in "Extracellular Microbial Polysaccharides", P. A. Snadford and A. Laskin Editors, ACS Symposium Series, No. 45, 242-264 (1977).

25. Sloneker, J. H. and Jeanes, A. "Exocellular Bacterial Polysaccharides from Xanthomonas Campestris. NRRL B-1459, Part(I):Constitution, Canadian Jo Chem.,Vol. 40, 2066 (1962).

26. Hill, H. J., Brew, J. R., Claridge, E. L., Hite, J. R., and Pope G. A., "The Behavior of Polymers in Porous Media", SPE 4748 (April 1974).

...al, E., Duda, J. L., Klaus, E. E., and Liu, H. T., "Solution ...perties of Mobility Control Polymers", SPE 6625 (Oct. 1977).

...nes, A., "Applications of Extracellular Microbial Polysaccharides-...lyelectrolytes:Review of Literature, Including Patents", J. ...lymer Sci.,Symposium No. 45, 209-227 (1974).

...intzis, F. R., Babcock, G. E., and Tobin, R.,"Studies on Dilute ...lutions and Dispersions of the Polysaccharides from Xanthomonas ...mpestries NRRL B-1459", Carbohydrate Research, Vol 13, 257-267 (1970).

...Meerker, J. M. "Mechanical Degradation of Partially Hydrolyzed ...olyacrylamide Solutions in Unconsolidated Porous Media", SPE ...ournal, (Aug. 1976)

...Pinker, G. E.,Bowman, R. W., and Pope, G. A.,"Determination of ...n-Site Mobility and Wellbore Impairment from Polymer Injectivity ...ata", J. Pet. Tech., (May 1976).

...Martin, F. D., "Laboratory Investigations in the Use of Polymers in Low Permeability Reservoirs", Paper SPE 5100, (Oct 1974).

...Vela, S., Peaceman, D. W., and Sandvik, E. I.,"Evaluation of Polymer Flooding in a Layered Reservoir with Crossflow, Retention, and Degradation", SPE Journal, (April 1976) 82-96.

...Mysels, K. J.,"Introduction to Colloid Chemistry", 10, Interscience Publishers, Inc., New York, NY. (1959).

35. Becher, P., "Emulsions:Theory and Practice", 36, Reinhold Publishing Corp., New York, N. Y. (1965).

36. Ibid., 46.

37. Becher, P., "Principles of Emulsion Technology", Reinhold Pilot Book, 3, Reinhold Publishing Corp., New York, N. Y. (1955).

38. Bowcott, J. E. and Schulman, J. H.,"Emulsions, Zeits Fur Elect." 59, Heft 4, 283 (1955).

39. Gogarty, W. B. and Olson, R. W."Use of Microemulsions in Miscible -Type Oil Recovery Procedure", U. S. Patent No. 3,254,714 (June 7, 1966).

40. Gogarty, W. B., and Tosch, W. C., "Miscible-Type Waterflooding: Oil Recovery with Micellar Solutions", J. Pet. Tech. 147-1414 (Dec. 1968).

... Davis, J. A.Jr., Gogarty, W. B., Jones, S. C., and Tosch, W. C., "Oil Recovery Using Micellar Solutions", API Drilling and Production Practices, 261-272 (1968).

... Davis, J. A. Jr., and Jones, S. C.,"Displacement Mechanicsms of Micellar Solutions", J. Pet. Tech. 1415-1428 (Dec. 1968).

... Gogarty, W. B., Meabon, H. P. and Milton, H. W. "Mobility Control Deisgn for Miscible Type Waterfloods Using Micellar Solutions", J. Pet. Tech., 141-147 (Feb. 1970).

... Gogarty, W. B., and Surkalo, H., "A Field Test of Micellar Solution Flooding", SPE 3439, J. Pet. Tech., 1161-1169 (Sept 1972).

... Jones, S. C., and Dreher, K. D.,"Cosurfactants in Micellar Systems Used for Tertiary Oil Recovery", SPE Journal, 161-167 (June 1976).

... Shah, D. O., Bansal, V. K., Chan, K. and Hsieh, W. C., "The Structure, Formation and Phase-Inversion of Microemulsion", Published in "Improved Oil Recovery by Surfactant and Polymer Flooding", D. O. Shah and R. S. Schechter, Editors, Academic Presss, 293-337(1977).

47. Thurston, G. B., "Biorheology", (1976) 13, 191.

48. Gogarty, W. B., Levy, G. L., and Fox, V. G. "Viscoelastic Effects in Polymer Flow through Porous Media", SPE 4025, (Oct 1972).

49. Laufer, G. Gutfinger, C. and Abuaf, N. "Flow of Dilute Polymer Solutions through a Packed Bed", I and EC Fundamentals, (1976) 15,74.

50. Ergun, S. "Fluid Flow through Packed Columns", Chem. Eng. Prog. 48, 89 (1952).

51. Kemblowski, Z. and Mertl, J., Chem. Eng. Sci. 29, 213 (1974).

52. Contraves A. G., Zurich, Schaffhauserstrasse 580, P. O. Box CH-8052, Zurich.

53. Glenco Scientific, Inc. 2802 White Oak Drive, Houston Texas 77007.

54. The Zenith Corp.432 Cherry St., West Neuton, Massachusetts 02165.

55. Validyne Engineering Corp., 19414 Londelius St., Northridge, Calif. 91324.

56. Texas Instrument Corp., Recorder Dept., P. O. Box 1443, Houston, Tx. 77001.

57. Instrumentation Specialties, Co., ISCO Model 328, Lincoln Nebraska,

58. Bear, Jacob. "Dynamics of Fluids in Porous Media", American Elsevier Publishing Co., 1972.

59. Tsaur, Kerming, "A Study of Polymer/Surfactant Interactions for Micellar/Polymer Flooding Appciations", Master's Thesis, The University of Texas at Austin. Dec 1978.

60. Jones,Kim :" A Rheological and Phase Behavior Study of Micro-emulsion ", Master's Thesis, in Progress, Department of Petroleum Engineering, University of Texas at Austin

TABLE 1

LIST OF EXPERIMENTS AND CHARACTERISTICS

EXP.NO.	SOLUTION NUMBER	TYPE OF COLUMN	SIZE OF GLASS BEADS (micron)	POROSITY (percent)	PERMEABILITY (darcy)	SPHERICITY FACTOR	RESIDUAL RESISTANCE FACTOR	
PF-1	1-a	first	100-110	44.8	8.7	0.63	-	1% NaCl
	1-b				8.2	0.61	1.07	1000 ppm P-700,1%NaCl
	1-c				8.2	0.61	-	1% NaCl
PF-2	2-a	second	100-110	39	6.0	0.72	-	1% NaCl
	2-b				5.2	0.67	1.15	500 ppm XF, 1% NaCl
	2-c				5.2	0.67	-	1% NaCl
PF-3	3-a	third	100-110	39	4.3	0.60	-	1% NaCl
	3-b				4.0	0.58	1.075	1000 ppm XF, 1% NaCl
	3-c				4.0	0.58	-	1% NaCl
	3-d				3.8	0.57	1.044	500 ppm XF, 1% NaCl
	3-e				3.8	0.57	-	1% NaCl, 0.1% NaCl
	3-f				3.45	0.54	1.11	1000 ppm XF,0.1% NaCl
	3-g				3.45	0.54	-	0.1% NaCl
PF-4	4-a	Bench top study for sheared and unsheared XF solution						
	4-b	third	100-110	40	6.1	0.68	-	1% NaCl
	4-c				5.4	0.64	1.14	1000 ppm XF,1% NaCl
	4-d				5.4	0.64	-	1% NaCl
PF-5	5-a	third	100-110	39	4.9	0.64	-	1% NaCl
	5-b				4.2	0.59	1.16	1000 ppm P-700,1%NaCl
	5-c				4.2	0.59	-	1% NaCl

TABLE I (cont'd)

LIST OF EXPERIMENTS AND CHARACTERISTICS OF POROUS MEDIA

EXP.NO.	SOLUTION NUMBER	TYPE OF COLUMN	SIZE OF GLASS BEADS (micron)	POROSITY (percent)	PERMEABILITY (darcy)	SPHERICITY FACTOR	RESIDUAL RESISTANCE FACTOR	
PF-6	6-a	third	100-110	39.3	4.1	0.58	-	1% NaCl
	6-b				3.75	0.55	1.10	500 ppm P-700,1%NaCl
	6-c				3.75	0.55	-	1% NaCl, 0.1 % NaCl
	6-d				3.6	0.54	1.04	1000 ppm P-700,0.1%NaCl
	6-e				3.6	0.54	-	0.1% NaCl
PF-7	7-a	third	250-300	38.7	38.9	0.70	-	1% NaCl
	7-b				37.9	0.69	1.026	1000 ppm P-700,1%NaCl
	7-c				37.9	0.69	-	1% NaCl
PF-8	8-a	third	250-300	40	37.4	0.65	-	1% NaCl
	8-b				37.1	0.65	1.008	1000 ppm P-700,1%NaCl
	8-c				37.1	0.65	-	1% NaCl,fresh water*
	8-d				35.7	0.64	1.039	500 ppm W.C.110,fresh*
	8-e				35.7	0.64	-	fresh water*
	8-f				35.5	0.63	1.006	as of 8-d(heated)
	8-g				35.5	0.63	-	fresh water*
	8-h				35.0	0.62	1.014	500 ppmW.C.160,fresh*
	8-i				35.0	0.62	-	fresh water*
MF-1	1-a	third	100-110	41	9.0	0.79	-	0.4% NaCl
	1-b				8.2	0.75	1.09	3.5% TRS 10-80 20% iso-octane 4.4% IBA 0.4% NaCl
	1-c				8.2	0.75	-	0.4% NaCl

*Fresh water: 0.02% NaCl, 0.005% $NaHCO_3$, 0.005% $CaCl_2$

TABLE 2

EXPERIMENTAL RESULTS FOR EXP. NO. PF-1a

FLOW RATE (cc/sec)	PRESSURE DROP (psi)	PERMEABILITY (darcy)
0.0281	0.6	7.74
0.0842	1.6	8.70
0.14	2.64	8.76

Pressure Drop measured across the total length, 1"x24" glass column.

Solution: 1% NaCl

TABLE 3

EXPERIMENTAL RESULTS FOR EXP. NO. PF-1b

FLOW RATE (cc/sec)	PRESSURE DROP psi)	APPARENT VISCOSITY (cp)	SHEAR RATE (sec^{-1})	REYNOLDS NUMBER
0.000527	0.095	8.2	1.4	1.5×10^{-5}
0.00115	0.185	7.32	3.0	3.7×10^{-5}
0.00225	0.36	7.28	6.0	7.4×10^{-5}
0.00346	0.54	7.1	9.2	1.2×10^{-4}
0.00467	0.698	6.8	12.4	1.6×10^{-4}
0.00538	0.78	6.6	14.2	1.9×10^{-4}
0.0083	1.26	7.0	21.7	2.8×10^{-4}
0.014	1.95	6.34	37	5.3×10^{-4}
0.028	3.6	5.87	74	1.1×10^{-3}
0.0056	7.4	6.06	147	2.2×10^{-3}
0.07	9.65	6.27	186	2.7×10^{-3}
0.084	11.65	6.31	223	3.2×10^{-3}
0.11	16.5	6.83	292	3.8×10^{-3}
0.139	22.3	7.3	368	4.5×10^{-3}
0.168	29.6	8.0	444	5.0×10^{-3}
0.193	37.7	8.0	512	5.2×10^{-3}
0.222	46.8	9.6	588	5.5×10^{-3}
0.25	54	9.83	663	6.1×10^{-3}
0.277	64	10.5	734	6.3×10^{-3}
0.305	76	11.34	808	6.4×10^{-3}

Pressure Drop measured across the total length, 1"x24" glass column.

Solution: 1000 ppm Pusher 700 in 1% NaCl

TABLE 4

EXPERIMENTAL RESULTS FOR EXP. NO. PF-1c

FLOW RATE (cc/sec)	PRESSURE DROP (psi)	PERMEABILITY (darcy)
0.0845	1.7	8.21
0.141	2.86	8.15

Pressure Drop measured across the total length, 1"x24" glass column.

Solution: 1% NaCl

TABLE 5

EXPERIMENTAL RESULTS FOR EXP. NO. PF-2a

FLOW RATE (cc/sec)	PRESSURE DROP (psi)	PERMEABILITY (darcy)	SHEAR RATE (sec^{-1})	REYNOLDS NUMBER	P_1 (psi)	P_2 (psi)	P_{Ergun} (psi)	$\frac{P_{Ergun}}{P_1}$	Pressure Drop / P_{Ergun}
0.00071	0.05	6.06	18.7	1.0×10^{-3}	0.0509	-	0.0509	1	0.982
0.00137	0.093	6.28	35.8	2.0×10^{-3}	0.098	-	0.098	1	0.949
0.00275	0.187	6.28	72.2	4.0×10^{-3}	0.197	-	0.197	1	0.949
0.004	0.3	5.69	105	5.8×10^{-3}	0.285	-	0.285	1	1.053
0.0055	0.42	5.63	145	8.1×10^{-2}	0.395	-	0.395	1	1.063
0.0085	0.62	5.87	224	1.2×10^{-2}	0.61	-	0.61	1	1.018
0.0139	0.962	6.16	363	2.0×10^{-2}	0.99	-	0.99	1	0.972
0.028	1.93	6.13	727	4.0×10^{-2}	1.98	-	1.98	1	0.975
0.055	3.89	6.03	1439	8.0×10^{-1}	3.92	-	3.92	1	0.992
0.083	5.95	5.96	2176	1.2×10^{-1}	5.93	0.0083	5.938	1.0013	1.002
0.11	8.03	5.85	2883	1.6×10^{-1}	7.85	0.015	7.865	1.0019	1.021
0.137	10	5.82	3584	2.0×10^{-1}	9.77	0.023	9.793	1.0023	1.024
0.17	12.1	6.0	4456	2.5×10^{-1}	12.14	0.035	12.174	1.0029	0.994
0.226	16.1	5.99	5924	3.3×10^{-1}	16.14	0.062	16.2	1.0037	0.994
0.282	20.3	5.92	7368	4.1×10^{-1}	20.08	0.096	20.18	1.005	1.006
0.347	24.7	6.0	9086	5.0×10^{-1}	24.76	0.15	24.91	1.006	0.992
0.4	29.2	5.92	10604	5.9×10^{-1}	28.9	0.198	29.1	1.007	1.003
0.462	33.6	5.87	12098	6.7×10^{-1}	32.97	0.258	33.23	1.008	1.011
0.519	38.1	5.81	13590	7.6×10^{-1}	37.04	0.33	37.37	1.009	1.022
0.495	35.9	5.89	12970	7.2×10^{-1}	35.34	0.297	35.64	1.009	1.007
0.58	43.8	5.65	15184	8.4×10	41.38	0.41	41.79	1.01	1.048
0.882	69.9	5.39	23100	1.3	62.95	0.94	63.89	1.015	1.094
1.162	97.1	5.11	30443	1.7	82.96	1.63	84.95	1.02	1.148
1.473	130	4.84	38583	2.1	105.14	2.63	107.77	1.025	1.206
2.04	197	4.42	53443	3.0	145.63	5.04	150.67	1.035	1.307
2.572	275	3.99	67383	3.7	183.62	8.01	191.63	1.044	1.435
3.265	371	3.76	85628	4.8	233.34	12.93	246.27	1.055	1.506
3.722	465	3.42	97576	5.4	265.9	16.8	282.7	1.063	1.645

Pressure Drop measured across the total length, 7/16" x 12" stainless steel column.

Solution : 1% NaCl

TABLE 6

EXPERIMENTAL RESULTS FOR EXP. NO. PF-2b

FLOW RATE (cc/sec)	PRESSURE DROP (psi)	APPARENT VISCOSITY (cp)	SHEAR RATE (sec^{-1})	REYNOLDS NUMBER
0.0005	0.404	8.89	11.6	1.2×10^{-4}
0.001	0.665	7.32	23	2.8×10^{-4}
0.0021	1.19	6.12	50	7.1×10^{-4}
0.00314	1.6	5.61	73	1.1×10^{-3}
0.0043	2.03	5.25	99	1.6×10^{-3}
0.0077	3.1	4.45	178	3.5×10^{-3}
0.013	4.65	3.93	303	6.7×10^{-3}
0.0263	7.9	3.30	614	1.5×10^{-2}
0.053	13	2.70	1220	3.4×10^{-2}
0.08	17.8	2.43	1843	5.8×10^{-2}
0.105	21.8	2.28	2448	8.5×10^{-2}
0.133	26.2	2.17	3080	1.1×10^{-1}
0.22	37.8	1.89	5166	2.2×10^{-1}
0.34	53.4	1.73	7783	4.0×10^{-1}
0.581	88.5	1.68	13546	7.0×10^{-1}
0.88	12.6	1.58	20529	1.1
1.171	164	1.54	27260	1.5
1.452	204	1.55	33823	1.9
1.943	289	1.64	45266	2.4
2.58	386	1.65	60158	3.2
3.12	485	1.71	72690	3.7
3.65	602	1.82	85070	4.1

Pressure Drop measured across the total length, 7/16"x12" stainless steel column.

Solution : 500 ppm XF in 1% NaCl

TABLE 7

EXPERIMENTAL RESULTS FOR EXP. NO. PF-2c

FLOW RATE (cc/sec)	PRESSURE DROP (psi)	PERMEABILITY (darcy)
0.0275	2.25	5.2
0.0825	6.83	5.2
0.1367	11.46	5.1
0.779	23.15	5.2

Pressure Drop measured across the total length, 7/16"x12" stainless steel column.

Solution : 1% NaCl

TABLE 5

EXPERIMENTAL RESULTS FOR EXP. NO. PF-3a

FLOW RATE (cc/sec)	PRESSURE DROP (psi)	PERMEABILITY (darcy)	SHEAR RATE (sec^{-1})	REYNOLDS NUMBER	P_1 (psi)	P_2 (psi)	P_{Ergun} (psi)	$\frac{P_{Ergun}}{P_1}$	Pressure Drop $\frac{}{P_{Ergun}}$
0.00072	0.0165	5.64	12	5.0×10^{-4}	0.0217	-	0.0217	1	0.76
0.00142	0.035	5.23	25	1.0×10^{-3}	0.0429	-	0.0429	1	0.82
0.00278	0.072	4.97	49	2.0×10^{-3}	0.0838	-	0.0838	1	0.86
0.00417	0.11	4.88	73	2.9×10^{-3}	0.0125	-	0.125	1	0.88
0.0055	0.15	4.72	57	3.9×10^{-3}	0.165	-	0.165	1	0.91
0.00817	0.23	4.58	144	5.7×10^{-3}	0.246	-	0.246	1	0.935
0.0133	0.39	4.39	234	9.3×10^{-2}	0.4	-	0.4	1	0.975
0.0272	0.78	4.49	469	1.9×10^{-2}	0.82	-	0.82	1	0.951
0.055	1.63	4.35	970	3.9×10^{-2}	1.658	0.0008	1.66	1.0006	0.983
0.082	2.51	4.22	1450	5.7×10^{-2}	2.48	0.0017	2.482	1.0008	1.01
0.137	4.2	4.20	2412	9.6×10^{-1}	4.13	0.0046	4.13	1.001	1.02
0.168	5.1	4.24	2959	1.2×10^{-1}	5.06	0.0069	5.07	1.002	1.006
0.225	6.8	4.26	3946	1.6×10^{-1}	6.75	0.012	6.762	1.002	1.006
0.28	8.52	4.23	4932	2.0×10^{-1}	8.44	0.019	8.46	1.0024	1.007
0.344	9.9	4.48	6060	2.4×10^{-1}	10.4	0.029	10.394	1.003	0.952
0.455	13.4	4.37	8005	3.2×10^{-1}	13.7	0.051	13.74	1.0037	0.975
0.516	15.1	4.40	9104	3.6×10^{-1}	15.57	0.066	15.64	1.004	0.966
0.577	17.2	4.32	10147	4.01×10^{-1}	17.35	0.082	17.43	1.005	0.987
0.9	26.8	4.33	15868	6.3×10^{-1}	27.14	0.2	27.34	1.0074	0.98
1.486	44.5	4.30	26213	1.0	44.83	0.545	45.38	1.012	0.981
2.04	63	4.17	35900	1.4	61.4	1.02	62.44	1.017	1.001
2.61	80	4.20	45932	1.8	78.58	1.67	80.25	1.021	0.997
3.25	98	4.27	57217	2.3	97.9	2.6	100.5	1.027	0.975
3.82	116	4.24	67363	2.7	15.2	3.6	118.8	1.031	0.976
4.478	134	4.30	78919	3.1	135	4.94	139.9	1.036	0.958
5.02	153	4.23	88502	3.5	151.4	6.21	157.6	1.041	0.971

Pressure Drop measured between two pressure taps 6" apart, 9/16"x12" stainless steel column.
Solution : 1% NaCl

TABLE 9

EXPERIMENTAL RESULTS FOR EXP. NO. PF-3b

FLOW RATE (cc/sec)	PRESSURE DROP (psi)	APPARENT VISCOSITY (cp)	SHEAR RATE (sec^{-1})	REYNOLDS NUMBER	DEBORAH NUMBER	APPARENT VISCOSITY / STEADY VISCOSITY
0.000361	0.39	30.68	5.27	7.3×10^{-6}	6.3×10^{-4}	0.935
0.000722	0.65	25.72	10.52	1.8×10^{-5}	1.3×10^{-3}	1.0
0.0015	1.06	20.19	21.9	4.6×10^{-5}	2.6×10^{-3}	1.057
0.0025	1.41	16.11	36.4	9.7×10^{-5}	4.3×10^{-3}	1.032
0.0034	1.75	14.70	50	1.4×10^{-4}	5.9×10^{-3}	1.05
0.0074	2.72	10.44	109	4.5×10^{-4}	1.3×10^{-2}	1.1
0.0125	3.8	8.69	182	9×10^{-4}	2.2×10^{-2}	1.207
0.0258	5.94	6.58	376	2.5×10^{-3}	4.5×10^{-2}	1.29
0.0533	8.33	5.0	777	6.7×10^{-3}	9.3×10^{-2}	1.3
0.077	12.2	4.53	1120	1×10^{-2}	1.3×10^{-1}	1.33
0.105	13.9	4.05	1531	1.6×10^{-2}	1.8×10^{-1}	1.32
0.132	17.4	3.77	1920	2.2×10^{-2}	2.3×10^{-1}	
0.16	20	3.57	2334	2.8×10^{-2}	2.7×10^{-1}	
0.216	24.4	3.23	3150	4.2×10^{-2}	3.7×10^{-1}	
0.329	33.2	2.88	4800	7.1×10^{-2}	5.6×10^{-1}	
0.385	37.2	2.76	5600	8.7×10^{-2}	6.6×10^{-1}	
0.447	41.3	2.64	6534	1.1×10^{-1}	7.7×10^{-1}	
0.503	45.2	2.57	7328	1.2×10^{-1}	8.6×10^{-1}	
0.59	51.6	2.50	8611	1.5×10^{-1}	1.0	
0.875	71	2.32	12765	1.7×10^{-1}	1.5	
1.178	91	2.21	17199	3.3×10^{-1}	2.0	
1.455	110	2.16	21236	4.2×10^{-1}	2.5	
2.007	147	2.09	29264	6×10^{-1}	3.4	
2.63	180	1.96	38366	8.4×10^{-1}	4.5	
3.096	210	1.94	45156	1.0	5.3	
3.244	214	1.88	47373	1.1	5.6	
3.714	247	1.90	54141	1.2	6.4	
4.316	275	1.82	63009	1.5	7.4	

Pressure Drop measured between two pressure taps 6" apart,

9/16"x12" stainless steel column.

Solution : 1000 ppm XF in 1% NaCl

TABLE 10

EXPERIMENTAL RESULTS FOR EXP. NO. PF-3c

FLOW RATE (cc/sec)	PRESSURE DROP (psi)	PERMEABILITY (darcy)
0.00194	0.048	3.88
0.00283	0.098	3.72
0.00567	0.18	4.06
0.00867	0.283	3.95
0.028	0.94	3.83
0.0833	2.72	3.95
0.1383	4.53	3.93
0.22	7.2	3.94
0.274	9.07	3.9
0.383	12.2	4.05
0.498	15.7	4.9
1.183	37.2	4.1
2.032	64.6	4.05
2.658	84	4.08

Pressure Drop measured between two pressure taps 6" apart, 9/16"x12" stainless steel column.

Solution : 1% NaCl

TABLE 11

EXPERIMENTAL RESULTS FOR EXP. NO. PF-3d

FLOW RATE (cc/sec)	PRESSURE DROP (psi) ↓ ↓	APPARENT VISCOSITY (cp)	SHEAR RATE (sec^{-1})	REYNOLDS NUMBER
0.000575	0.31/0.17/0.08	8.08	8.4	4.9×10^{-5}
0.00111	0.467/0.26/0.13	6.4	16.3	1.2×10^{-4}
0.0022	0.875/0.45/0.24	5.55	33	2.5×10^{-4}
0.00344	1.24/0.65/0.334	5.17	51	4.2×10^{-4}
0.0047	1.57/0.8/0.42	4.65	69	6.2×10^{-3}
0.00767	2.37/1.19/0.63	4.24	113	1.1×10^{-3}
0.0137	3.65/1.83/1.0	3.66	201	2.3×10^{-3}
0.0265	6.06/3.05/1.74	3.14	390	5.2×10^{-2}
0.0533	9.9/5.26/2.9	2.7	780	1.2×10^{-2}
0.08	13.4/7.28/3.9	2.49	1175	2.0×10^{-2}
0.107	16.8/9/4.4	2.31	1568	2.8×10^{-2}
0.134	20/10.9/5.3	2.22	1974	3.7×10^{-2}
0.214	29.2/15.8/7.5	2.02	3150	6.5×10^{-1}
0.322	40.7/22.1/10.1	1.88	4724	1.1×10^{-1}
0.433	51.5/28.1/12.65	1.77	6370	1.5×10^{-1}
0.6	65/36/16	1.64	8810	2.2×10^{-1}
0.9	93/50/23	1.53	13162	3.4×10^{-1}
1.17	115/60.2/28.8	1.4	17181	4.7×10^{-1}
1.457	140/71/35	1.33	21388	5.9×10^{-1}
2.09	186/92/47	1.20	30719	1.1
2.62	235/114/59.5	1.19	38475	1.3
3.24	280/137/71.3	1.16	47595	1.7
3.5	302/148/77.5	1.16	51414	1.8

Pressure Drops measured across the total length(12"), between two pressure taps(6") and between the inlet and the first pressure tap(3") respectively, 9/16"x12" stainless steel column. The pressure drop measured between two pressure taps 6" apart was used in calculation.

Solution : 500 ppm XF in 1% NaCl

TABLE 12

EXPERIMENTAL RESULTS FOR EXP. NO. PF-3e

FLOW RATE (cc/sec)	PRESSURE DROP (psi)	PERMEABILITY (darcy)
0.000722	0.0265	3.51
0.00144	0.051	3.65
0.00283	0.1	3.65
0.00567	0.21	3.48
0.0137	0.49	3.59
0.0278	0.95	3.77
0.0825	2.87	3.70
0.138	4.8	3.71
0.223	7.7	3.74
0.278	9.1	3.94
0.39	12.8	3.91
0.442	14.7	3.87
0.5	16.6	3.88
0.5683	19.9	3.68
1.17	39.2	3.84
2.08	68.2	3.93
2.345	77.4	3.90
2.61	85.1	3.95

Pressure Drop measured between two pressure taps 6" apart, 9/16"x12" stainless steel column.

Solution : 1% NaCl

TABLE 13

EXPERIMENTAL RESULTS FOR EXP. NO. PF-3f

FLOW RATE (cc/sec)	PRESSURE DROP (psi)	APPARENT VISCOSITY (cp)	SHEAR RATE (sec^{-1})	REYNOLDS NUMBER
0.00044	0.46	25.53	7.0	1.0×10^{-5}
0.00097	0.82	24.8	15.3	2.7×10^{-5}
0.0021	1.29	15.06	33	8.2×10^{-5}
0.0033	1.69	12.5	52	1.6×10^{-4}
0.0045	2.06	11.8	70	2.3×10^{-4}
0.00717	2.7	9.28	112	4.5×10^{-4}
0.0125	3.78	7,45	196	9.7×10^{-4}
0.0263	6.08	5.70	411	2.7×10^{-3}
0.0525	9.47	4.45	821	6.9×10^{-3}
0.08	12	3.70	1252	1.3×10^{-2}
0.107	14.7	3.40	1677	1.8×10^{-2}
0.135	17.3	3.16	2113	2.5×10^{-2}
0.213	24.5	2.83	3337	4.4×10^{-2}
0.273	28.9	2.61	4281	6.1×10^{-2}
0.323	33.2	2.54	5032	7.4×10^{-2}
0.378	37.5	2.45	5908	9.0×10^{-2}
0.433	41.9	2.38	6785	1.1×10^{-1}
0.49	46	2.32	7661	1.2×10^{-1}
0.59	55	2,30	9238	1.5×10^{-1}
0.89	75	2.08	12920	2.5×10^{-1}
1.174	90	1.89	18376	3.6×10^{-1}
1.47	113	1.90	22970	4.5×10^{-1}
2.06	150	1.80	32245	6.7×10^{-1}
2.312	168	1.79	36170	7.5×10^{-1}
2.614	186	1.76	40907	8.6×10^{-1}

Pressure Drop measured between two pressure taps 6" apart.

9/16"x12" stainless steel column.

Solution : 1000 ppm XF in 0.1 % NaCl

TABLE 14

EXPERIMENTAL RESULTS FOR EXP. NO. PF-3g

FLOW RATE (cc/sec)	PRESSURE DROP (psi)	PERMEABILITY (darcy)
0.00069	0.026	3.44
0.00283	0.11	3.32
0.00583	0.23	3.27
0.0137	0.52	3.39
0.0272	1.05	3.34
0.0816	3.1	3.39
0.138	5.2	3.41
0.222	8.3	3.44
0.333	12.3	3.49
0.387	14.2	3.51
0.494	18.2	3.50
0.574	21	3.52
1.155	42.5	3.50
2.04	75.4	3.47
2.35	86	3.52
2.61	95	3.54

Pressure Drop measured between two pressure taps 6" apart, 9/16"x12" stainless steel column.

Solution : 0.1 % NaCl

TABLE 15

EXPERIMENT RESULTS FOR EXP. NO. PF-4b

FLOW RATE (cc/sec)	PRESSURE DROP (psi)	PERMEABILITY (darcy)	SHEAR RATE (sec^{-1})	REYNOLDS NUMBER	P_1 (psi)	P_2 (psi)	P_{Ergun} (psi)	$\frac{P_{Ergun}}{P_1}$	$\frac{\text{Pressure Drop}}{P_{Ergun}}$
0.00147	0.031	6.12	21	$1.2x10^{-3}$	0.031	-	0.031	1	1.0
0.00294	0.064	5.93	41.9	$2.4x10^{-3}$	0.062	-	0.0621	1	1.03
0.006	0.132	5.86	85	$4.8x10^{-3}$	0.127	-	0.127	1	1.043
0.008	0.185	5.6	114	$6.5x10^{-3}$	0.69	-	0.169	1	1.095
0.0139	0.32	5.6	198	$1.1x10^{-2}$	0.293	-	0.293	1	1.092
0.0267	0.615	6.0	380	$2.2x10^{-2}$	0.564	0.00014	0.564	1.00025	1.091
0.0558	1.2	5.97	795	$4.5x10^{-2}$	1.178	0.00062	1.179	1.005	1.018
0.0825	1.78	5.95	1176	$6.7x10^{-2}$	1.742	0.00136	1.743	1.0008	1.021
0.11	2.38	5.99	1567	$8.9x10^{-1}$	2.322	0.0024	2.325	1.001	1.023
0.138	2.98	5.90	1968	$1.1x10^{-1}$	2.917	0.0038	2.921	1.0013	1.019
0.22	4.8	5.91	3144	$1.8x10^{-1}$	4.66	0.0097	4.67	1.002	1.028
0.333	7.26	5.94	4739	$2.7x10^{-1}$	7.02	0.022	7.04	1.003	1.031
0.394	8.5	5.90	5582	$3.2x10^{-1}$	8.27	0.03	8.3	1.0036	1.024
0.444	9.7	5.90	6322	$3.6x10^{-1}$	9.37	0.039	9.41	1.0042	1.031
0.594	12.2	6.27	8452	$4.8x10^{-1}$	12.53	0.07	12.6	1.0056	0.97
0.91	18.4	6.38	12940	$7.3x10^{-1}$	19.17	0.164	19.33	1.0086	0.952
1.19	24	6.38	16927	$9.6x10^{-1}$	25.08	0.28	25.36	1.01	0.946
1.49	30.3	6.32	21165	1.2	31.36	0.439	31.8	1.014	0.953
2.05	42.3	6.24	29184	1.7	43.24	0.835	44.1	1.019	0.96
2.62	54.3	6.21	37272	2.1	55.23	1.362	56.6	1.025	096
3.226	66.8	6.22	46021	2.6	68.2	2.07	70.27	1.03	0.951
3.92	79.8	6.33	55817	3.2	82.7	3.05	85.75	1.037	0.931
4.38	91.4	6.17	62333	3.5	92.36	3.81	96.17	1.041	0.95

Pressure Drop measured between two pressure taps 6" apart,9/16"x12" stainless steel column.

Solution : 1% NaCl

TABLE 16

EXPERIMENTAL RESULTS FOR EXP. NO. PF-4c

FLOW RATE (cc/sec)	PRESSURE DROP (psi)	APPARENT VISCOSITY (cp)	SHEAR RATE (sec^{-1})	REYNOLDS NUMBER
0.00044	0.339	29.3	5.4	$1x10^{-5}$
0.00106	0.565	20.5	12.8	$3.6x10^{-5}$
0.00228	0.86	14.5	27	$1.1x10^{-4}$
0.00342	1.1	12.35	41	$1.9x10^{-4}$
0.00467	1.35	11.1	56	$2.9x10^{-4}$
0.007171	1.75	9.36	87	$5.3x10^{-4}$
0.0123	2.47	7.68	149	$1.1x10^{-3}$
0.025	3.87	5.94	301	$2.9x10^{-3}$
0.0517	6.2	4.6	624	$7.8x10^{-3}$
0.0783	8.2	4.01	947	$1.4x10^{-2}$
0.105	9.9	3.62	1267	$2.0x10^{-2}$
0.132	11.6	3.38	1590	$2.7x10^{-2}$
0.158	13.1	3.19	1901	$3.4x10^{-2}$
0.213	16.3	2.93	2575	$5.1x10^{-2}$
0.318	22.2	2.68	3844	$8.3x10^{-2}$
0.372	25.1	2.59	4501	$1.0x10^{-1}$
0.48	30.7	2.46	5776	$1.4x10^{-1}$
0.312	21.4	2.63	3767	$8.3x10^{-2}$
0.6	35.4	2.26	7244	$1.9x10^{-1}$
0.892	48.9	2.10	10780	$3.0x10^{-1}$
1.17	61.9	2.04	4083	$4.0x10^{-1}$
1.43	74	1.98	17309	$5x10^{-1}$
2.01	100	1.91	24206	$7.3x10^{-1}$
2.65	124	1.79	32030	1.03
3.16	147	1.78	38251	1.24
3.81	174	1.75	45978	1.52
4.41	193	1.72	53184	1.78
4.71	213	1.72	56874	1.91

Pressure Drop measured between tow pressure tap 6" apart,

9/16"x12" stainless steel column.

Solution : 1000 ppm XF in 1% NaCl

TABLE 17

EXPERIMENTAL RESULTS FOR EXP. NO. PF-4d

FLOW RATE (cc/sec)	PRESSURE DROP (psi)	PERMEABILITY (darcy)
0.0015	0.0375	5.15
0.0029	0.07	5.37
0.0058	0.138	5.38
0.0138	0.355	5.02
0.0272	0.674	5.2
0.0817	1.98	5.32
0.137	3.29	5.37
0.22	5.2	5.45
0.33	7.77	5.48
0.385	9.12	5.44

Pressure Drop measured between two pressure taps 6" apart, 9/16"x12" stainless steel column.

Solution : 1% NaCl

TABLE 18

EXPERIMENTAL RESULTS FOR EXP. NO. PF-5a

FLOW RATE (cc/sec)	PRESSURE DROP (psi)	PERMEABILITY (darcy)	SHEAR RATE (sec^{-1})	REYNOLDS NUMBER	P_1 (psi)	P_2 (psi)	P_{Ergun} (psi)	$\frac{P_{Ergun}}{P_1}$	Pressure Drop / P_{Ergun}
0.00072	0.021	4.43	11.9	5.4×10^{-4}	0.019	-	0.019	1	1.1
0.00144	0.042	4.42	24	1.1×10^{-3}	0.038	-	0.038	1	1.0
0.0029	0.081	4.6	47.6	2.2×10^{-3}	0.0758	-	0.0758	1	1.07
0.0043	0.119	4.69	71	3.2×10^{-3}	0.114	-	0.114	1	1.045
0.00583	0.156	4.81	96	4.4×10^{-3}	0.153	-	0.153	1	1.018
0.0083	0.222	4.83	137	6.3×10^{-2}	0.219	-	0.219	1	1.014
0.0138	0.373	4.76	228	1.0×10^{-2}	0.363	-	0.363	1	1.03
0.028	0.759	4.75	463	2.1×10^{-2}	0.737	0.0002	0.737	1.00027	1.03
0.055	1.43	4.95	909	4.1×10^{-2}	1.45	0.0008	1.45	1.0007	0.986
0.0825	2.15	4.94	1364	6.1×10^{-2}	2.17	0.0019	2.175	1.0009	0.99
0.11	2.9	4.89	1818	8.3×10^{-1}	2.9	0.0033	2.903	1.001	0.99
0.14	3.64	4.95	2313	1.1×10^{-1}	3.68	0.0054	3.69	1.0014	0.986
0.223	5.87	4.90	3700	1.7×10^{-1}	5.9	0.014	5.914	1.0024	0.993
0.281	7.45	4.86	4652	2.1×10^{-1}	7.4	0.022	7.43	1.0027	1.003
0.333	8.9	4.82	5498	2.5×10^{-1}	8.76	0.03	8.79	1.0034	1.013
0.444	11.6	4.93	7348	3.3×10^{-1}	11.7	0.054	11.76	1.0046	0.986
0.504	13.15	4.93	8326	3.8×10^{-1}	13.26	0.07	13.33	1.0053	0.987
0.59	15.3	4.96	9726	4.4×10^{-1}	15.5	0.095	15.6	1.0061	0.981
0.9	24	4.90	14907	6.8×10^{-1}	23.75	0.223	23.97	1.0093	1.001
1.17	30.7	4.91	19294	8.8×10^{-1}	30.74	0.373	31.11	1.012	0.987
1.476	38.1	4.99	24395	1.1	38.87	0.6	39.47	1.015	0.965
2.083	53.85	4.98	34360	1.6	54.74	1.183	55.92	1.022	0.963
2.666	69.1	4.97	44139	2.0	70.3	1.95	72.27	1.028	0.956
3.215	84.9	4.88	53125	2.4	84.64	2.83	87.47	1.033	0.971
3.475	92.6	4.83	57407	2.6	91.46	3.3	94.76	1.036	0.977

Pressure Drop measured between two pressure taps 6" apart, 9/16"x12" stainless steel column.

Solution : 1% NaCl

TABLE 19

EXPERIMENTAL RESULTS FOR EXP. NO. PF-5b

FLOW RATE (cc/sec)	PRESSURE DROP (psi)	APPARENT VISCOSITY (cp)	SHEAR RATE (sec^{-1})	REYNOLDS NUMBER	DEBORAH NUMBER	APPARENT VISCOSITY / STEADY VISCOSITY
0.0006	0.162	8.16	8.4	4.7×10^{-5}	1.0×10^{-3}	1.02
0.00128	0.302	7.14	18	1.2×10^{-4}	2.1×10^{-3}	1.0
0.0026	0.538	6.28	36	2.7×10^{-4}	4.4×10^{-3}	0.98
0.004	0.783	5.91	56	4.4×10^{-4}	6.7×10^{-3}	1.0
0.0053	0.99	5.61	74	6.1×10^{-4}	9.0×10^{-3}	1.0
0.008	1.47	5.55	111	9.3×10^{-3}	1.3×10^{-2}	1.028
0.0133	2.59	5.87	186	1.5×10^{-3}	2.2×10^{-2}	1.236
0.0253	6.3	7.52	352	2.2×10^{-3}	4.2×10^{-2}	1.77
0.0478	19	12.02	666	2.6×10^{-3}	8.0×10^{-2}	3.08
0.0702	38.1	16.4	978	2.8×10^{-3}	1.2×10^{-1}	4.55
0.0883	58.5	20	1230	2.8×10^{-3}	1.5×10^{-1}	5.71
0.106	80.8	23.03	1476	3.0×10^{-3}	1.8×10^{-1}	6.77
0.12	97	24.4	1671	3.2×10^{-3}	2.0×10^{-1}	7.29
0.1267	105	25	1764	3.3×10^{-3}	2.1×10^{-1}	7.59
0.135	119	26.6	1880	3.3×10^{-3}	2.3×10^{-1}	8.14
0.148	139	28.3	2065	3.4×10^{-3}	2.3×10^{-1}	8.8
0.16	160	30.21	2228	3.4×10^{-3}	2.5×10^{-1}	9.47
0.162	155	28.91	2255	3.6×10^{-3}	2.7×10^{-1}	9.09
0.173	180	31.52	2401	3.5×10^{-3}	$2.9\times1-^{-1}$	10.1
0.189	195	31.17	2631	3.9×10^{-3}	3.2×10^{-1}	10.1
0.194	217	33.72	2707	3.7×10^{-3}	3.3×10^{-1}	10.91
0.203	235	35.01	2825	3.7×10^{-3}	3.4×10^{-1}	11.52
0.227	272	36.25	3157	4.0×10^{-3}	3.8×10^{-1}	12.08

Pressure Drop measured between two pressure taps 6" apart, 9/16" x 12" stainless steel column.

Solution : 1000 ppm Pusher 700 in 1% NaCl

TABLE 20

EXPERIMENTAL RESULTS FOR EXP. NO. PF.5c

FLOW RATE (cc/sec)	PRESSURE DROP (psi)	PERMEABILITY (darcy)
0.00144	0.051	3.65
0.00283	0.088	4.15
0.00583	0.17	4.42
0.0133	0.396	4.33
0.0278	0.85	4.21
0.0833	2.49	4.31
0.138	4.2	4.24
0.22	6.87	4.13
0.277	8.7	4.11
0.331	10.2	4.19
0.389	11.9	4.21

Pressure Drop measured between two pressure taps 6" apart, 9/16"x12" stainless steel column.

Solution : 1% NaCl

TABLE 21

EXPERIMENTAL RESULTS FOR EXP. NO. PF-6a

FLOW RATE (cc/sec)	PRESSURE DROP (psi)	PERMEABILITY (darcy)	SHEAR RATE (sec^{-1})	REYNOLDS NUMBER	P_1 (psi)	P_2 (psi)	P_{Ergun} (psi)	$\frac{P_{Ergun}}{P_1}$	$\frac{\text{Pressure Drop}}{P_{Ergun}}$
0.00144	0.045	4.12	26	9.8×10^{-4}	0.0446	-	0.0448	1	1.0
0.0029	0.09	4.12	51	2×10^{-3}	0.0895	-	0.0895	1	1.001
0.006	0.185	4.15	107	4.1×10^{-3}	0.187	-	0.187	1	0.99
0.0083	0.27	4.08	148	5.7×10^{-3}	0.259	-	0.259	1	1.04
0.0142	0.44	4.16	251	9.7×10^{-2}	0.44	-	0.44	1	1.0
0.0283	0.87	4.19	503	1.9×10^{-2}	0.881	0.0002	0.8812	1.0002	0.985
0.0554	1.7	4.20	983	3.8×10^{-2}	1.72	0.0008	1.72	1.0004	0.988
0.0842	2.6	4.17	1495	5.8×10^{-2}	2.62	0.00175	2.622	1.0007	0.992
0.11	3.46	4.10	1961	7.5×10^{-2}	3.43	0.003	3.433	1.0009	1.008
0.139	4.36	4.12	2472	9.5×10^{-2}	4.33	0.0048	4.333	1.001	1.004
0.168	5.27	4.09	2983	1.2×10^{-1}	5.24	0.007	5.231	1.0013	1.0075
0.223	7.05	4.08	3978	1.5×10^{-1}	6.9	0.0124	6.98	1.0018	1.0097
0.28	8.9	4.04	4944	1.9×10^{-1}	8.66	0.019	8.68	1.0022	1.025
0.387	12.2	4.09	6876	2.6×10^{-1}	12	0.037	12.08	1.0031	1.01
0.504	15.8	4.11	8959	3.4×10^{-1}	15.7	0.063	15.76	1.004	1.0023
0.15	4.6	4.21	2671	1.0×10^{-1}	4.68	0.0056	4.69	1.0012	0.982
0.3	9.2	4.18	5313	2.0×10^{-1}	9.3	0.0222	9.32	1.0024	0.987
0.558	18.2	4.16	10456	4.1×10^{-1}	18.3	0.086	18.39	1.0047	0.99
0.878	27.5	4.12	15599	6.0×10^{-1}	27.3	0.19	27.5	1.007	1.0004
1.19	36.6	4.18	21111	8.0×10^{-1}	37	0.35	37.32	1.0095	0.981
1.474	45.5	4.17	26169	1.01	45.82	0.538	46.36	1.012	0.982

Pressure Drop measured between two pressure taps 6" apart, 9/16"x12" stainless steel column.

Solution : 1% NaCl

TABLE 22

EXPERIMENTAL RESULTS FOR EXP. NO. PF-6b

FLOW RATE (cc/sec)	PRESSURE DROP (psi)	APPARENT VISCOSITY (cp)	SHEAR RATE (sec^{-1})	REYNOLDS NUMBER
0.00072	0.071	2.65	10.5	1.6×10^{-4}
0.00136	0.132	2.60	20	3.1×10^{-4}
0.00267	0.247	2.48	39	6.4×10^{-4}
0.00408	0.374	2.45	59	1×10^{-3}
0.0055	0.49	2.39	80	1.4×10^{-3}
0.008	0.7	2.34	117	2×10^{-3}
0.0135	1.26	2.50	197	3.2×10^{-3}
0.027	2.94	2.92	394	$55. \times 10^{-3}$
0.0516	8,86	4.6	753	6.7×10^{-3}
0.0754	16.4	5.83	1098	7.7×10^{-3}
0.1	27.7	7.42	1456	8.1×10^{-3}
0.1217	41	9.02	1773	8.1×10^{-3}
0.1367	48	9.40	1990	8.7×10^{-3}
0.187	82.7	11.84	2724	9.4×10^{-3}
~~0.56~~ 0.2554	~~104~~ 140	14.67	3728	1×10^{-2}
0.313	193	16.52	4556	1.1×10^{-2}
0.388	270	18.62	5656	1.3×10^{-2}
0.426	316	19.9	6203	1.3×10^{-2}
0.456	351	20.64	6634	1.3×10^{-2}

Pressure Drop measured between two pressure taps 6" apart, 9/16"x12" stainless steel column.

Solution : 500 ppm Pusher 700 in 1% NaCl

TABLE 23

EXPERIMENTAL RESULTS FOR EXP. NO. PF-6c

FLOW RATE (cc/sec)	PRESSURE DROP (psi)	PERMEABILITY (darcy)
0.0825	2.8	3.8
0.137	4.74	3.71
0.22	7.7	3.68
0.333	11.3	3.80
0.392	13.3	3.79
0.494	17.1	3.72

Pressure Drop measured between two pressure taps 6" apart, 9/16"x12" stainless steel column.

Solution : 1% NaCl

TABLE 24

EXPERIMENTAL RESULTS FOR EXP. NO. PF-6d

FLOW RATE (cc/sec)	PRESSURE DROP (psi)	APPARENT VISCOSITY (cp)	SHEAR RATE (sec^{-1})	REYNOLDS NUMBER	DEBORAH NUMBER	APPARENT VISCOSITY / STEADY VISCOSITY
0.00039	0.5	33.05	5.9	6.9×10^{-6}	3.8×10^{-3}	0.93
0.00081	0.83	26.48	12.1	1.8×10^{-5}	7.8×10^{-3}	0.93
0.00169	1.54	23.27	26	4.3×10^{-5}	1.7×10^{-2}	1.07
0.00251	2.3	23.52	38	6.3×10^{-5}	2.5×10^{-2}	1.27
0.00354	3.12	22.66	53	9×10^{-5}	3.4×10^{-2}	1.36
0.00633	4.79	149.46	97	1.9×10^{-4}	6.3×10^{-2}	1.48
0.0103	8.4	20.9	156	2.9×10^{-4}	1.0×10^{-1}	1.90
0.0203	16.9	21.37	306	5.6×10^{-4}	2.0×10^{-1}	2.55
0.0394	37.3	24.32	596	9.5×10^{-4}	3.9×10^{-1}	3.77
0.0481	47.7	25.47	724	1.1×10^{-3}	10.7×10^{-1}	4.29
0.0725	81	28.73	1093	1.5×10^{-3}	7.1×10^{-1}	5.63
0.095	115	31.12	1433	1.8×10^{-3}	9.3×10^{-1}	6.76
0.115	147.5	32.98	1734	2.0×10^{-3}	1.1	7.67
0.153	214	36.08	2300	2.5×10^{-3}	1.5	9.38
0.173	253	37.45	2612	2.7×10^{-3}	1.7	10.42
0.213	331	39.89	3215	3.1×10^{-3}	2.1	11.9

Pressure Drop measured between two pressure taps 6" apart, 9/16"x12" stainless steel column.

Solution : 1000 ppm Pusher 700 in 0.1% NaCl

TABLE 25

EXPERIMENTAL RESULTS FOR EXP. NO. PF-6e

FLOW RATE (cc/sec)	PRESSURE DROP (psi)	PERMEABILITY (darcy)
0.028	0.926	3.70
0.082	2.89	3.64
0.138	4.9	3.64
0.22	8.04	3.52
0.333	11.8	3.64
0.386	13.8	3.60
0.497	17.9	3.58

Pressure Drop measured between two pressure taps 6" apart, 9/16"x12" stainless steel column.

Solution : 0.1% NaCl

TABLE 26

EXPERIMENTAL RESULTS FOR EXP. NO. PF-7a

FLOW RATE (cc/sec)	PRESSURE DROP (psi)	PERMEABILITY (darcy)	SHEAR RATE (sec^{-1})	REYNOLDS NUMBER	P_1 (psi)	P_2 (psi)	P_{Ergun} (psi)	$\frac{P_{Ergun}}{P_1}$	Pressure Drop $\frac{}{P_{Ergun}}$
0.00783	0.025	44.4	47	0.017	0.026	-	0.026	1	0.961
0.014	0.046	39.2	83	0.03	0.0464	-	0.0464	1	0.99
0.028	0.095	37.9	166	0.06	0.093	-	0.093	1	1.02
0.0564	0.19	38.4	334	0.12	0.187	0.0003	0.1873	1.0014	1.016
0.0833	0.275	39.1	494	0.18	0.276	0.0006	0.2766	1.002	0.99
0.113	0.38	38.4	672	0.24	0.376	0.0011	0.377	1.0027	1.01
0.141	0.48	38.7	834	0.3	0.467	0.0016	0.4686	1.0034	1.01
0.222	0.74	38.6	1318	0.48	0.738	0.0041	0.742	1.0056	0.99
0.316	1.04	39.1	1868	0.67	1.05	0.0082	1.053	1.0077	0.988
0.603	1.98	39.2	3574	1.3	2.0	0.03	2.03	1.015	0.975
0.908	2.98	39.3	5380	1.9	3.01	0.0682	3.08	1.023	0.968
1.19	3.9	39.3	7044	2.5	3.94	0.117	4.057	1.03	0.961
1.5	4.93	39.2	8888	3.2	4.97	0.186	5.156	1.037	0.956
2.083	6.9	38.9	12324	4.5	6.89	0.358	7.248	1.052	0.952
2.67	9.0	38.2	15808	5.7	8.85	0.59	9.44	1.067	0.953
3.2	10.8	38.2	18960	6.9	10.6	0.85	11.45	1.08	0.943
3.94	13	39	23345	8.4	13.1	1.285	14.36	1.099	0.905
4.47	15	38.4	26449	9.6	14.8	1.65	16.45	1.11	0.912
4.99	17.4	37	29568	10.7	16.6	2.06	18.6	1.124	0.935

Pressure Drop measured between two pressure taps 6" apart, 9/16"x12" stainless steel column.

Solution : 1% NaCl

TABLE 27

EXPERIMENTAL RESULTS FOR EXP. NO. PF-7b

FLOW RATE (cc/sec)	PRESSURE DROP (psi) ↓ ↓	APPARENT VISCOSITY (cp)	SHEAR RATE (sec^{-1})	REYNOLDS NUMBER	DEBORAH NUMBER	APPARENT VISCOSITY / STEADY VISCOSITY
0.00078	0.05/0.024	8.35	3.7	1.7×10^{-4}	4.4×10^{-4}	1.0
0.00147	0.09/0.044	8.09	6.9	3.2×10^{-4}	8.3×10^{-3}	1.011
0.0029	0.17/0.084	7.87	13.5	7.1×10^{-3}	1.6×10^{-3}	1.056
0.00425	0.24/0.119	7.58	20	1.1×10^{-3}	2.4×10^{-3}	1.057
0.00583	0.30/0.153	7.1	28	1.6×10^{-3}	3.3×10^{-3}	1.044
0.00817	0.45/0.21	6.96	38	2.3×10^{-3}	4.6×10^{-3}	1.088
0.0138	0.67/0.33	6.46	65	4.2×10^{-3}	7.8×10^{-2}	1.11
0.0273	1.21/0.6	5.94	128	8.9×10^{-2}	1.5×10^{-2}	1.13
0.0557	2.31/1.13	5.49	262	2.0×10^{-2}	3.1×10^{-2}	1.25
0.0818	3.9/1.94	6.42	385	2.5×10^{-2}	4.6×10^{-2}	1.51
0.112	6.05/3	7.27	527	3.0×10^{-2}	6.3×10^{-2}	1.86
0.137	8.72/4.34	8.59	642	3.1×10^{-2}	7.7×10^{-2}	2.23
0.138	9.8/4.9	9.65	647	2.8×10^{-2}	7.7×10^{-2}	2.51
0.167	13.6/6.9	11.2	782	2.9×10^{-2}	9.4×10^{-1}	3.0
0.217	22/11	13.74	1019	3.1×10^{-2}	1.2×10^{-1}	3.82
0.272	32/16	15.94	1279	3.3×10^{-2}	1.5×10^{-1}	4.55
0.32	42.4/21.2	17.93	1505	3.5×10^{-2}	1.8×10^{-1}	5.26
0.296	36/18	16.46	1392	3.5×10^{-2}	1.7×10^{-1}	5.00
0.444	69.3/34.6	21.1	2084	4.1×10^{-2}	2.5×10^{-1}	6.6
0.731	148/74	27.4	3438	5.1×10^{-2}	4.1×10^{-1}	9.29
0.872	188/94	29.3	4100	5.8×10^{-2}	4.9×10^{-1}	10.25
1.022	234/117	31	4807	6.4×10^{-2}	5.7×10^{-1}	11.27
1.195	280/140	31.71	5620	7.3×10^{-2}	6.7×10^{-1}	11.74
1.284	324/162	34.2	6034	7.3×10^{-2}	7.2×10^{-1}	12.7
1.458	375/187.5	34.8	6854	8.2×10^{-2}	8.1×10^{-1}	13.23
1.503	408/204	36.73	7072	8.0×10^{-2}	8.4×10^{-1}	14.13
1.724	458/229	35.95	8110	9.3×10^{-2}	9.4×10^{-1}	14.1
1.85	500/250	36.58	8697	9.8×10^{-2}	1.04	14.5
1.933	534/267	37.4	9088	1.0×10^{-1}	1.09	15.1

Pressure Drops measured across the total length(12") and two pressure taps 6" apart. The latter was used in calculation, 9/16 "x12" stainless steel column.

Solution : 1000 ppm Pusher 700 in 1% NaCl

TABLE 28

EXPERIMENTAL RESULTS FOR EXP. NO. PF-7c

FLOW RATE (cc/sec)	PRESSURE DROP (psi)	PERMEABILITY (darcy)
0.0273	0.109	39.12
0.0558	0.19	37.85
0.083	0.29	3.70
0.141	0.49	3.70
0.225	0.782	37.1
0.339	1.15	37.96
0.394	1.33	38.2
0.511	1.7	38.73

Pressure Drop measured between two pressure taps 6" apart, 9/16"x12" stainless steel column,

Solution : 1% NaCl

TABLE 29

EXPERIMENTAL DATA FOR EXP. NO. PF-8a

FLOW RATE (cc/sec)	PRESSURE DROP (psi)	PERMEABILITY (darcy)	SHEAR RATE (sec^{-1})	REYNOLDS NUMBER	P_1 (psi)	P_2 (psi)	P_{Ergun} (psi)	$\frac{P_{Ergun}}{P_1}$	Pressure Drop / P_{Ergun}
0.394	0.916	37.0	2264	0.79	0.892	0.0082	0.90	1.009	1.018
0.501	1.15	37.4	2881	1.01	1.134	0.0133	1.147	1.01	1.003
0.508	1.17	37.3	2927	1.02	1.152	0.0137	1.166	1.012	1.003
0.442	1.0	37.9	2540	0.89	1.0	0.01	1.01	1.01	0.99
0.575	1.35	36.6	3304	1.16	1.3	0.0175	1.318	1.014	1.024
0.897	2.0	38.5	5163	1.81	2.03	0.0428	2.07	1.02	0.97
1.184	2.73	37.3	6810	2.38	2.68	0.0745	2.76	1.03	0.99
1.484	3.44	37.0	8541	2.99	3.36	0.117	3.48	1.036	0.99
2.07	4.91	36.2	11910	4.16	4.69	0.228	4.92	1.05	1.0
2.68	6.4	35.9	15416	5.39	6.07	0.382	6.45	1.06	0.99
3.25	7.94	35.2	18720	6.55	7.37	0.563	7.93	1.076	1.0
3.83	9.5	34.6	21996	7.69	8.66	0.777	9.44	1.09	1.01
3.84	9.0	36.6	22088	7.72	8.70	0.783	9.48	1.09	0.95
4.41	10.4	36.5	25392	8.88	10.0	1.035	11.0	1.10	0.95

Pressure Drop measured across the total length, 9/16"x4" stainless steel column.

Solution : 1% NaCl

TABLE 30

EXPERIMENTAL DATA FOR EXP. NO. PF-8b

FLOW RATE (cc/sec)	PRESSURE DROP (psi)	APPARENT VISCOSITY (cp)	SHEAR RATE (sec^{-1})	REYNOLDS NUMBER
0.0561	0.85	6.05	254	0.017
0.085	1.55	7.28	384	0.022
0.143	3.58	9.97	648	0.027
0.23	7.5	10.0	1039	0.033
0.2867	10.3	14.3	1296	0.037
0.433	20.6	19	1957	0.042
0.585	30	20.5	2644	0.053
0.75	41	21.9	3385	0.063
0.884	52.8	23.8	3995	0.069
1.193	79.1	26.5	5391	0.083
1.29	92	28.5	5829	0.084
1.453	106.5	29.3	6566	0.092
1.725	136	31.5	7795	0.10
2.04	165	32.3	9218	0.12
2.26	194.5	34.4	10200	0.121
2.65	225	33.8	12000	0.15
2.92	262	35.9	13177	0.15
3.19	295	36.9	14415	0.16
3.48	326	37.4	15700	0.17
3.76	355	37.7	16990	0.18
4.03	384	38	18193	0.20
4.27	410	38.3	19290	0.21
4.45	429	38.5	20100	0.214

Pressure Drop measured across the total length, 9/16"x4" stainless steel column.

Solution : 1000 ppm Pusher 700 in 1% NaCl

TABLE 31

EXPERIMENTAL RESULTS FOR EXP. NO. PF-8c

FLOW RATE (cc/sec)	PRESSURE DROP (psi)	PERMEABILITY (darcy)
0.289	0.67	
0.431	1.01	35.65
0.596	1.35	37.8
1.196	2.73	37.6
1.447	3.4	36.6

Pressure Drop measured across the total length, 9/16"x4" stainless steel column.

Solution : 1% NaCl

TABLE 32

EXPERIMENTAL RESULTS FOR EXP. NO. PF-8d

FLOW RATE (cc/sec)	PRESSURE DROP (psi)	APPARENT VISCOSITY (cp)	SHEAR RATE (sec^{-1})	REYNOLDS NUMBER
0.00278	0.05	6.9	16.4	7.3×10^{-4}
0.0055	0.09	6.3	32	1.6×10^{-3}
0.008	0.127	6.1	47	2.4×10^{-3}
0.0138	0.196	5.43	81	4.6×10^{-3}
0.0276	0.329	4.56	163	1.1×10^{-2}
0.055	0.576	4.01	324	2.5×10^{-2}
0.0833	0.819	3.76	490	4.0×10^{-2}
0.14	1.31	3.58	824	7.0×10^{-2}
0.223	2.1	3.6	1314	1.1×10^{-1}
0.28	2.67	3.65	1648	1.4×10^{-1}
0.334	3.25	3.72	1966	1.6×10^{-1}
0.42	4.185	3.81	2472	2.0×10^{-1}
0.438	4.8	4.19	2578	1.9×10^{-1}
0.596	6.6	4.24	3502	2.5×10^{-1}
0.877	10.3	4.49	5162	3.5×10^{-1}
1.12	14.8	5.05	6592	4.0×10^{-1}
1.426	19.8	5.31	8393	4.8×10^{-1}
1.742	25.2	5.53	10253	5.7×10^{-1}
2.014	30.8	5.85	11854	6.2×10^{-1}
2.264	36.4	6.15	13326	6.6×10^{-1}
2.524	42.4	6.42	14856	7.1×10^{-1}
2.8	48	6.56	16480	7.7×10^{-1}
3.04	54	6.79	17893	8.1×10^{-1}
3.24	59.7	7.05	19070	8.3×10^{-1}
3.537	65.5	7.08	20819	9.0×10^{-1}
3.71	70.6	7.28	21837	9.2×10^{-1}
3.87	75.2	7.43	22780	9.4×10^{-1}
5.157	118	8.75	30354	1.06

Pressure Drop measured across the total length, 9/16 " x 4" stainless steel column.

Solution : 500 ppm Water Cut 110 in fresh water

TABLE 33

EXPERIMENTAL RESULTS FOR EXP. NO. PF-8e

FLOW RATE (cc/sec)	PRESSURE DROP (psi)	PERMEABILITY (darcy)
0.293	0.7	35.9
0.436	1.05	35.7
0.581	1.4	35.6
0.87	2.1	34.6
1.183	2.84	34.8
1.483	3.6	34.4

Pressure Drop measured across the total length, 9/16"x4" stainless steel column.

Solution : fresh water

TABLE 34

EXPERIMENTAL RESULTS FOR EXP. NO. PF-8f

FLOW RATE (cc/sec)	PRESSURE DROP (psi)	APPARENT VISCOSITY (cp)	SHEAR RATE (sec^{-1})	REYNOLDS NUMBER
0.00067	0.007	3.97	3.1	3.0×10^{-4}
0.00139	0.014	3.83	6.4	6.5×10^{-4}
0.0028	0.03	4.0	13	1.3×10^{-3}
0.0055	0.058	4.0	25	2.5×10^{-3}
0.0081	0.08	3.75	37	3.9×10^{-3}
0.0138	0.134	3.69	64	6.7×10^{-3}
0.028	0.23	3.12	129	1.6×10^{-2}
0.0563	0.415	2.80	260	3.6×10^{-2}
0.0833	0.59	2.70	384	5.6×10^{-2}
0.14	0.92	2.50	645	1.0×10^{-1}
0.298	1.76	2.24	1374	2.4×10^{-1}
0.591	3.4	2.19	2725	4.9×10^{-1}
0.9	5.03	2.12	4149	7.6×10^{-1}
1.466	8.44	2.19	6758	1.2
2.04	11.8	2.20	9404	1.7
2.61	15.2	2.21	12032	2.1
3.07	18.9	2.34	14153	2.4
3.64	22.4	2.34	16780	2.8
4.2	26	2.35	19362	3.2
4.55	29	2.42	20976	3.4
4.69	30.2	2.45	21621	3.5

Pressure Drop measured across the total length, 9/16" x 4" stainless steel column.

Solution : 500 ppm Water Cut 110 in fresh water, solution had been heated and cooled down before injected.

TABLE 35

EXPERIMENTAL RESULTS FOR EXP. NO. PF-8g

FLOW RATE (cc/sec)	PRESSURE DROP (psi)	PERMEABILITY (darcy)
0.29	0.7	35.6
0.432	1.04	35.6
0.576	1.384	35.7
0.855	2.08	35.3
1.152	2.79	35.5
1.419	3.52	34.6

Pressure Drop measured across the total length, 9/16"x4" stainless steel column.

Solution : fresh water

TABLE 36

EXPERIMENTAL RESULTS FOR EXP. NO. PF-8h

FLOW RATE (cc/sec)	PRESSURE DROP (psi)	APPARENT VISCOSITY (cp)	SHEAR RATE (sec^{-1})	REYNOLDS NUMBER
0.0013	0.0058	1.67	7.7	1.4×10^{-3}
0.00272	0.01	1.37	16.2	3.5×10^{-3}
0.0057	0.019	1.25	34	8.1×10^{-3}
0.00817	0.028	1.29	49	1.1×10^{-2}
0.014	0.046	1.23	83	2.0×10^{-2}
0.0278	0.089	1.20	165	4.1×10^{-2}
0.0554	0.169	1.14	329	8.6×10^{-2}
0.148	0.48	1.22	880	2.2×10^{-1}
0.299	0.91	1.14	1777	4.7×10^{-1}
0.449	1.35	1.13	2669	7.1×10^{-1}
0.594	1.82	1.15	3530	9.2×10^{-1}
0.9	2.8	1.17	5350	1.4
1.18	3.98	1.26	7014	1.7
1.483	5.45	1.39	8756	1.9
2.06	9.45	1.72	12245	2.1
2.574	14	2.04	15300	2.2
3.131	19.5	2.34	18610	2.4
3.61	24.7	2.57	21460	2.5
4.185	30	2.69	24875	2.8
4.56	34.1	2.80	27100	2.9
4.71	36	2.87	28000	2.9

Pressure Drop measured across the total length, 9/16 " x 4" stainless steel column.

Solution : 500 ppm Water Cut 160 in fresh water

TABLE 37

EXPERIMENTAL RESULTS FOR EXP. NO. PF-8i

FLOW RATE (cc/sec)	PRESSURE DROP (psi)	PERMEABILITY (darcy)
0.086	0.22	33.6
0/148	0.552	36.1
0.292	0.72	34.8
0.58	1.44	34.6
0.90	2.15	3.6
1.164	2,85	35.1
1.453	3.6	34.7

Pressure Drop measured across the total length, 9/16"x4" stainless steel column.

Solution : fresh water

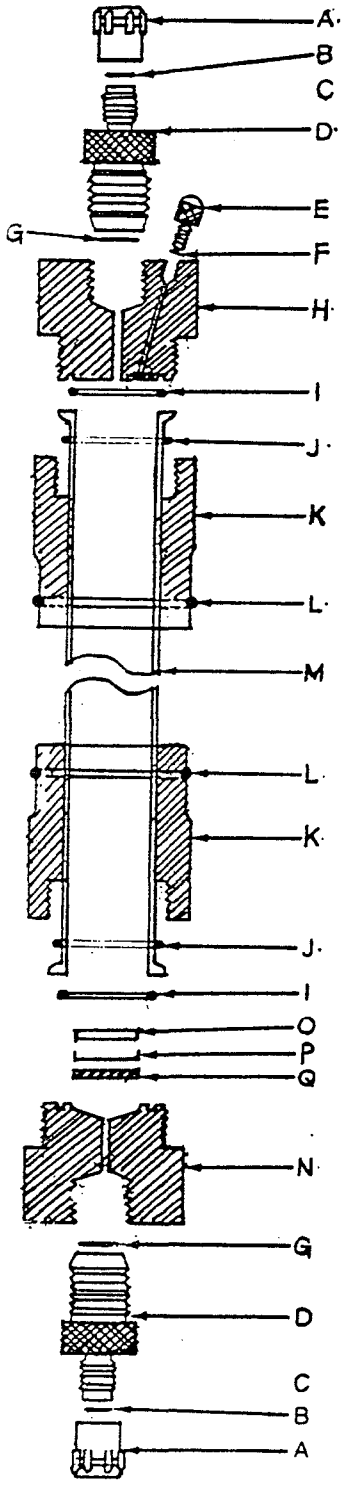

A Multifit Nut
B Multifit O Ring
C Ferrule
D Multifut Tubing Connector
E Vent Plug
F Vent Plug O Ring
H Upper End Plate
I Face Seal O Ring
J Collar Compression O Ring
K Collar
L Water Jacket O Ring
M Heavy Wall Borosilicate Glass Column
L Water Jacket O Ring
K Collar
J Collar Compression O Ring
I Face Seal O Ring
O Retainer Ring
P Fine Mesh Cloth Support
Q Support Grid
N Lower End Plate
G Fitting Seal O Ring
D Multifit Tubing Connector
C Ferrule
B Multifit O Ring
A Multifit Nut

FIGURE 1: Details of Construction of the First Type Column

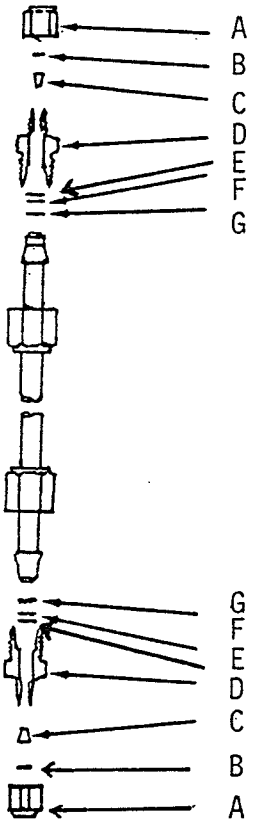

A Nut, 1/8"
B Back Ferrule, 1/8"
C Front Ferrule, 1/8"
D Zero Dead Volume End Piece
E Support Grid
F Screen, 10 micron
G Snap Ring

FIGURE 2: Details of Construction of the Second Type Column

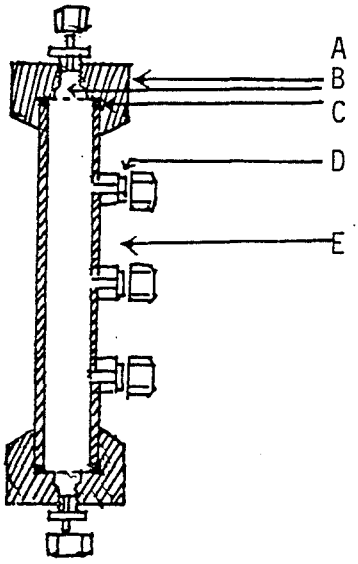

A Upper End Cap
B Tapered Void Space
C O Ring, Support Grid, 10 µm Screen
D Screen, 74 micron
E Packed Column

FIGURE 3: Details of Construction of the Third Type Column

A Reservoir of Metering Fluid (Mineral Oil)

B Zenith Metering Unit

C Reservoir of Injected Fluid

D Porous Flow Test Cell

E Validyne Pressure Transducer

F Carrier Demodulator

G Chart Recorder

H Sample Collector

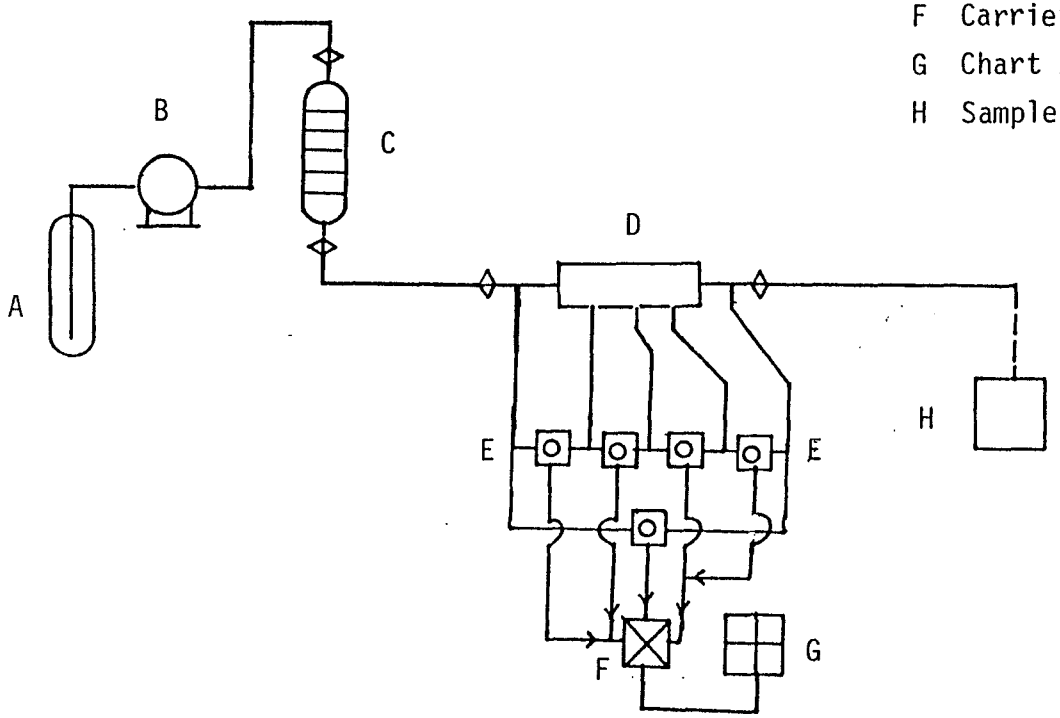

FIGURE 4: Schematic Diagram of Packed Bed Flow System

FIGURE 5
EXPT PF-1B

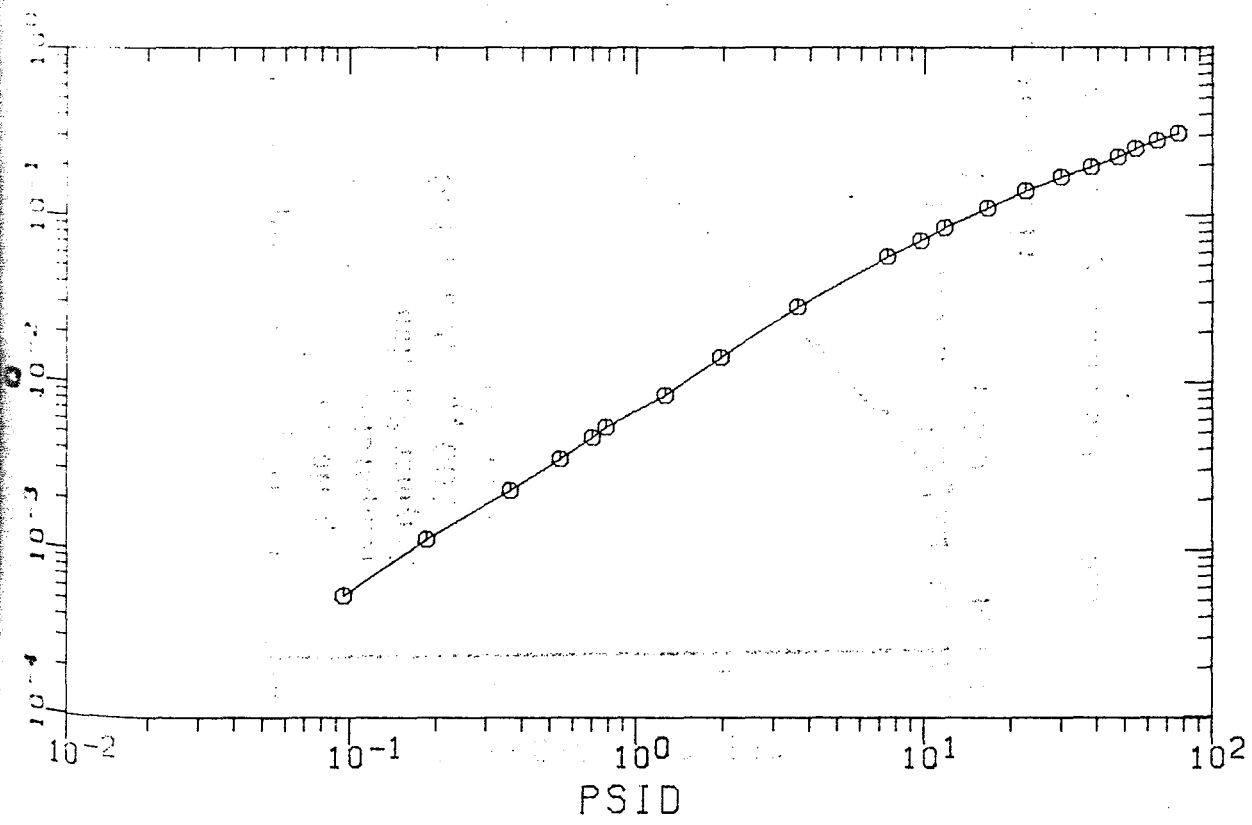

FIGURE 6
EXPT PF-1B

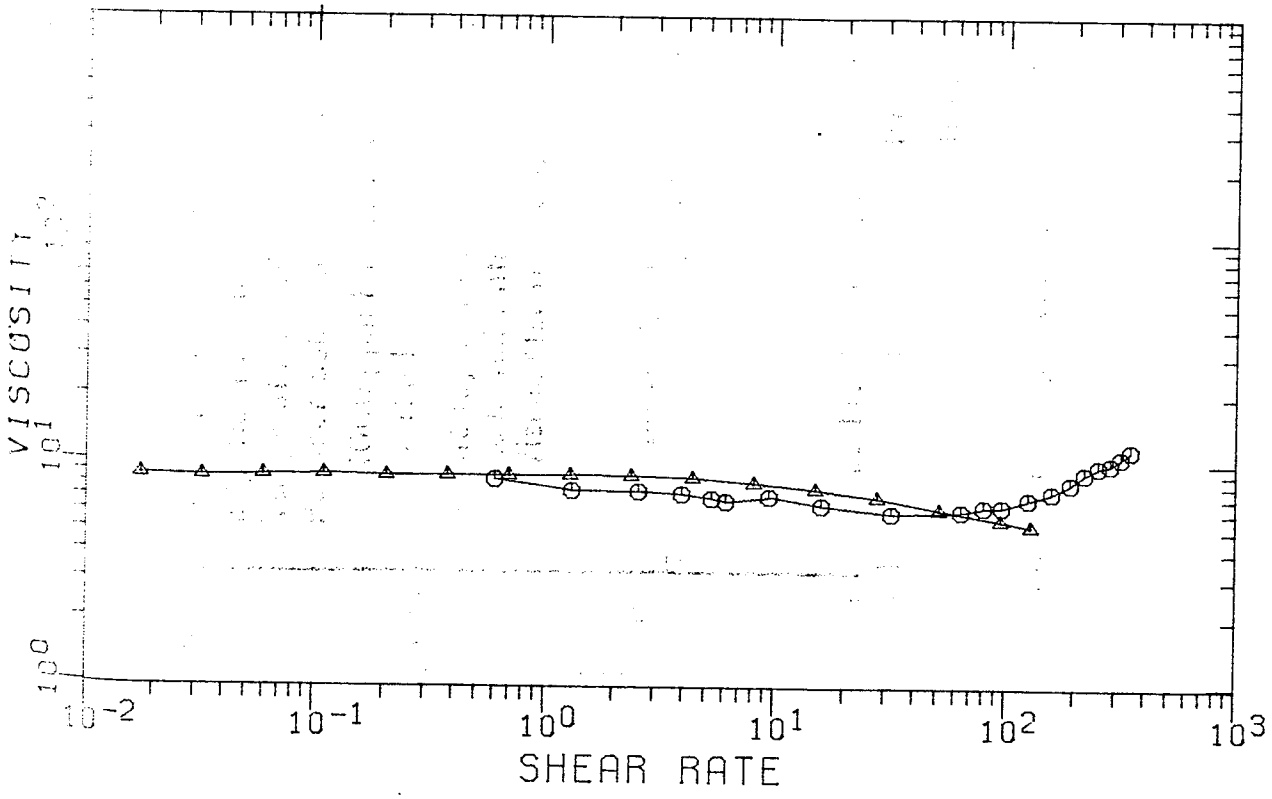

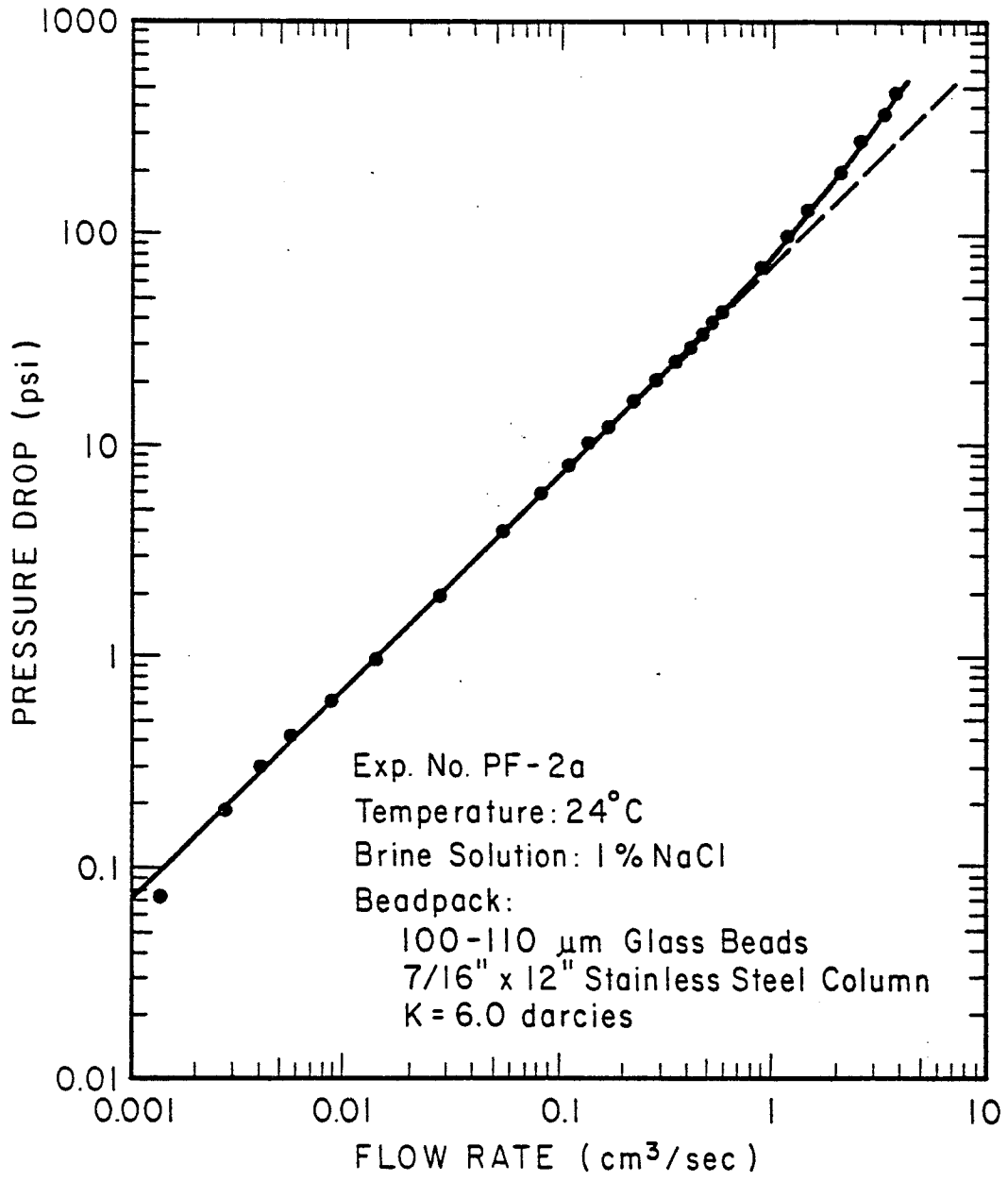

FIGURE 7. Pressure Drop - Flow Rate Data for Brine Solution in Beadpack

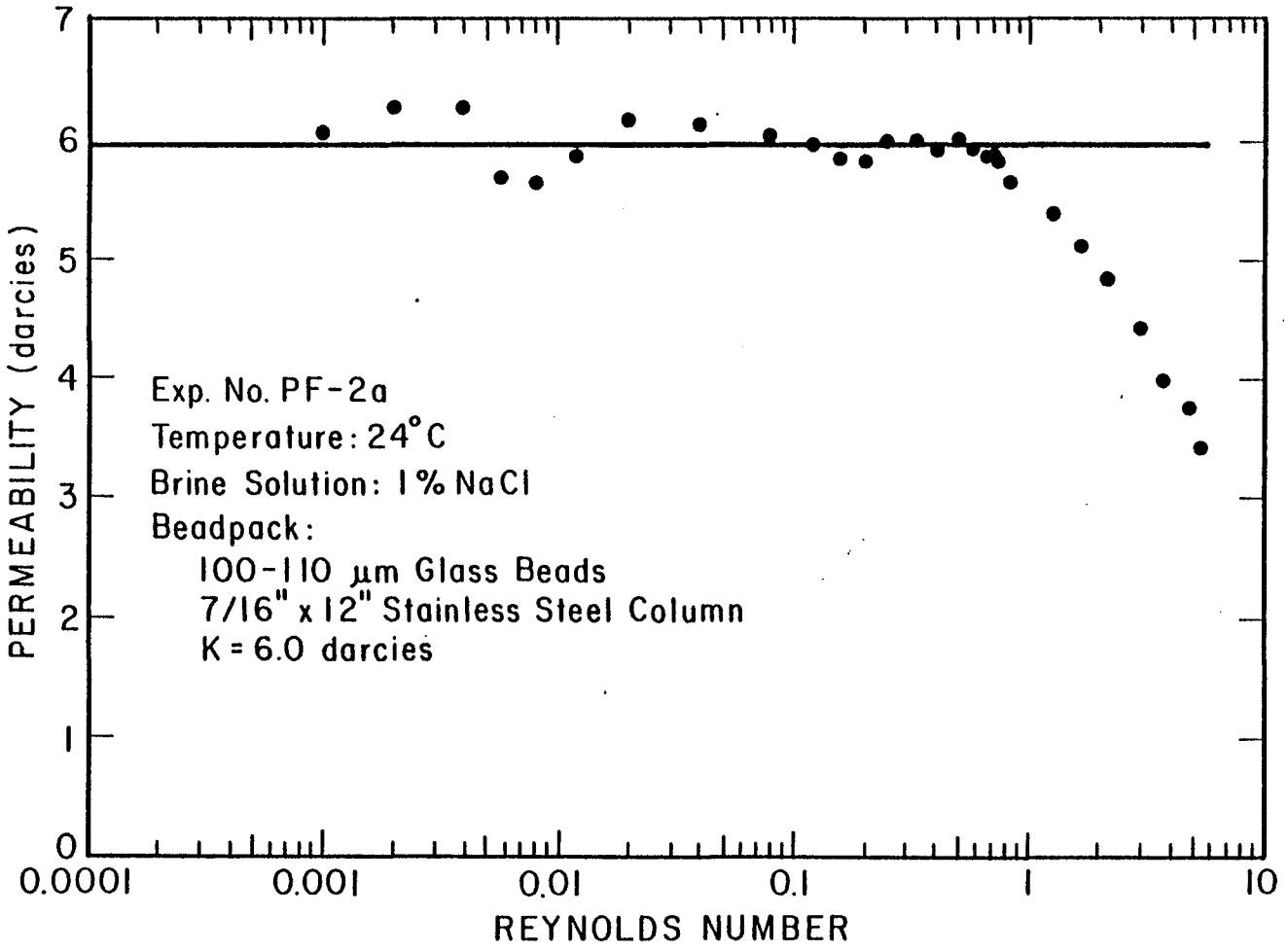

FIGURE 8. Beadpack Permeability to Brine

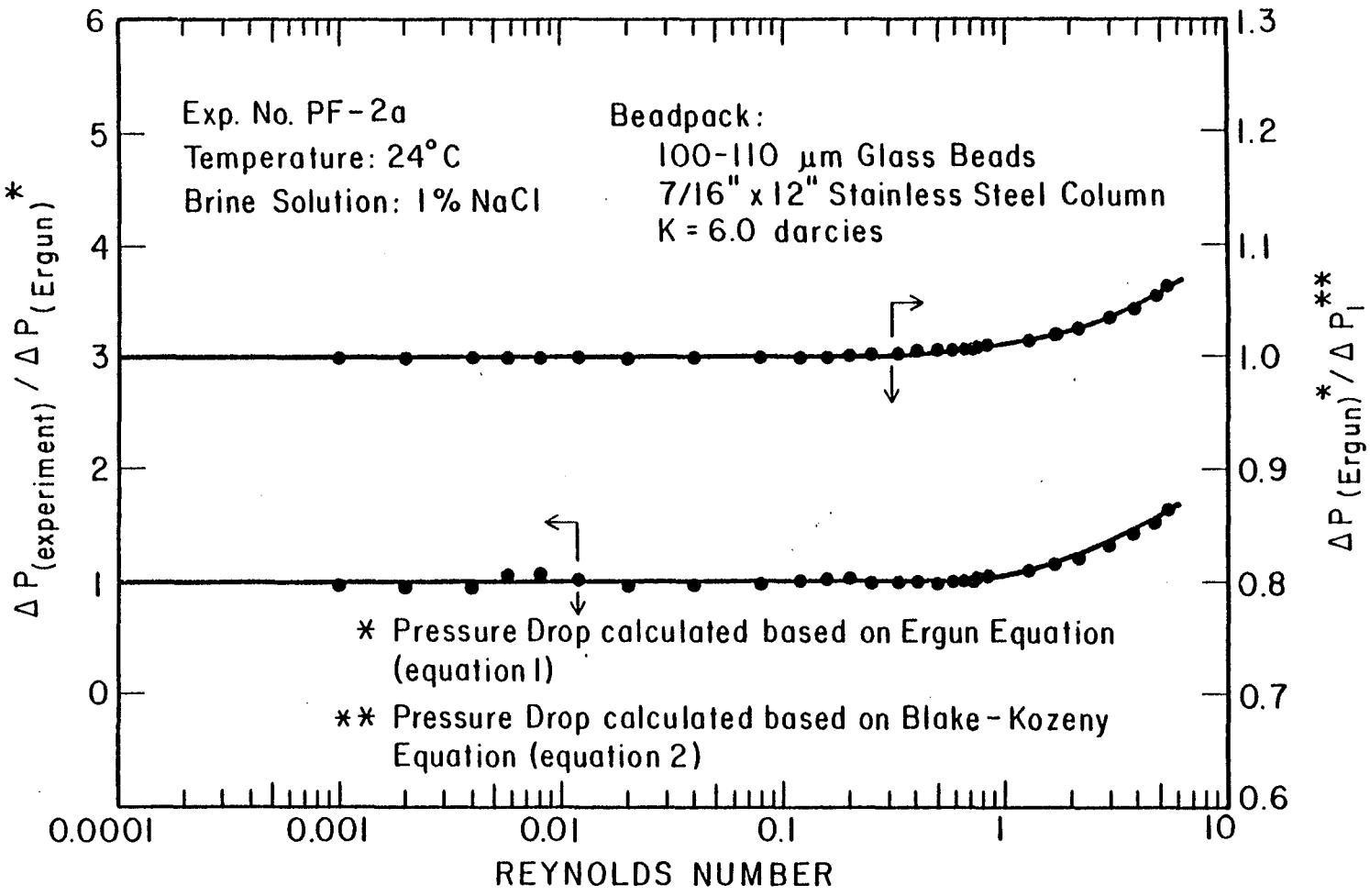

FIGURE 9. Comparison of Pressure Drops and Percent of Inertial Effect

FIGURE 10
EXPT PF-2B

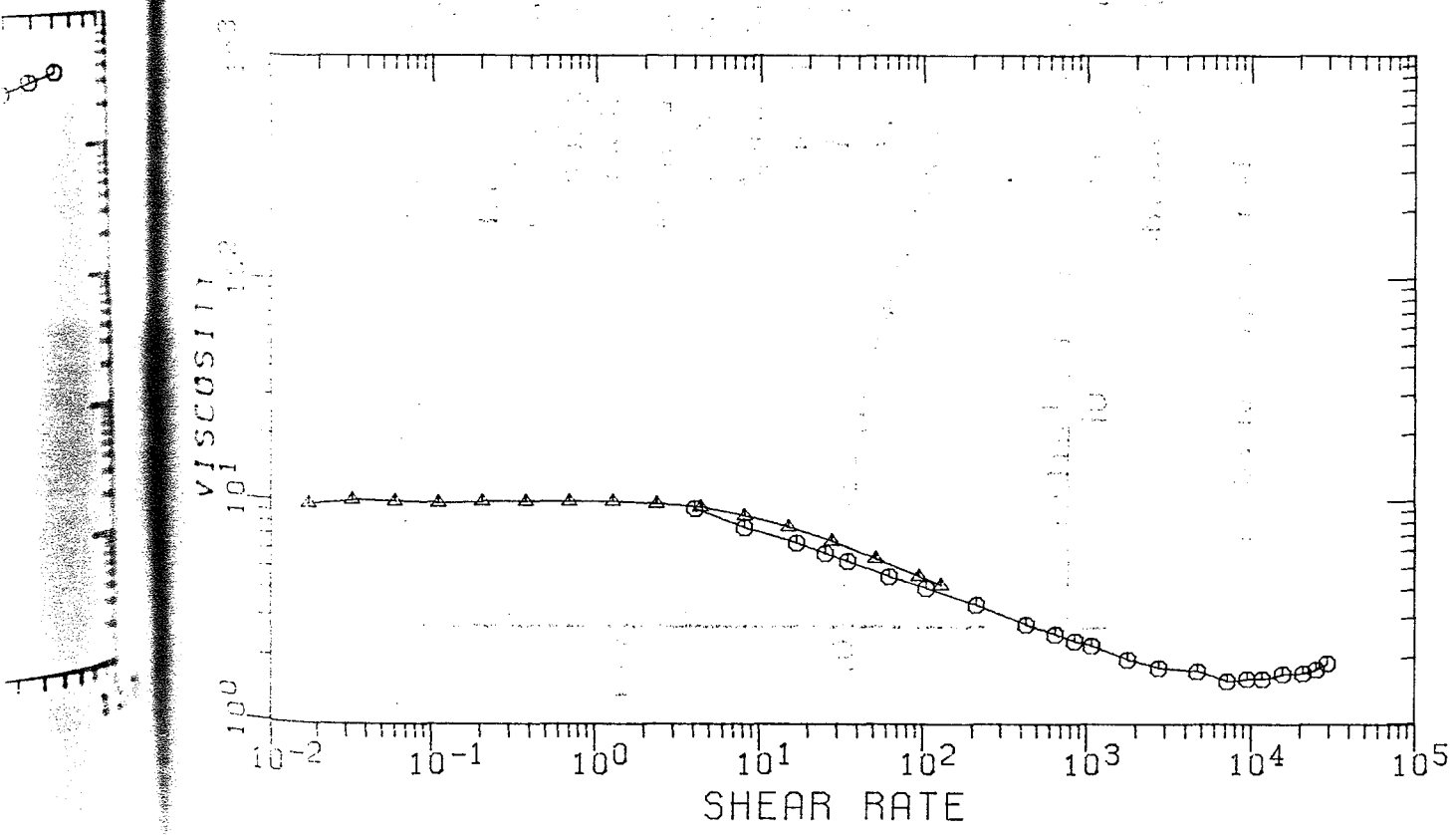

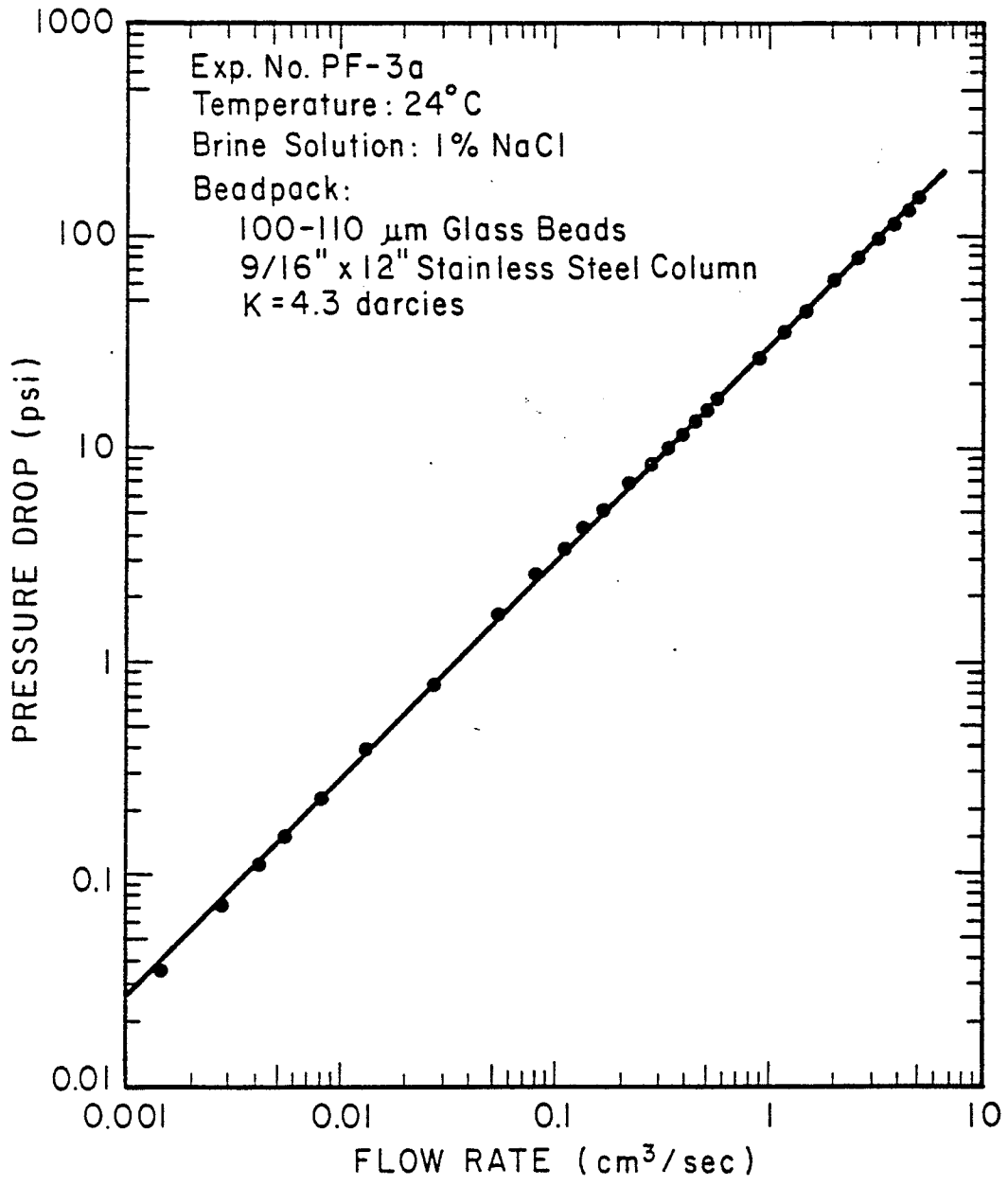

FIGURE 11. Pressure Drop - Flow Rate Data for Brine Solution in Beadpack

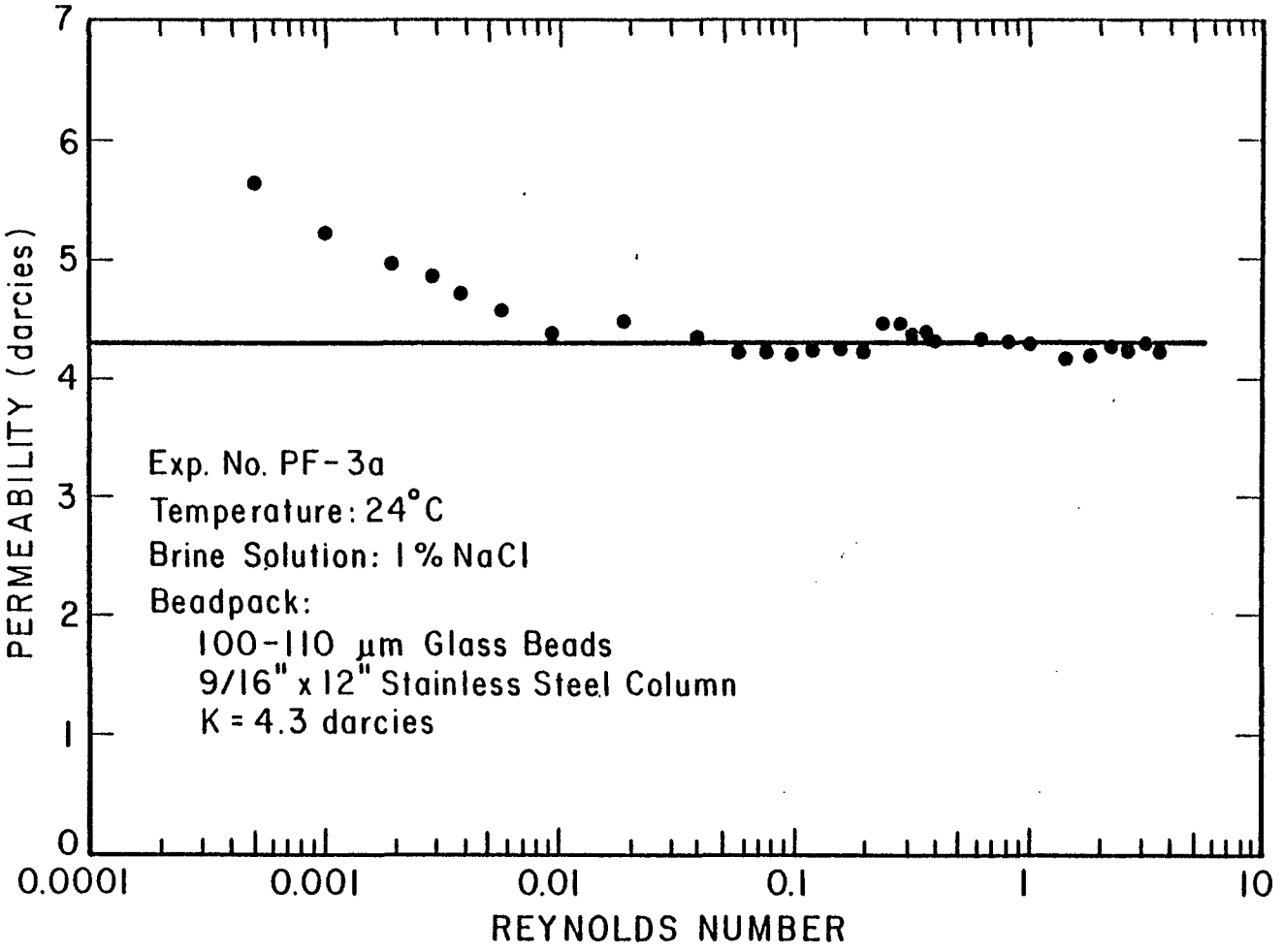

FIGURE 12. Beadpack Permeability to Brine

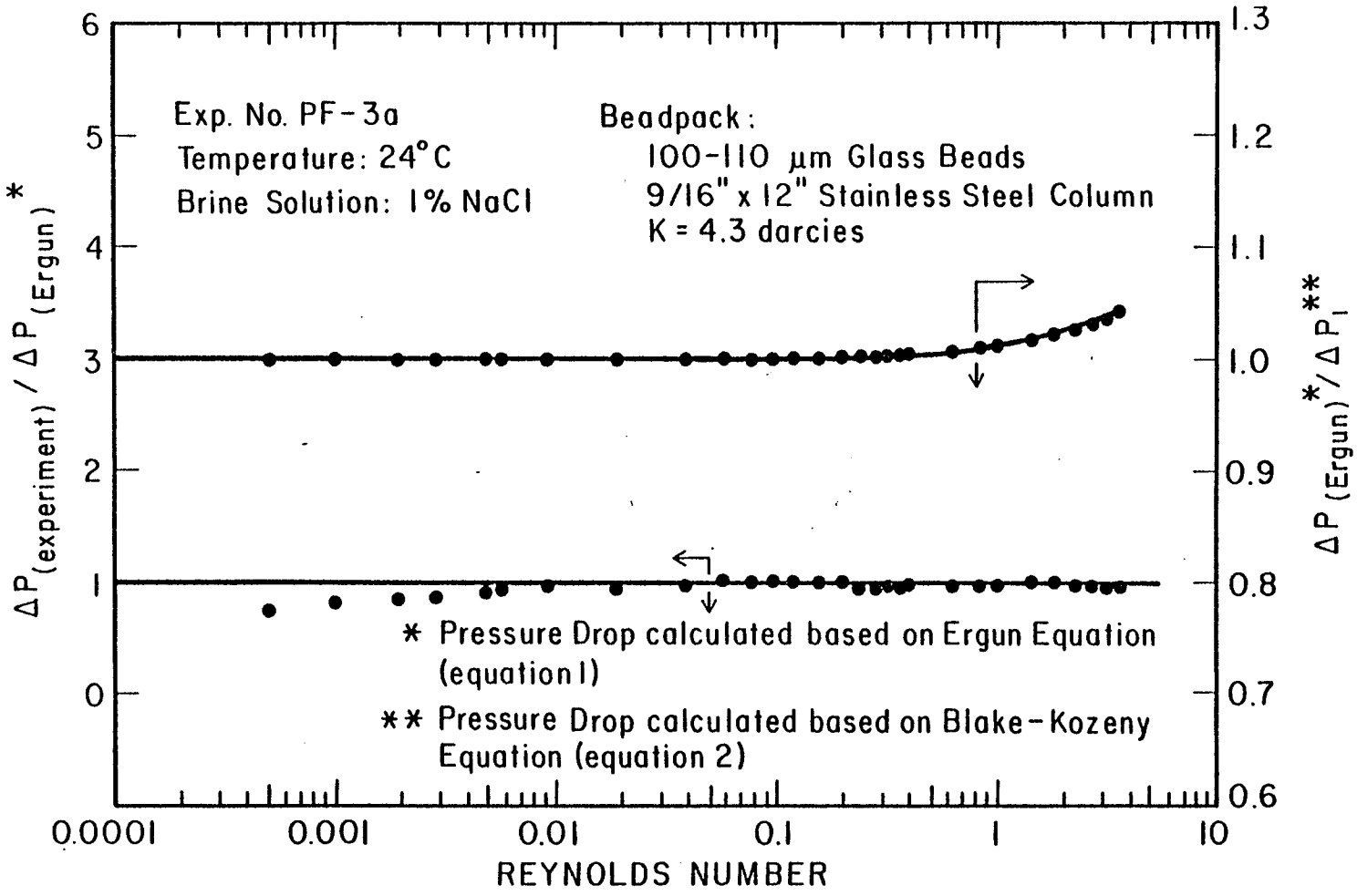

FIGURE 13. Comparison of Pressure Drops and Percent of Initial Effect

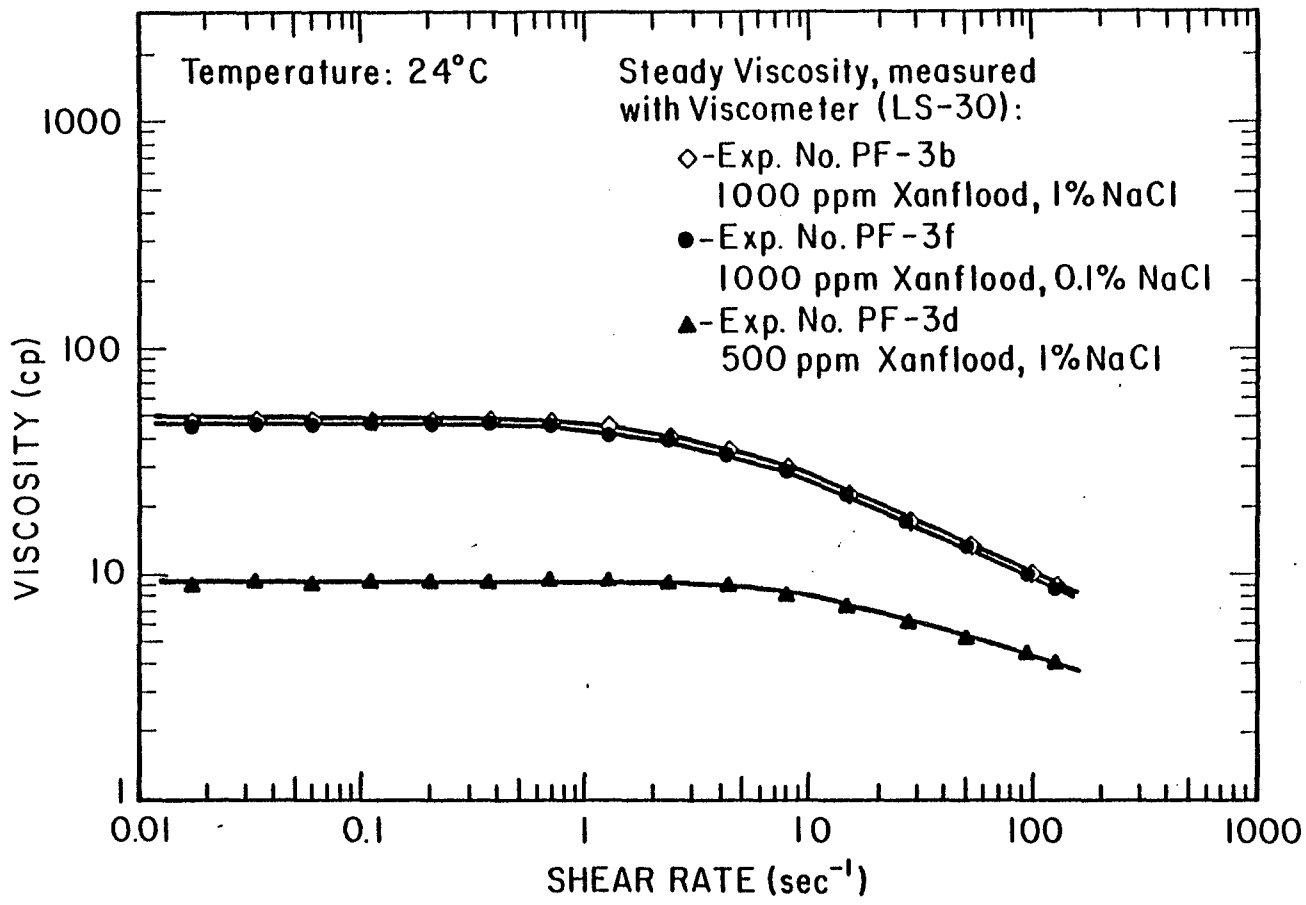

FIGURE 14. Steady Viscosity of Xanflood Polymer

FIGURE 15
EXPT PF-3B

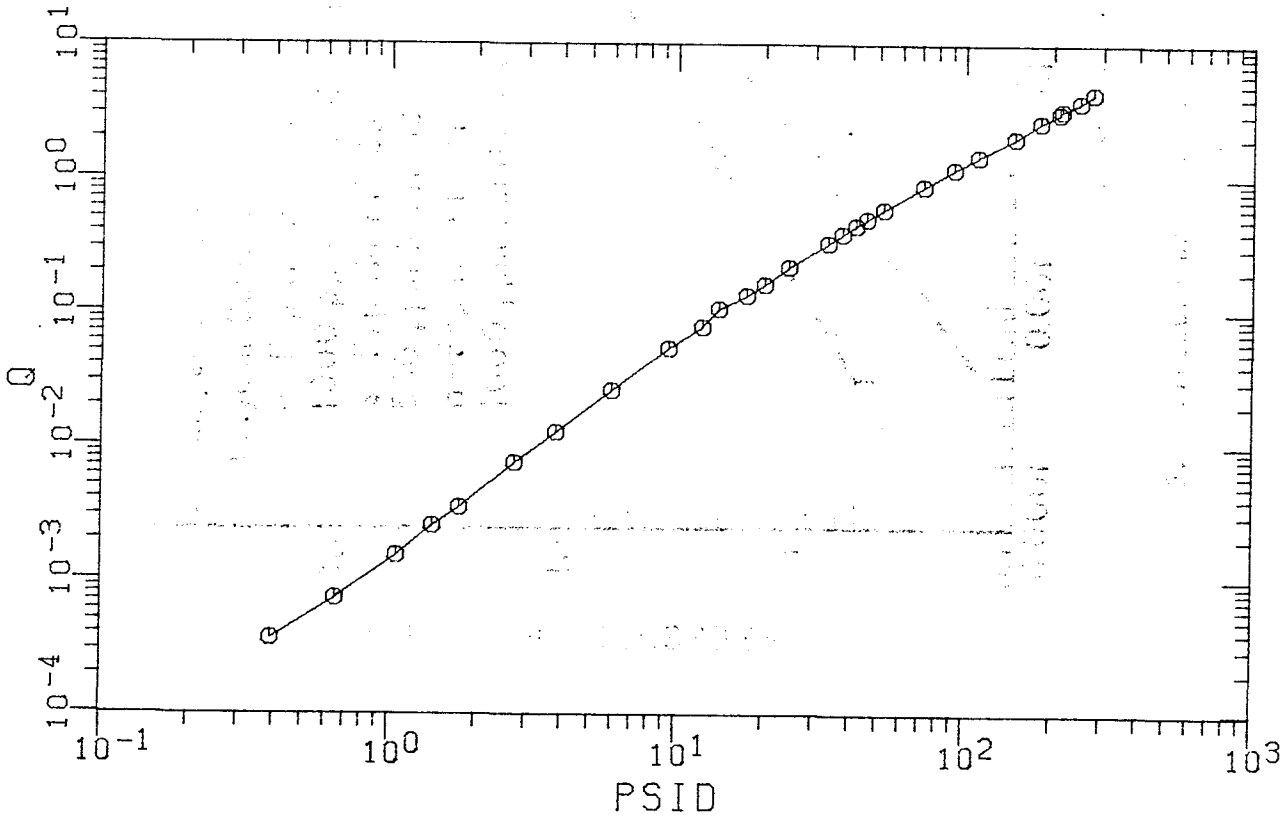

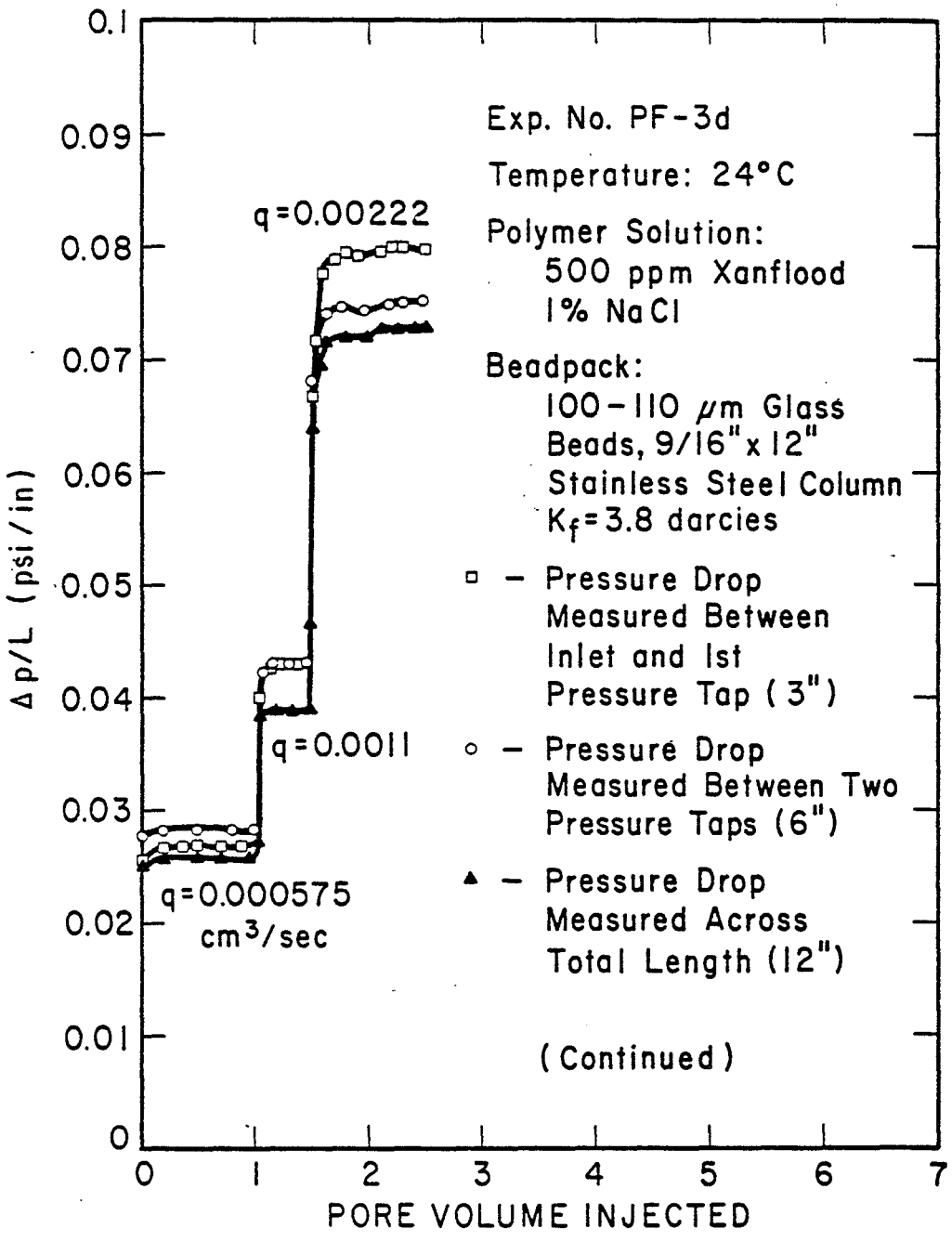

FIGURE 16. Pressure Gradient Versus Number of Pore Volume Injected for Xanflood Polymer in Beadpack

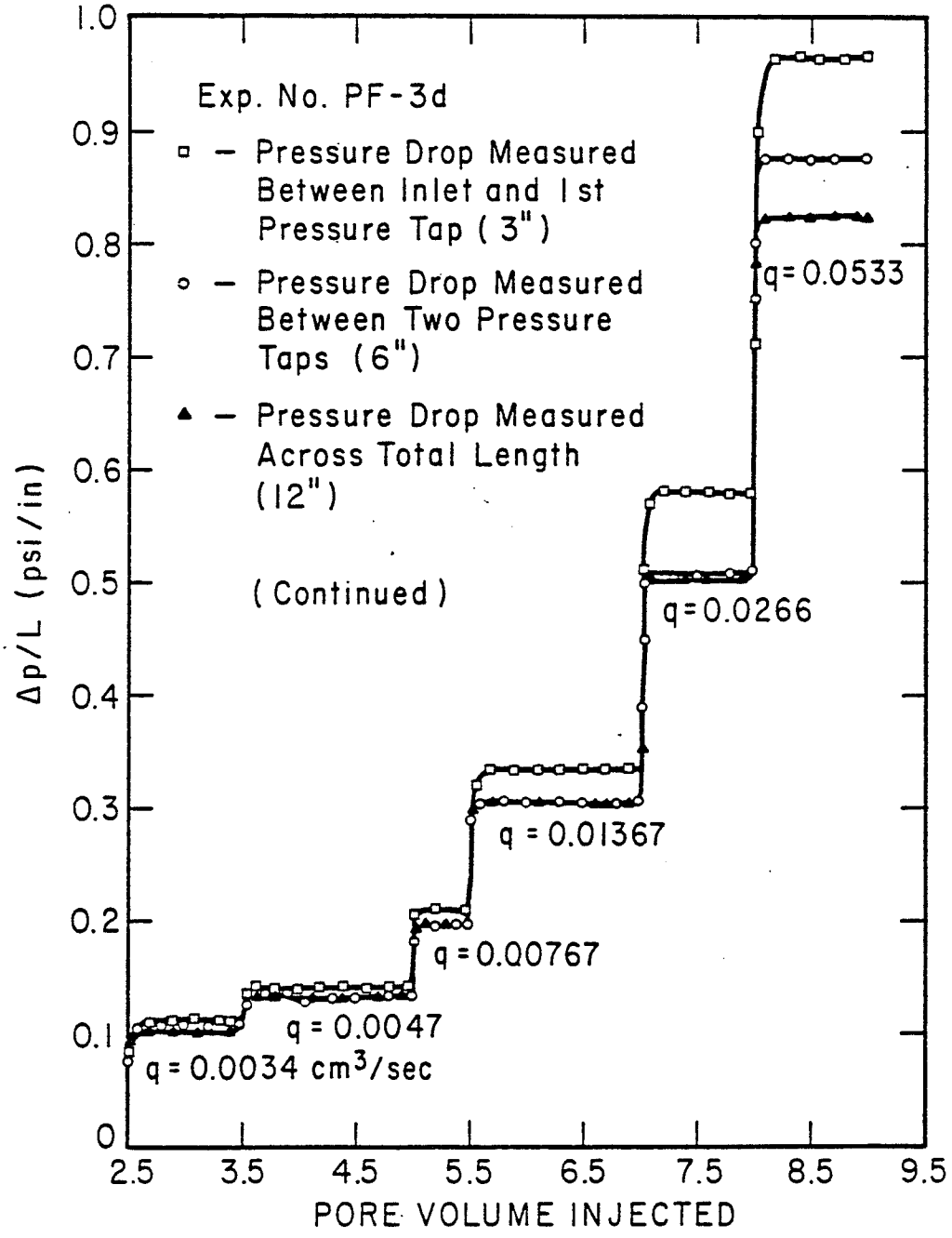

FIGURE 16. Pressure Gradient Versus Number of Pore Volume Injected for Xanflood Polymer in Beadpack

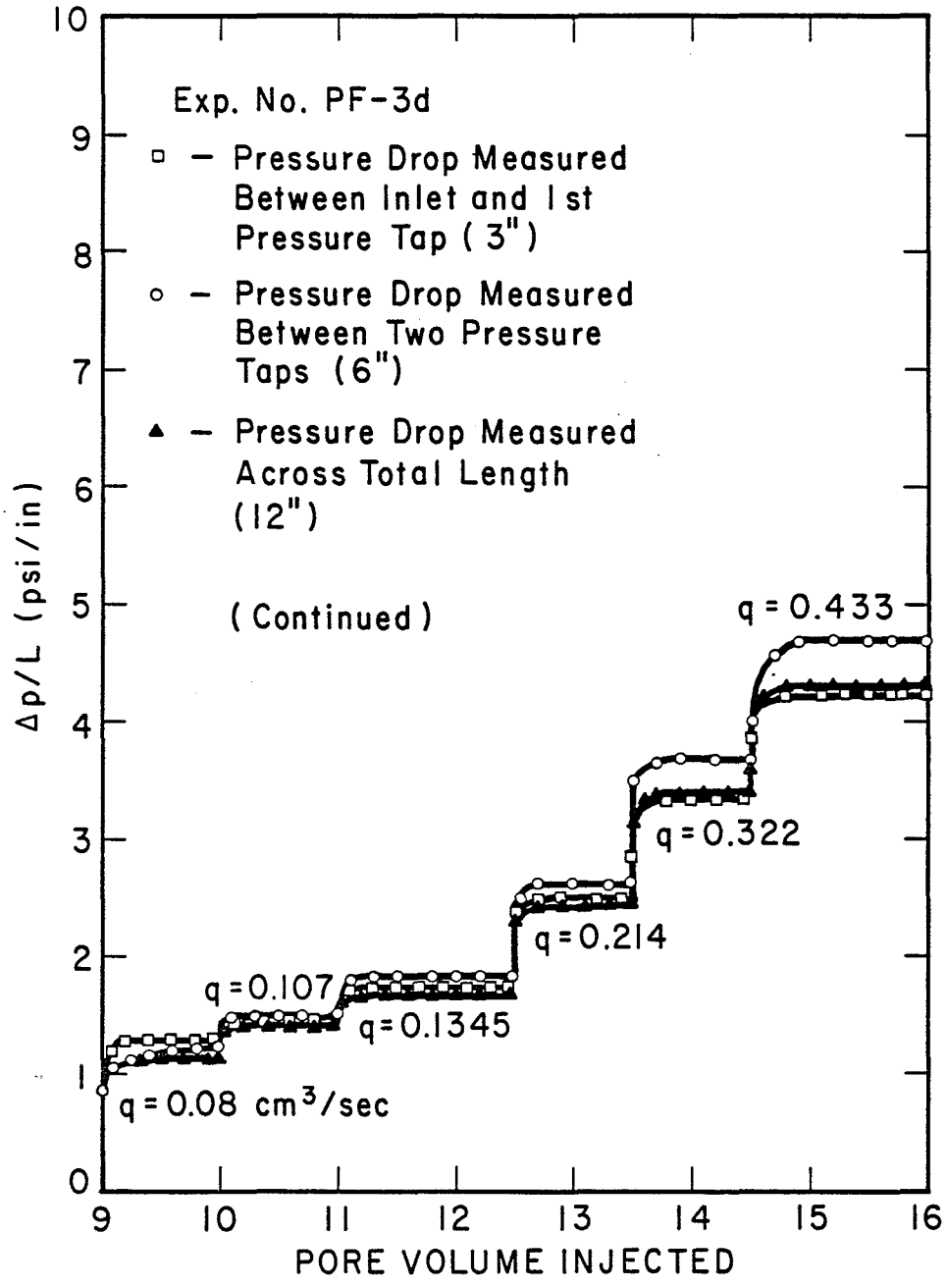

FIGURE 16. Pressure Gradient Versus Number of Pore Volume Injected for Xanflood Polymer in Beadpack

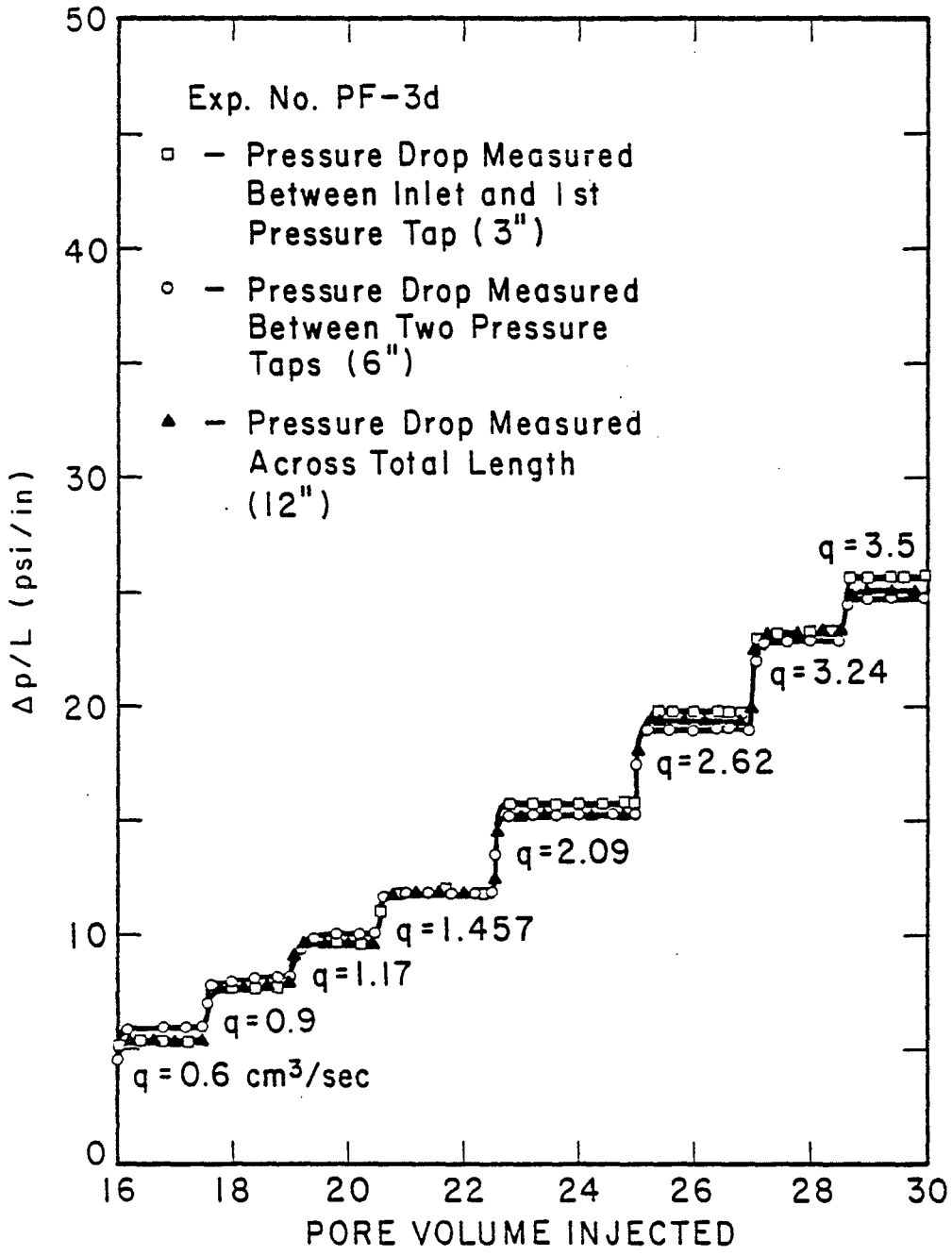

FIGURE 16. Pressure Gradient Versus Number of Pore Volume Injected for Xanflood Polymer in Beadpack

FIGURE 17
EXPT PF-3D

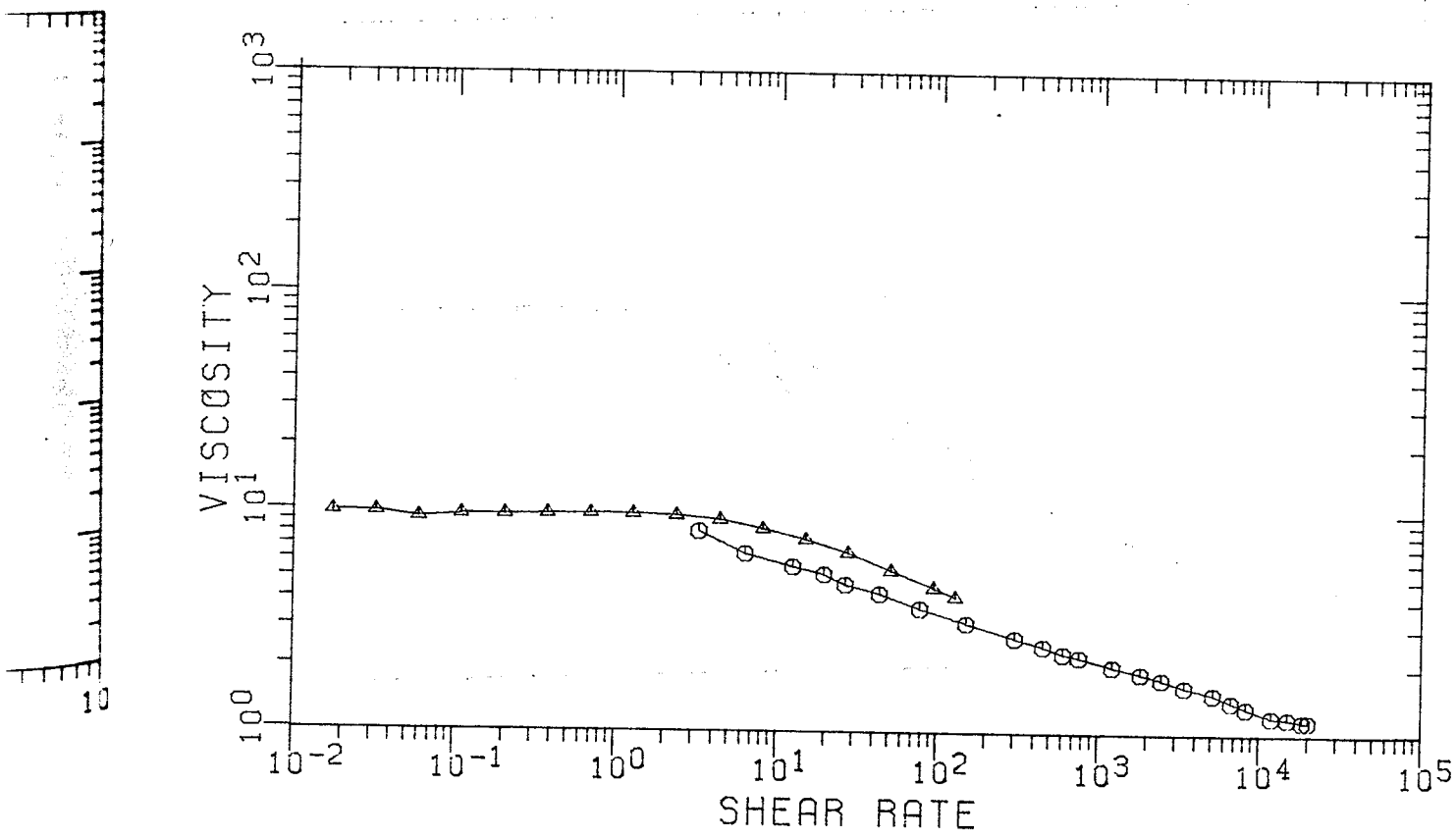

FIGURE 18
EXPT PF-3F

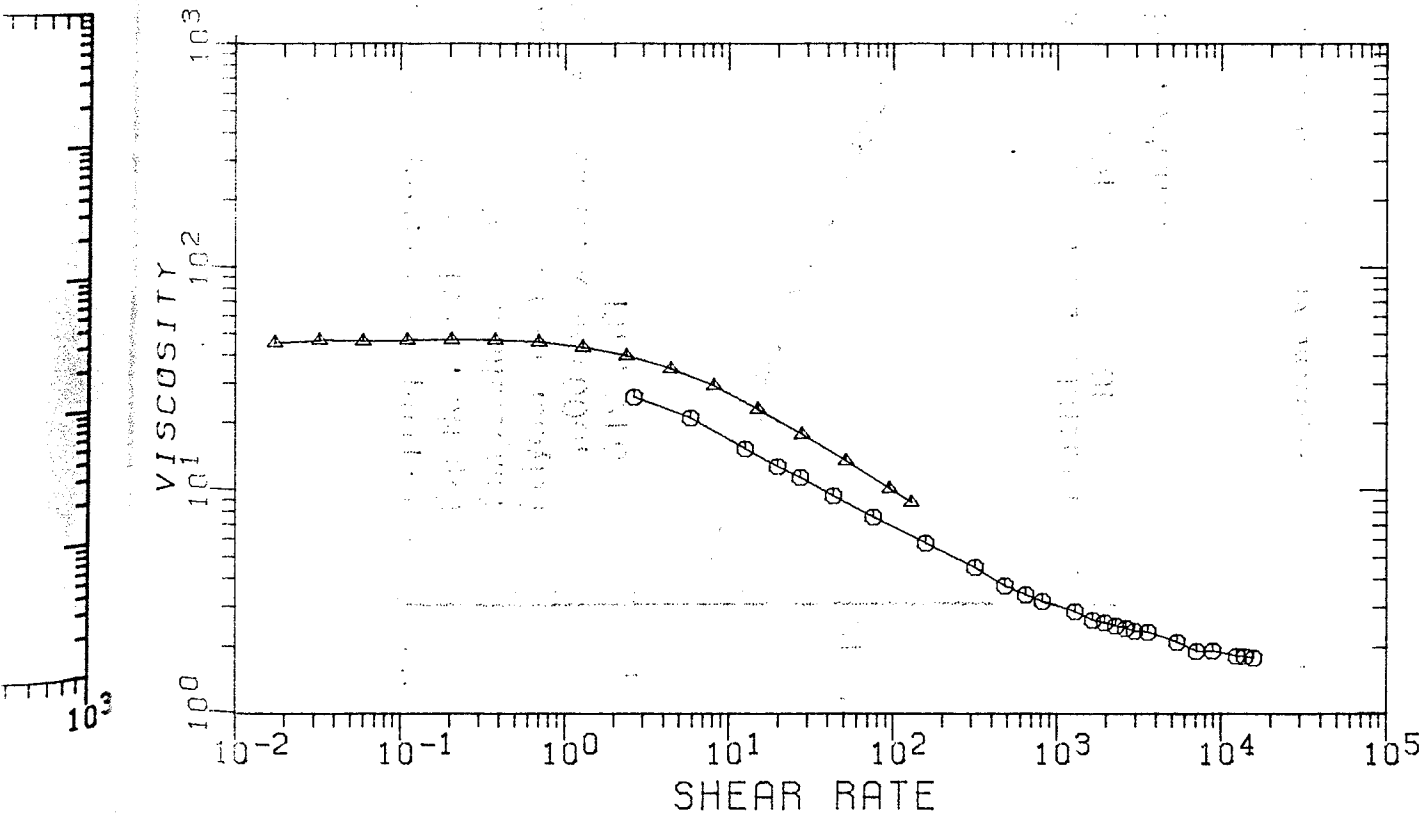

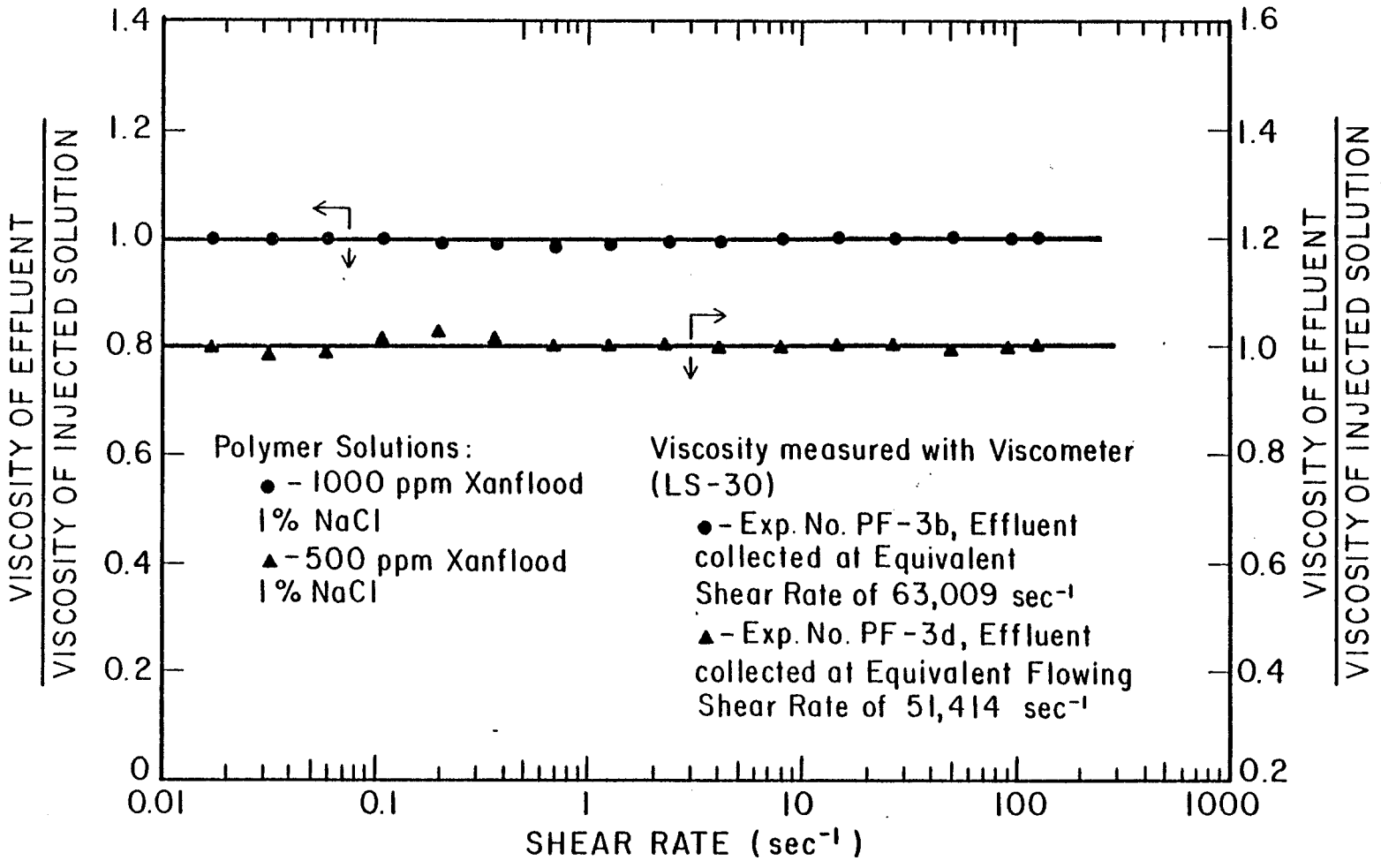

FIGURE 19. Comparison of Viscosity of Effluents to the Injected Polymer Solutions

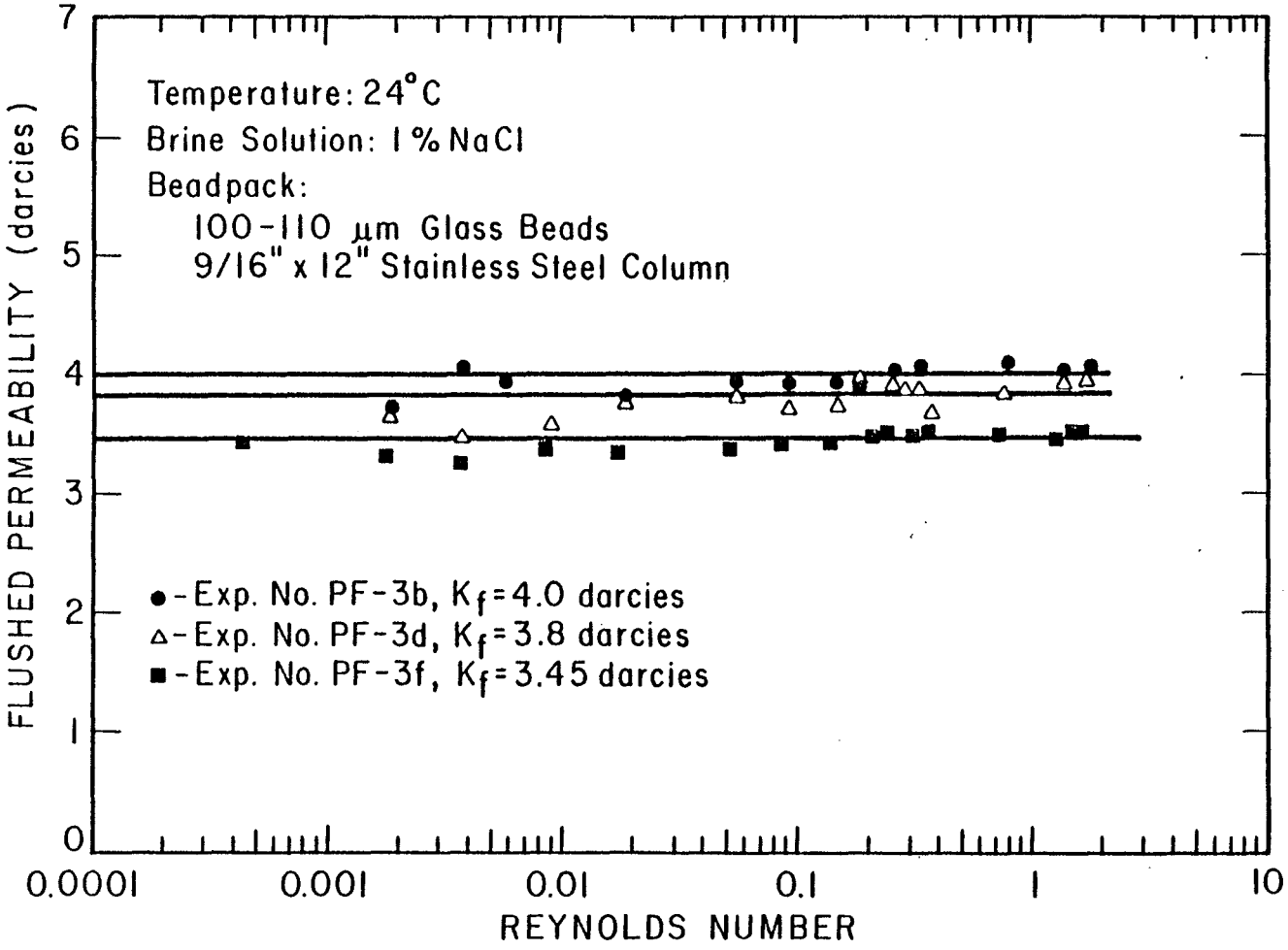

FIGURE 20. Flushed Permeability of Beadpack to Brine

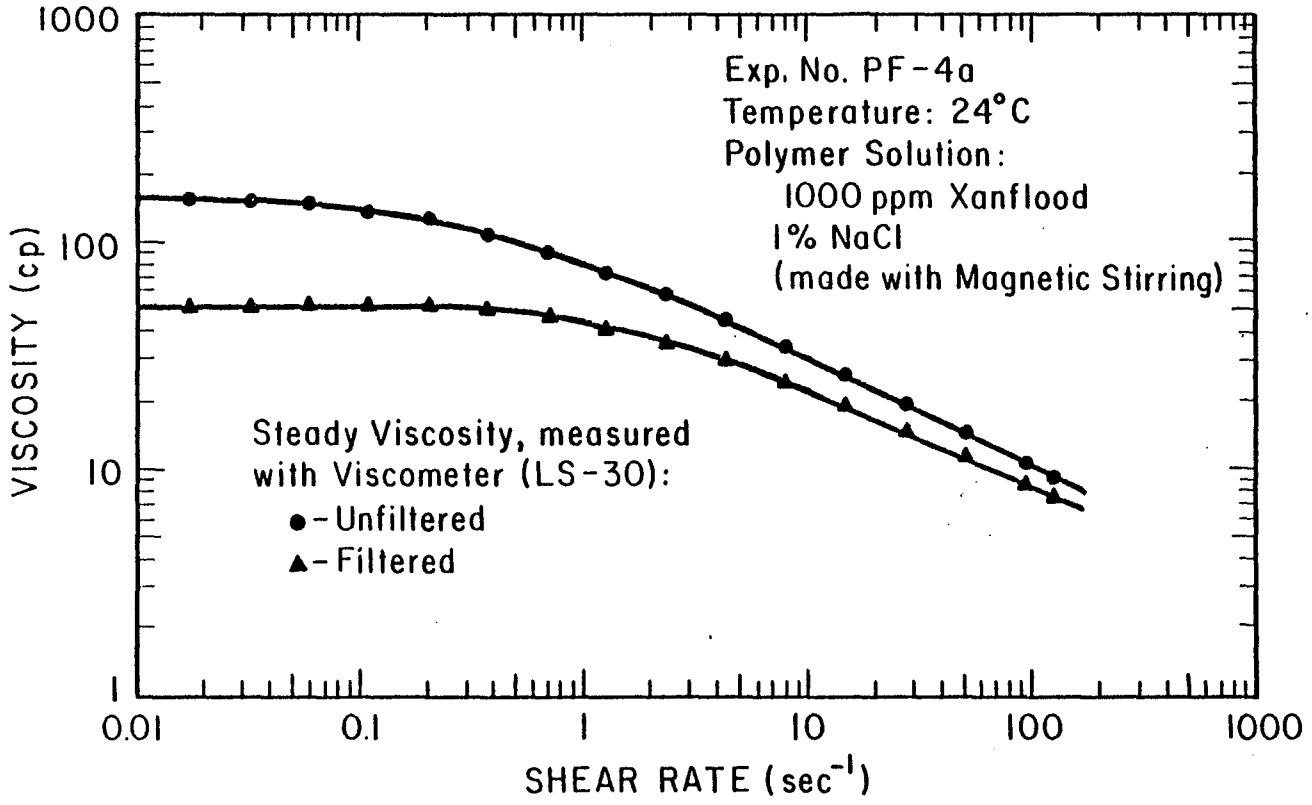

FIGURE 21. Viscosity of Unsheared Xanflood Polymer Solutions

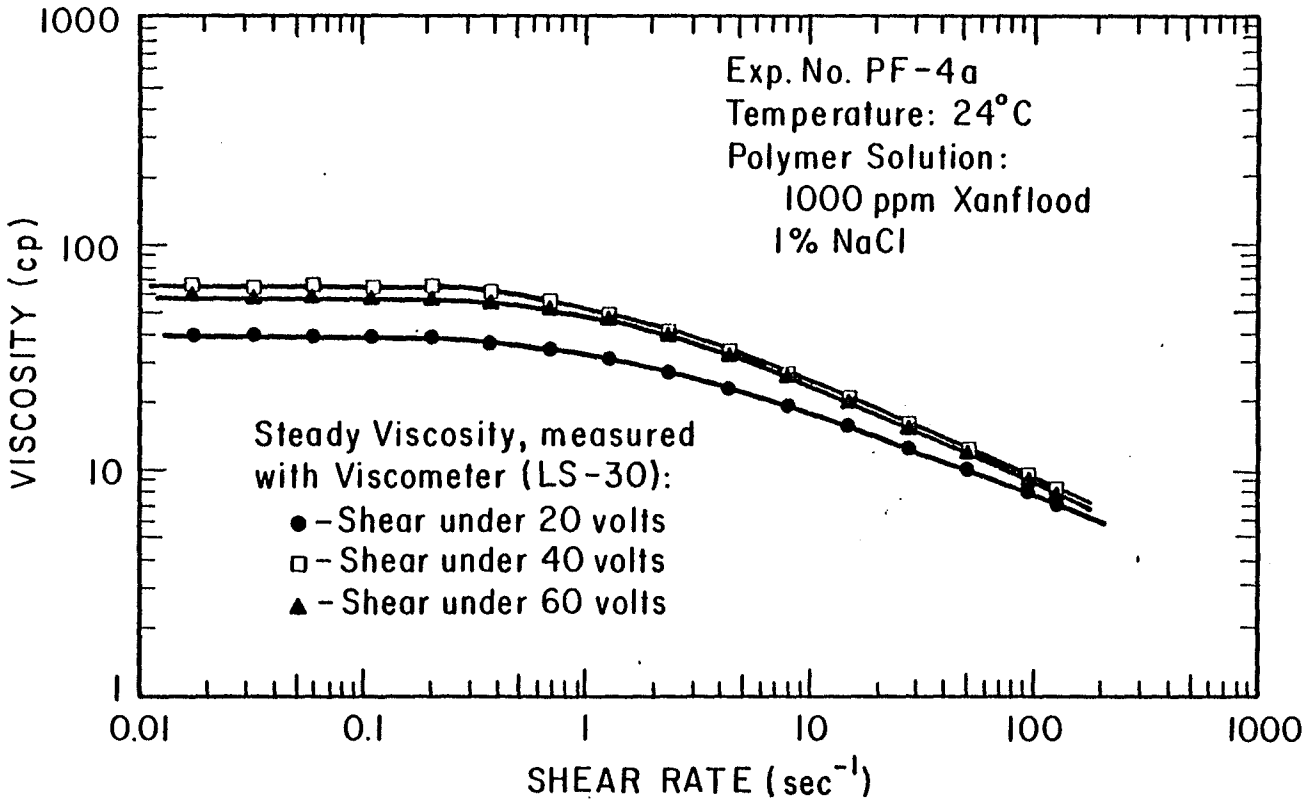

FIGURE 22. Viscosity of Xanflood Polymer Solution Made at Different Degree of Shearing

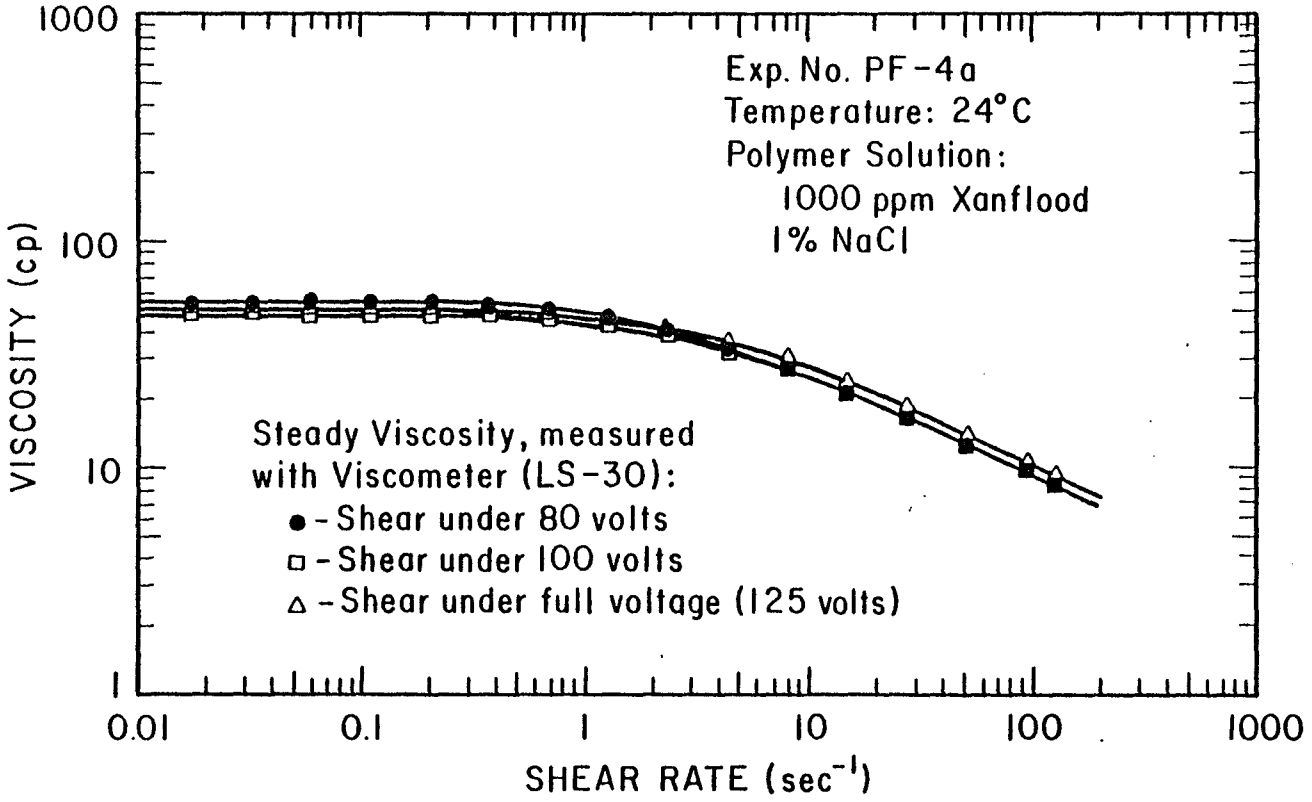

FIGURE 23. Viscosity of Xanflood Polymer Solution Made at Different Degree of Shearing

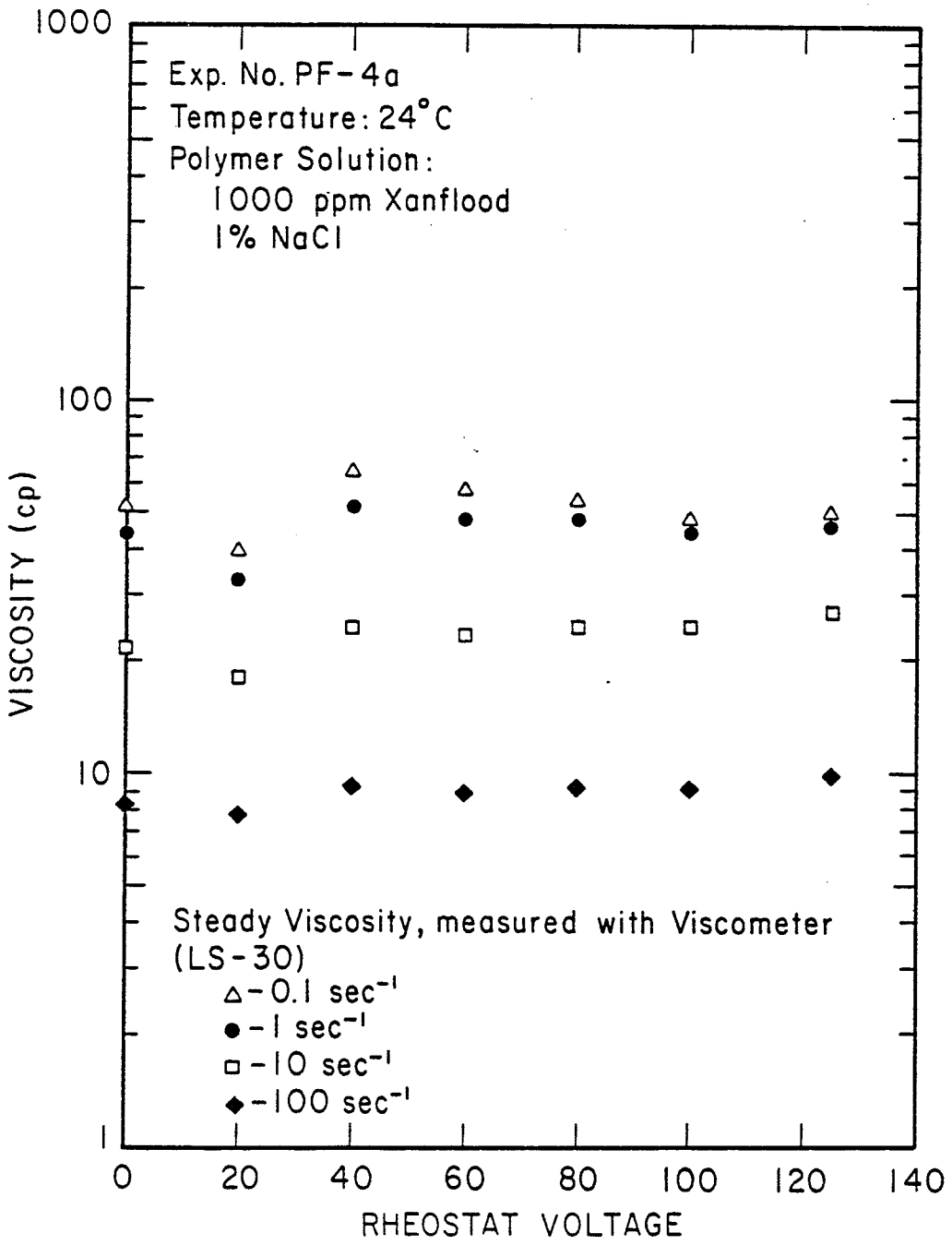

FIGURE 24. Viscosity of Xanflood Polymer Solution Made at Different Degree of Shearing

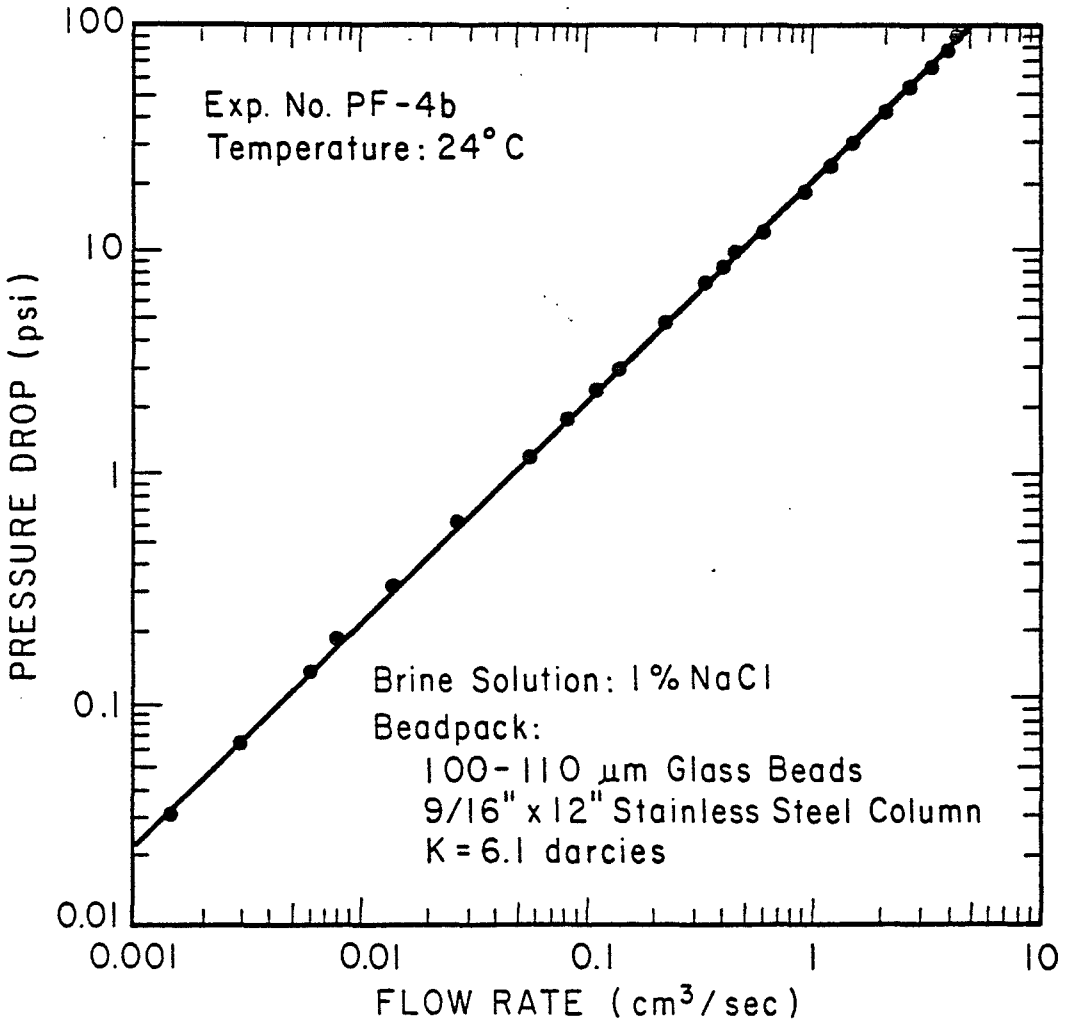

FIGURE 25. Pressure Drop-Flow Rate Data for Brine in Beadpack

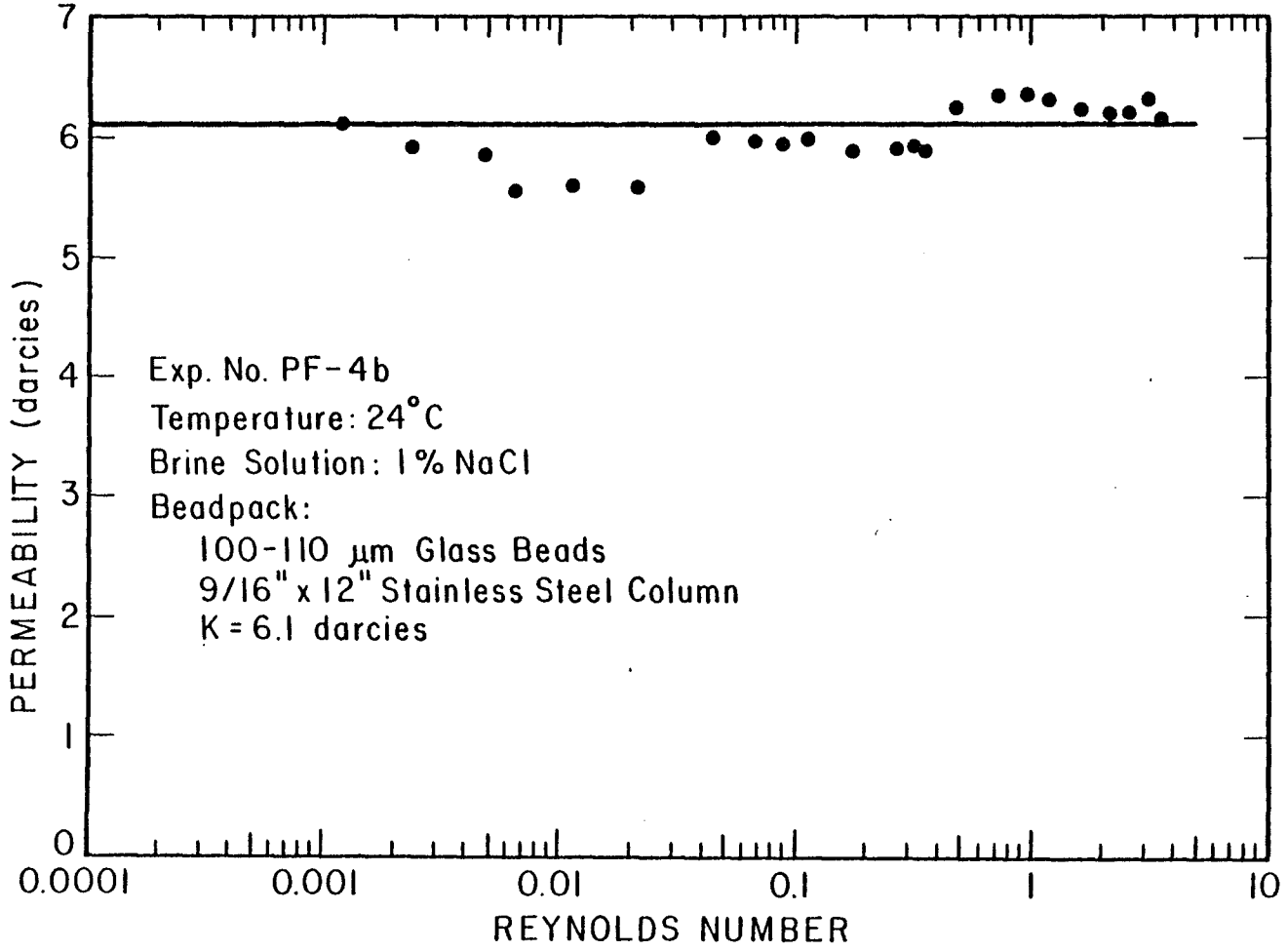

FIGURE 26. Beadpack Permeability to Brine

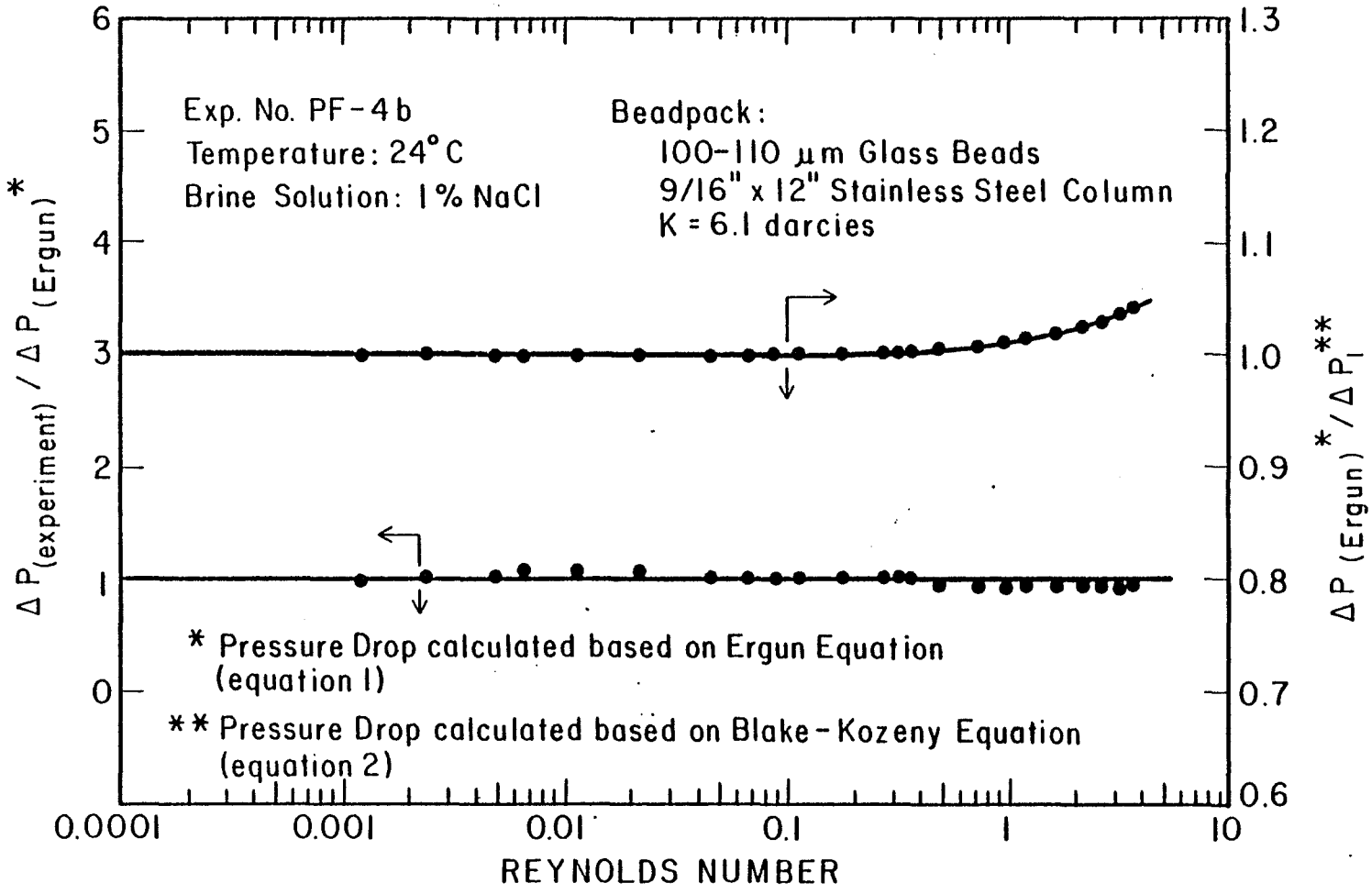

FIGURE 27. Comparison of Pressure Drops and Percent of Inertial Effect

FIGURE 28
EXPT PF-4C

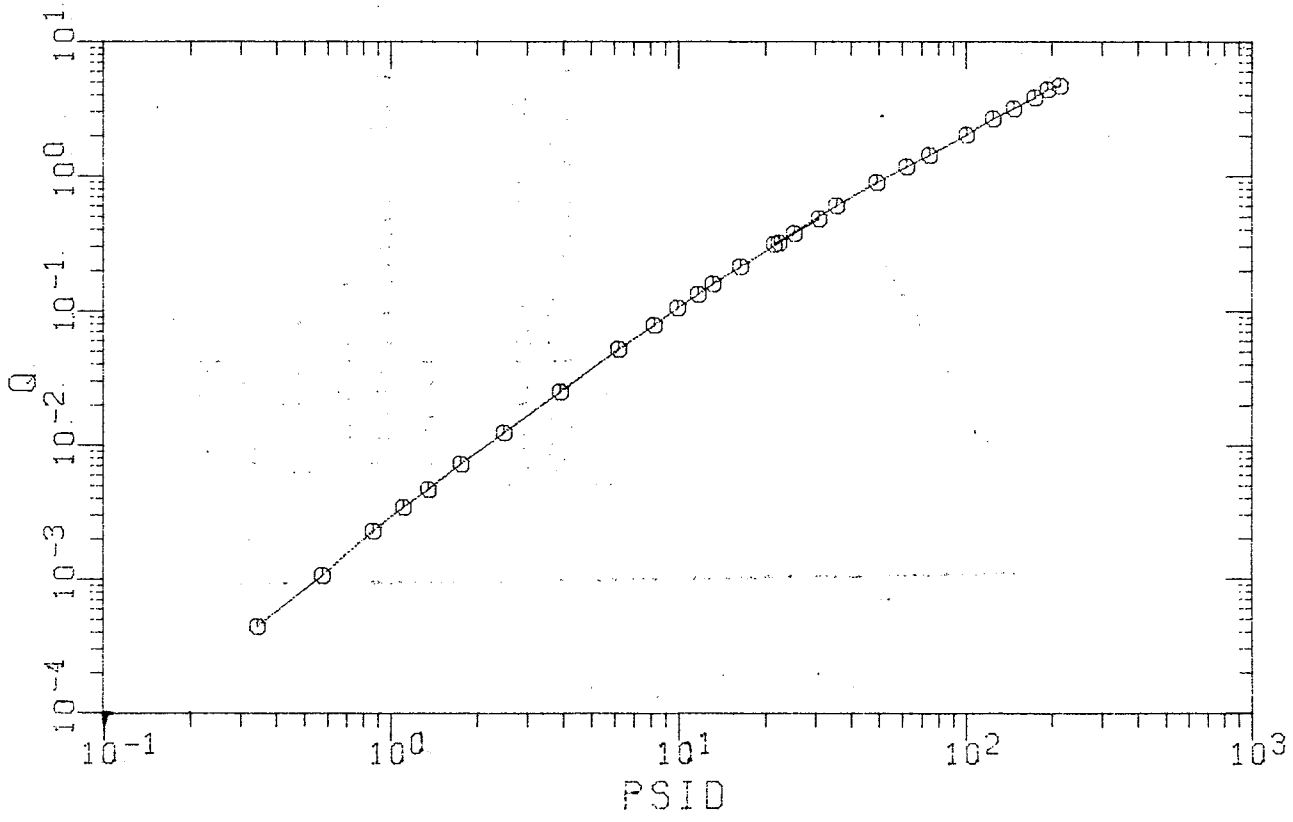

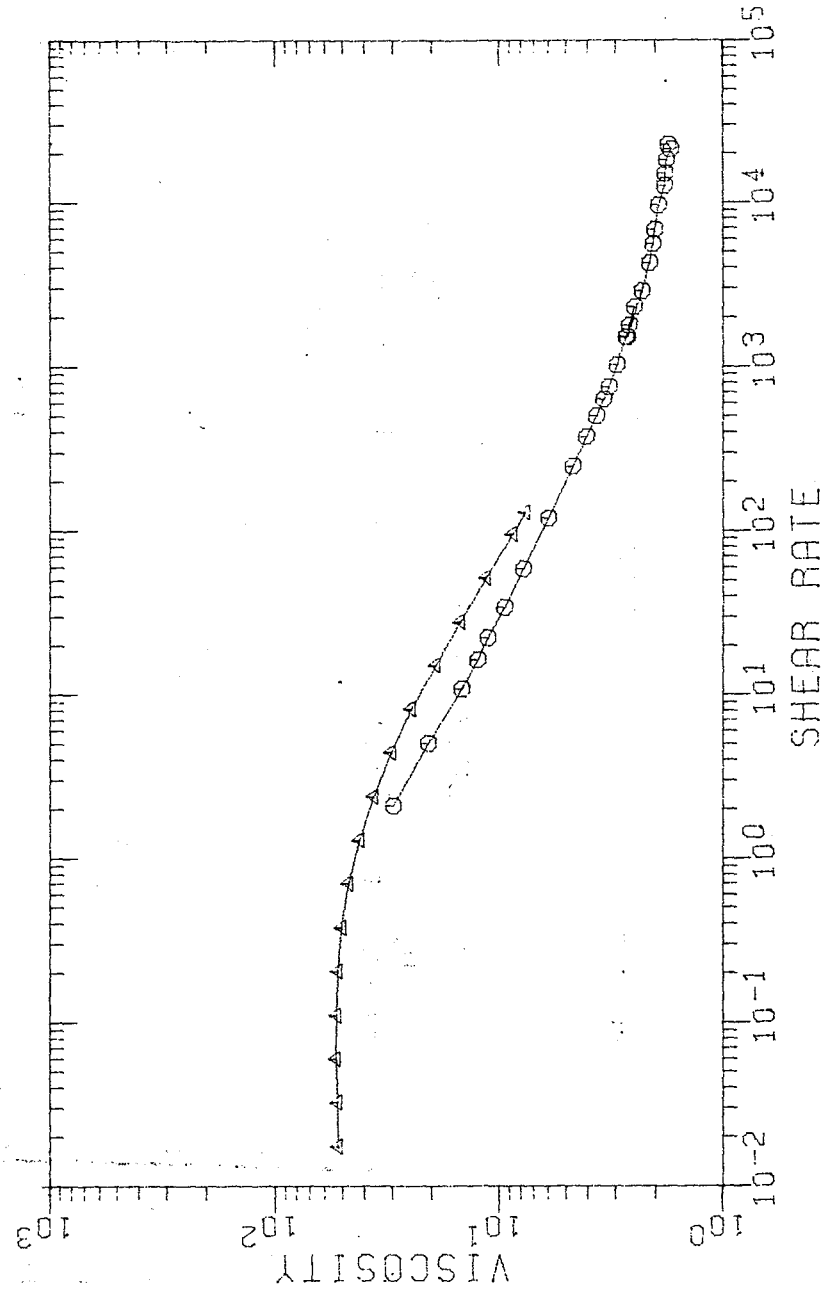
VISCOSITY
SHEAR RATE
10^0
10^1
10^2
10^3
10^-2
10^-1
10^0
10^1
10^2
10^3
10^4
10^5

FIGURE 29

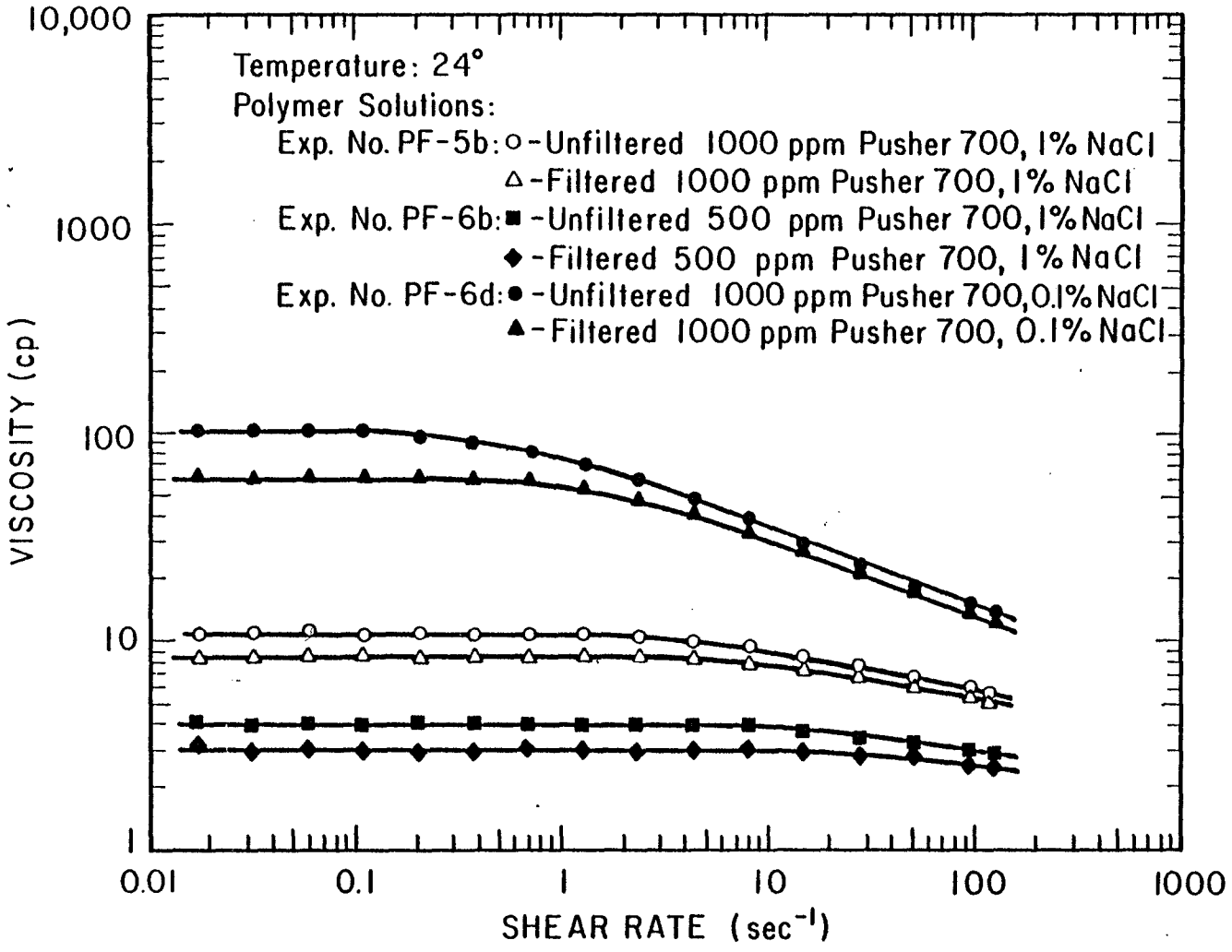

FIGURE 30. Steady Viscosity of Pusher 700 Polymer Solutions

FIGURE 31A
EXPT PF-5B

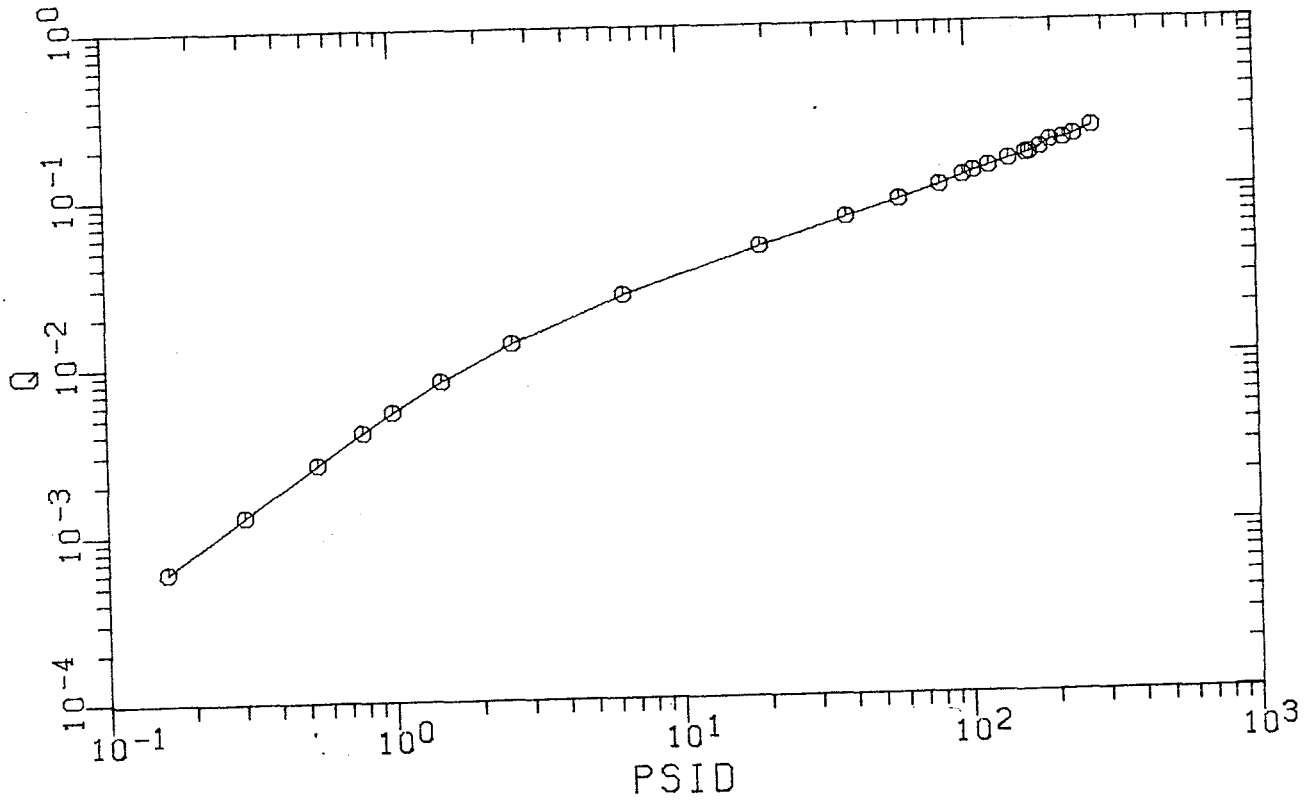

FIGURE 32A
EXPT PF-5B

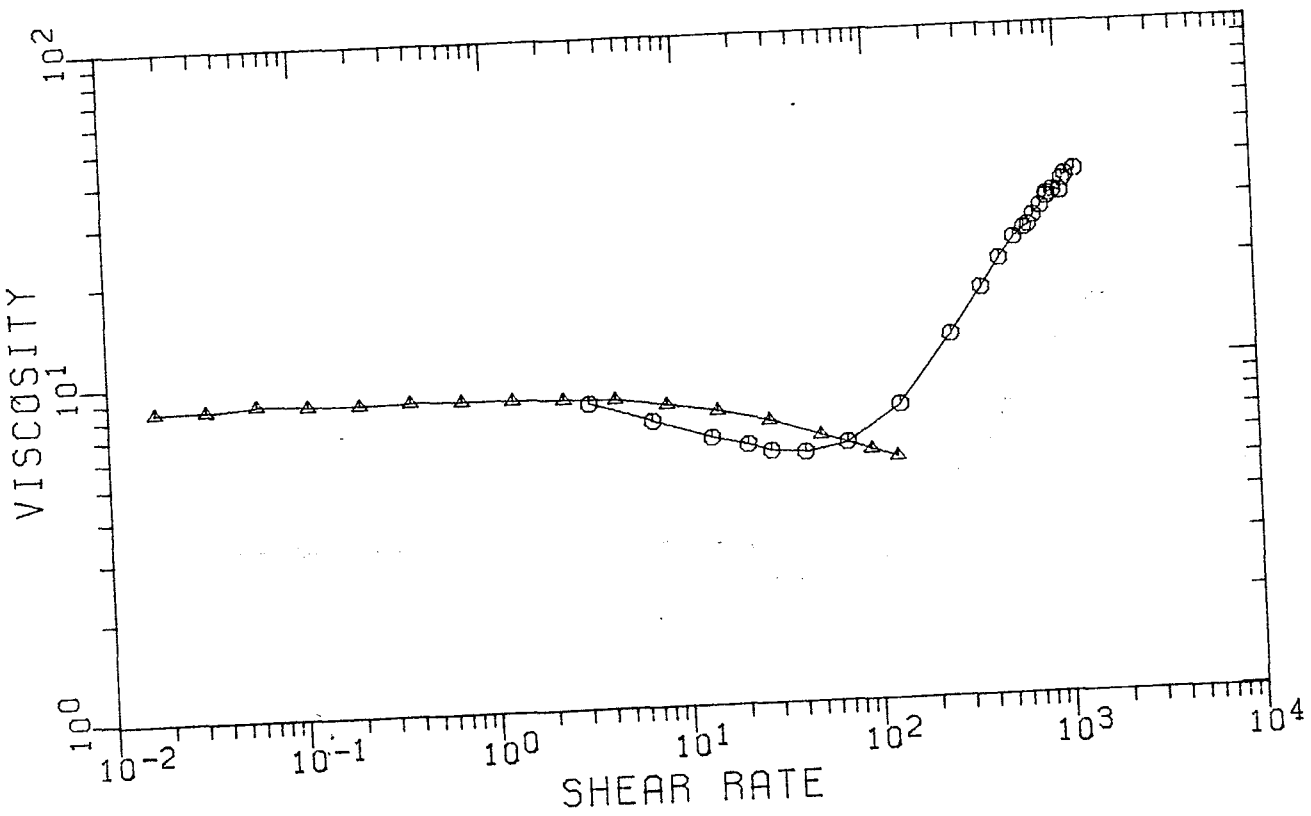

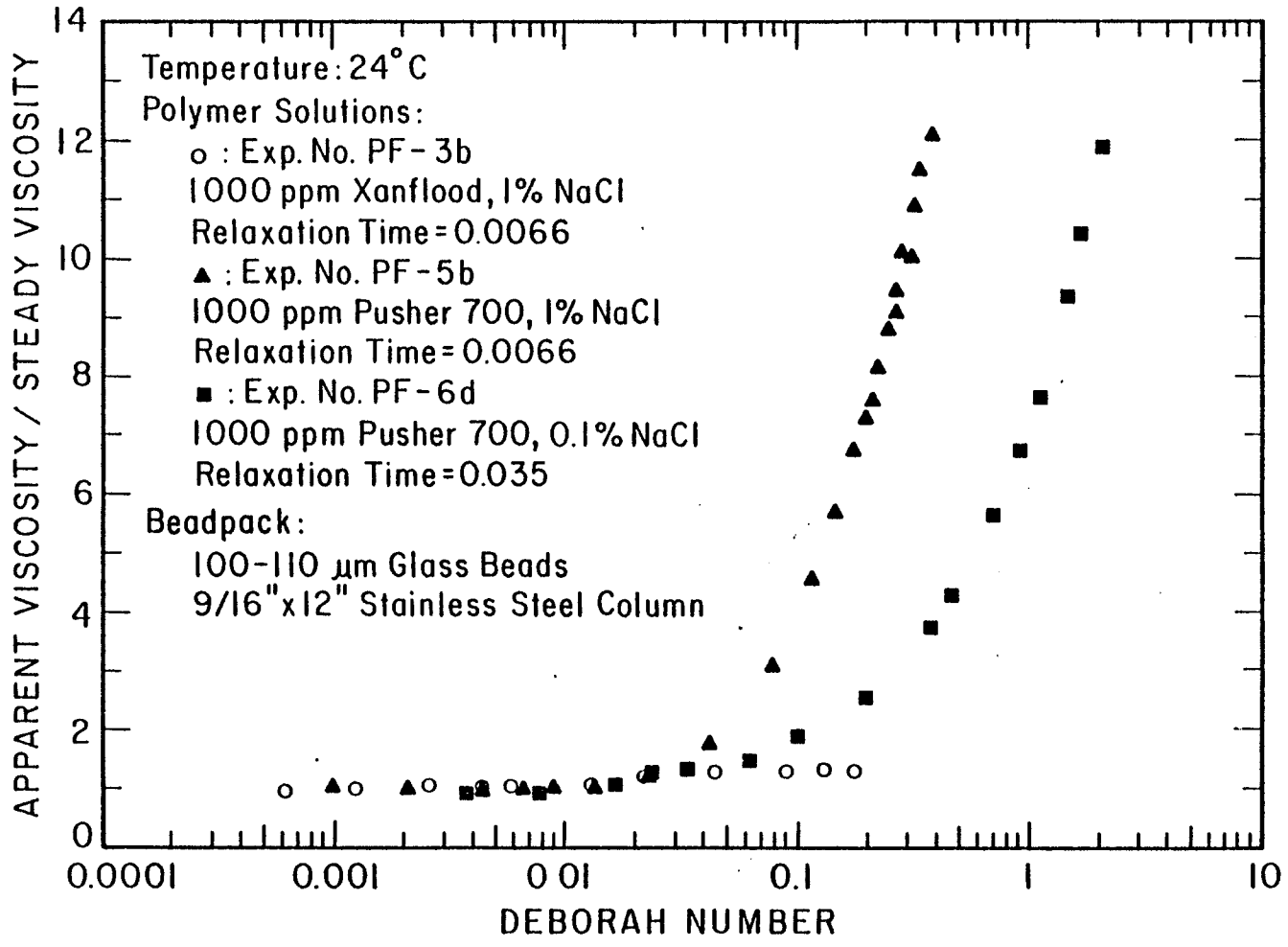

Figure 33. Effects of Polymer Type and Salt Concentration on the Viscoelasticity

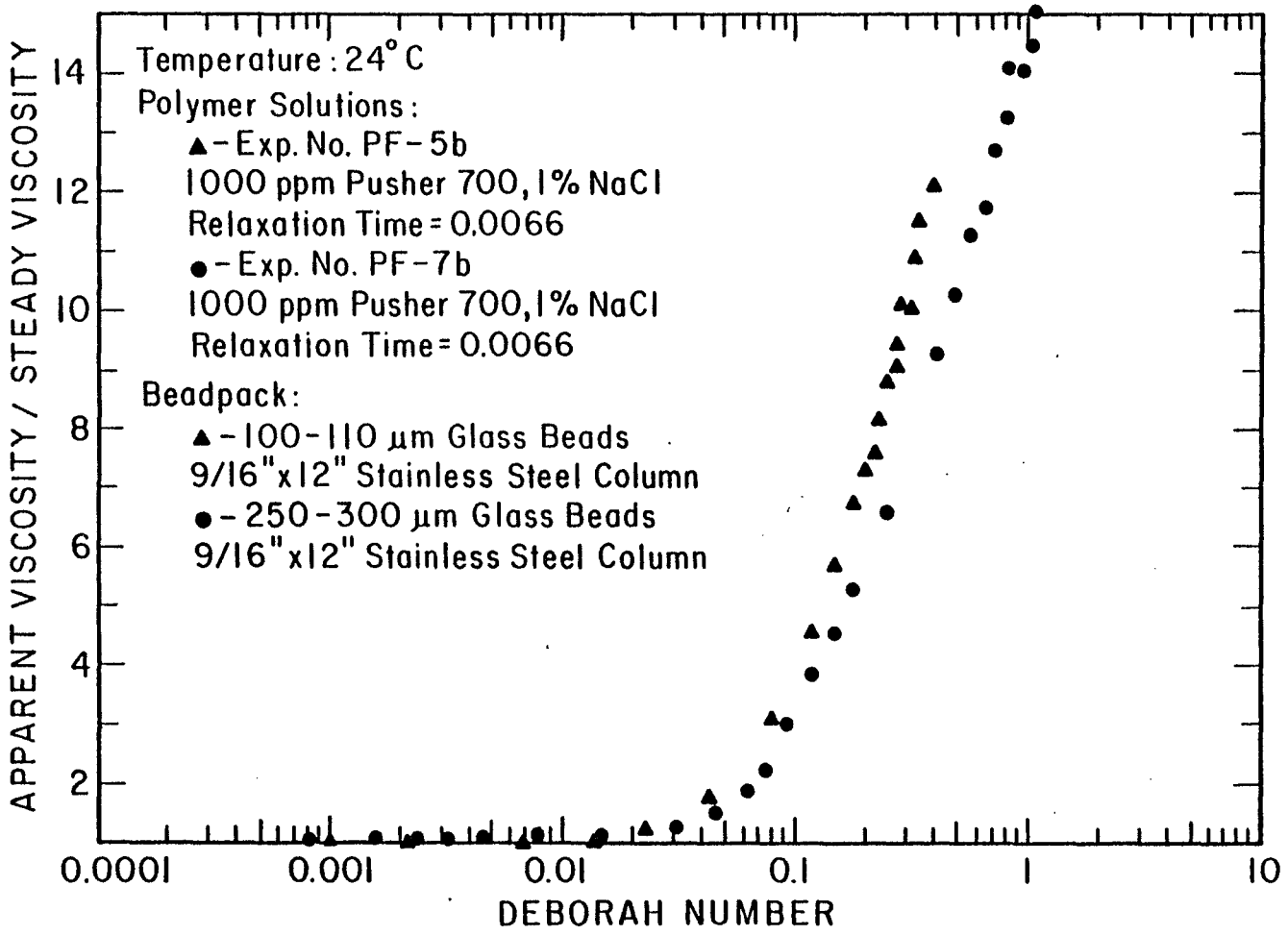

Figure 34. Effects of Bead Size on the Viscoelasticity of Pusher 700 Polymer

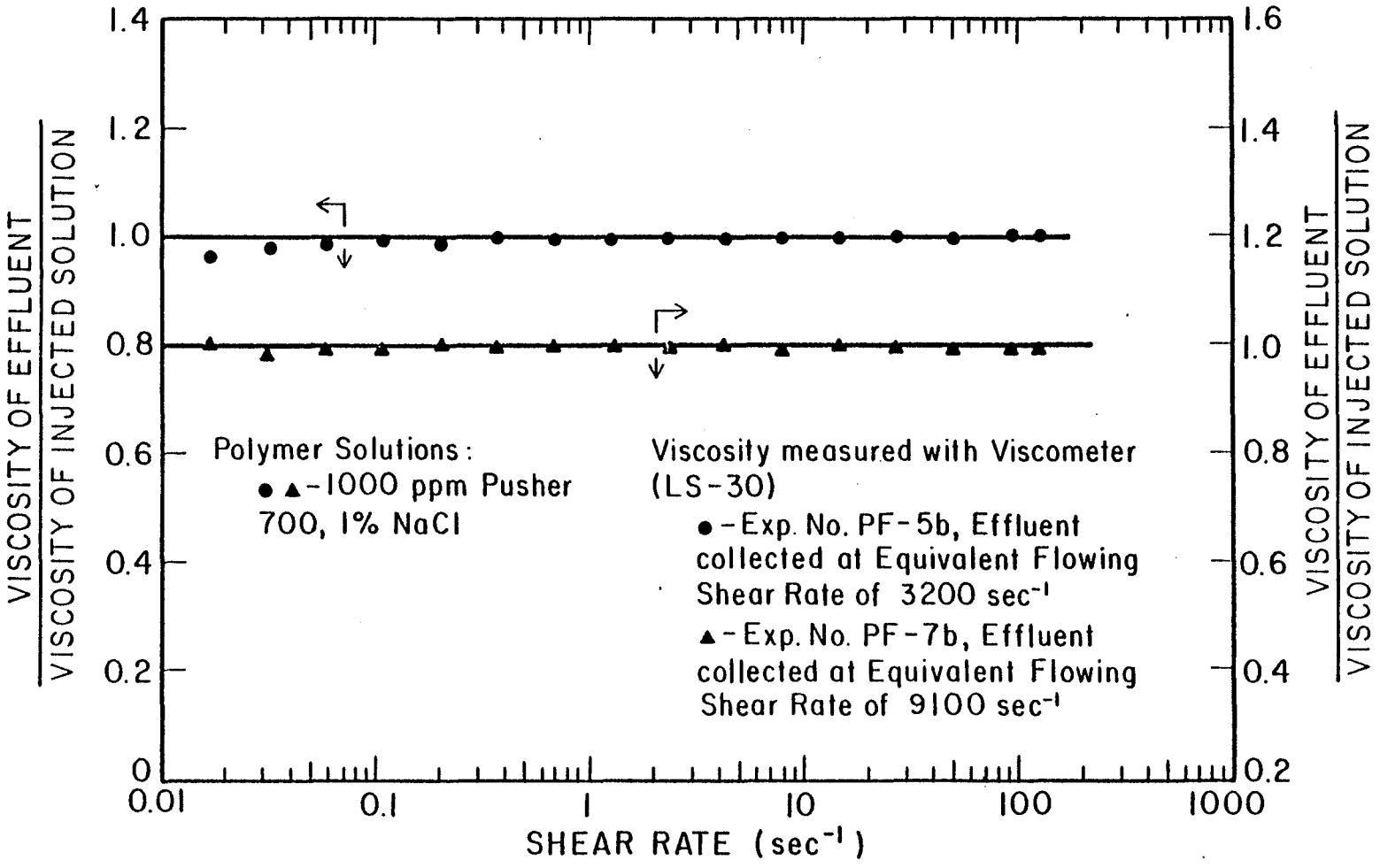

Figure 35. Comparison of Viscosity of Effluent to the Injected Polymer Solution

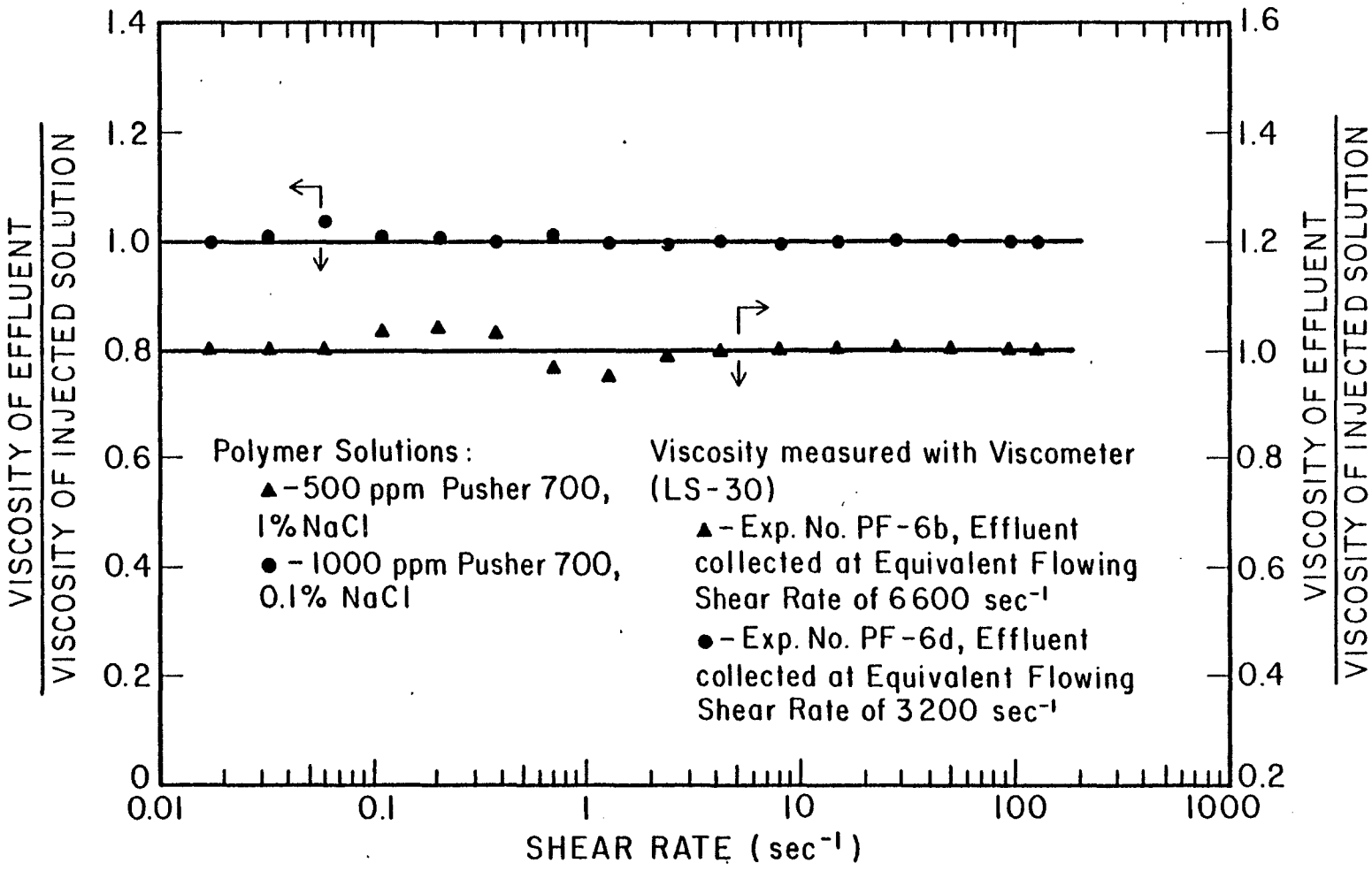

FIGURE 36. Comparison of Viscosity of Effluent to the Injected Polymer Solution

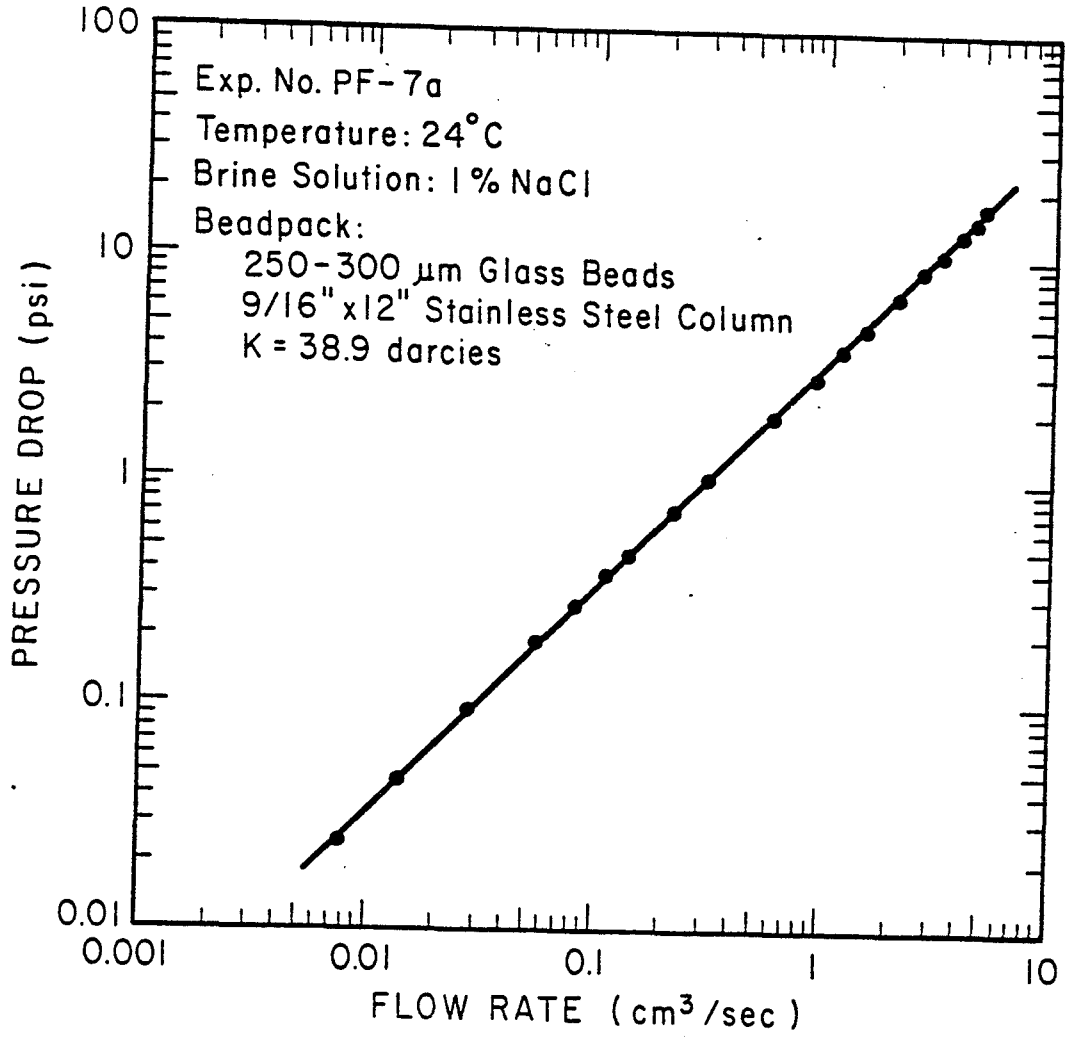

FIGURE 37. Pressure Drop-Flow Rate Data for Brine in Beadpack

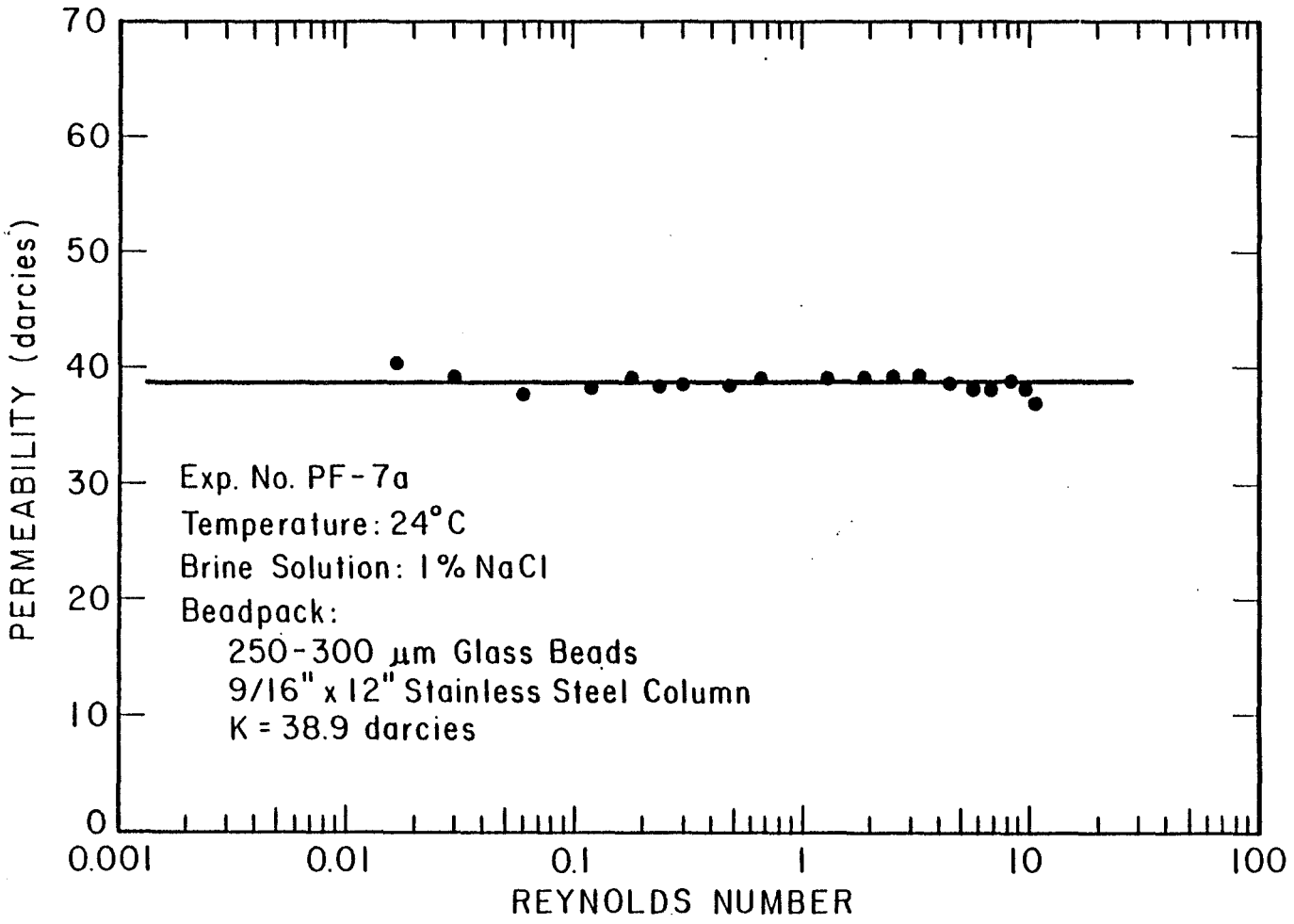

FIGURE 38. Beadpack Permeability to Brine

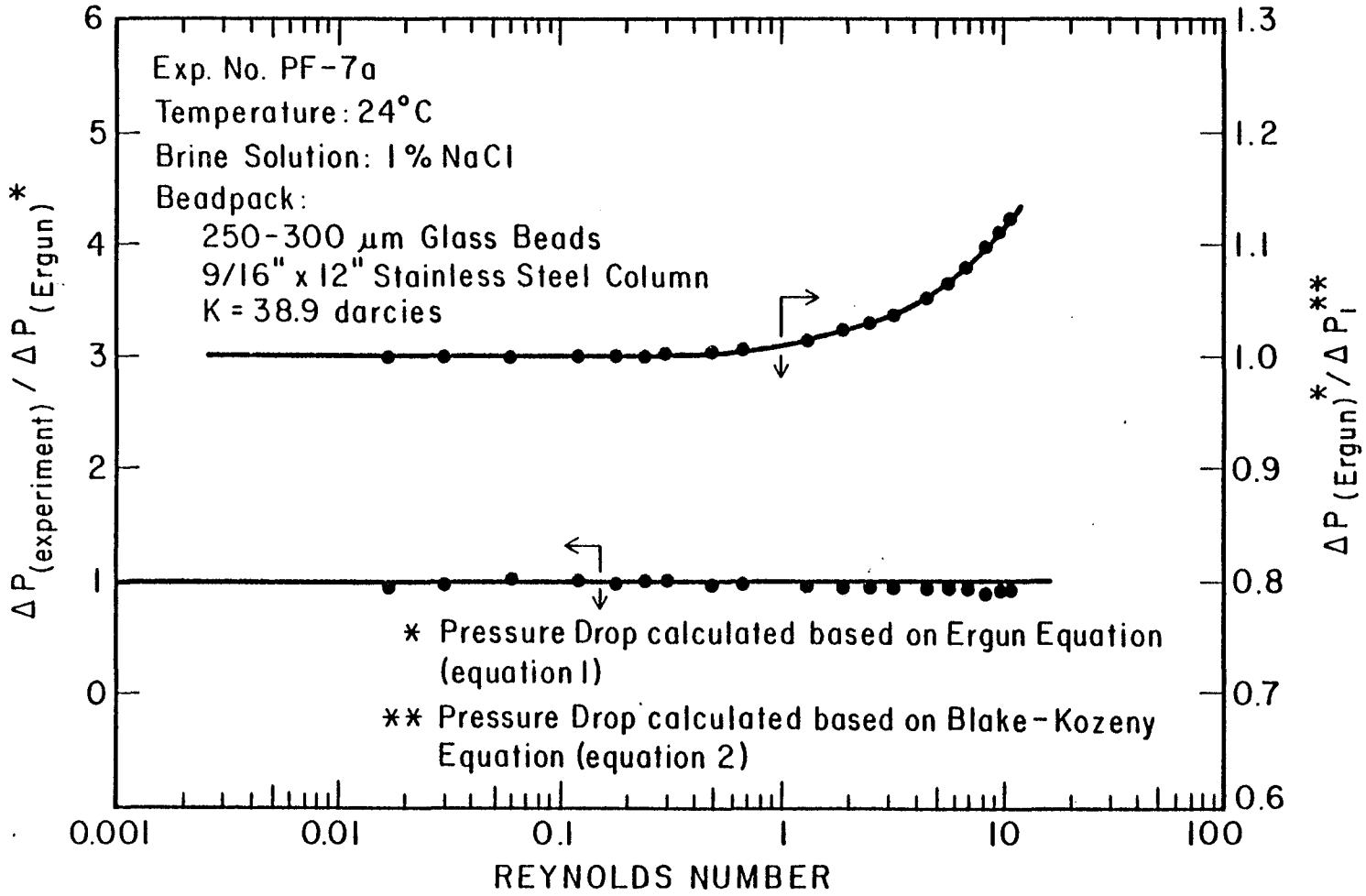

FIGURE 39. Comparison of Pressure Drop and Percent of Inertial Effect

FIGURE 40
EXPT PF-7B

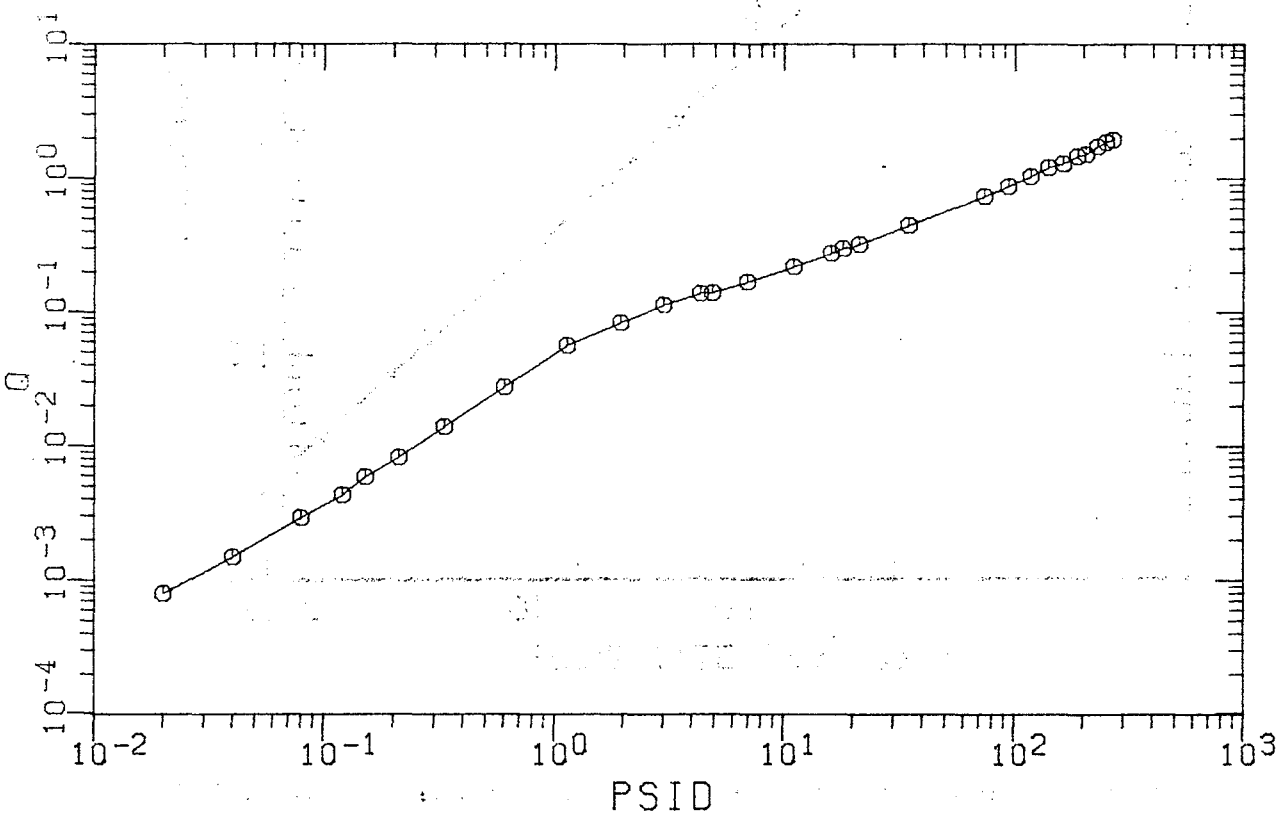

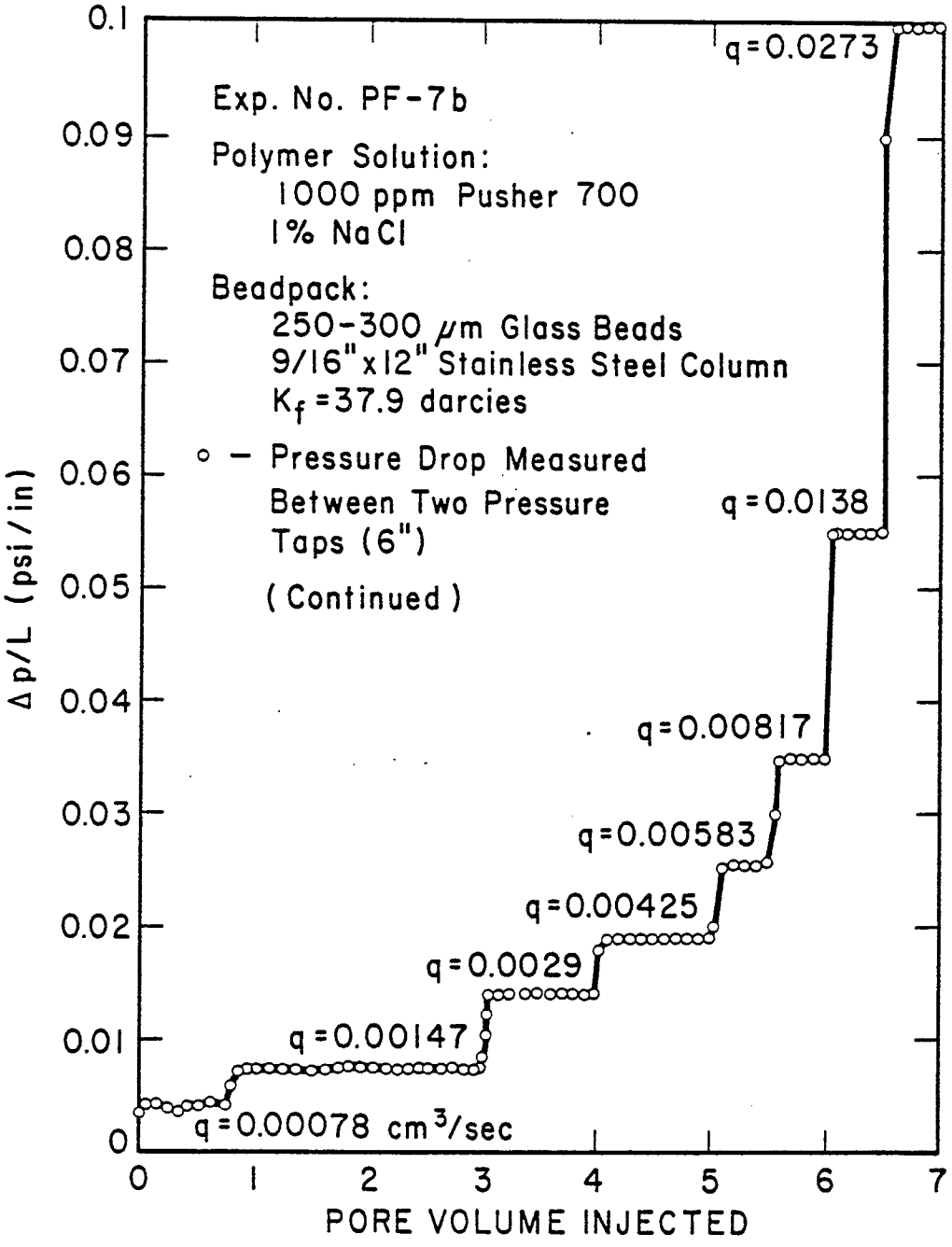

FIGURE 41. Pressure Gradient for Pusher 700 Polymer Solution in Beadpack

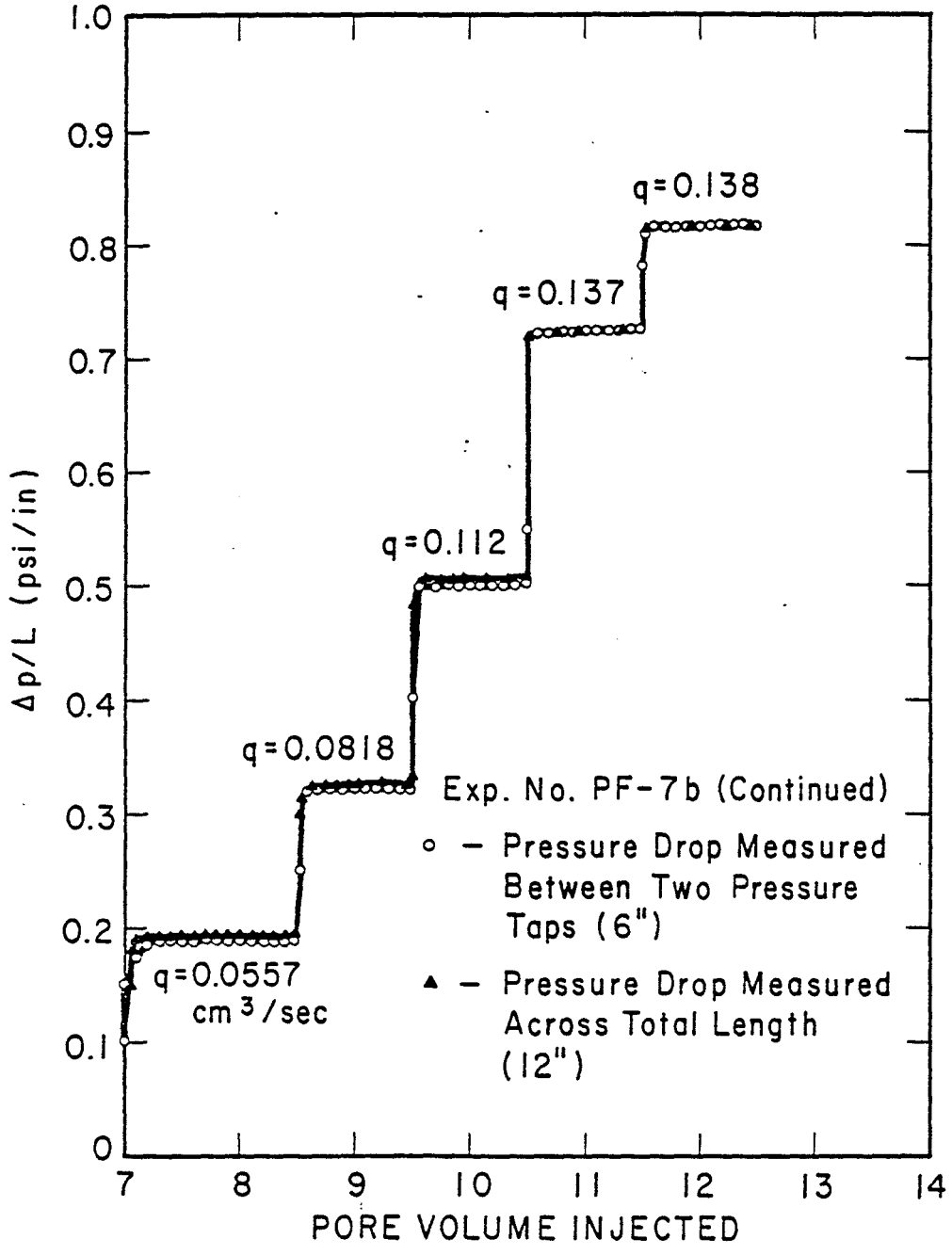

FIGURE 41. Pressure Gradient for Pusher 700 Polymer Solution in Beadpack

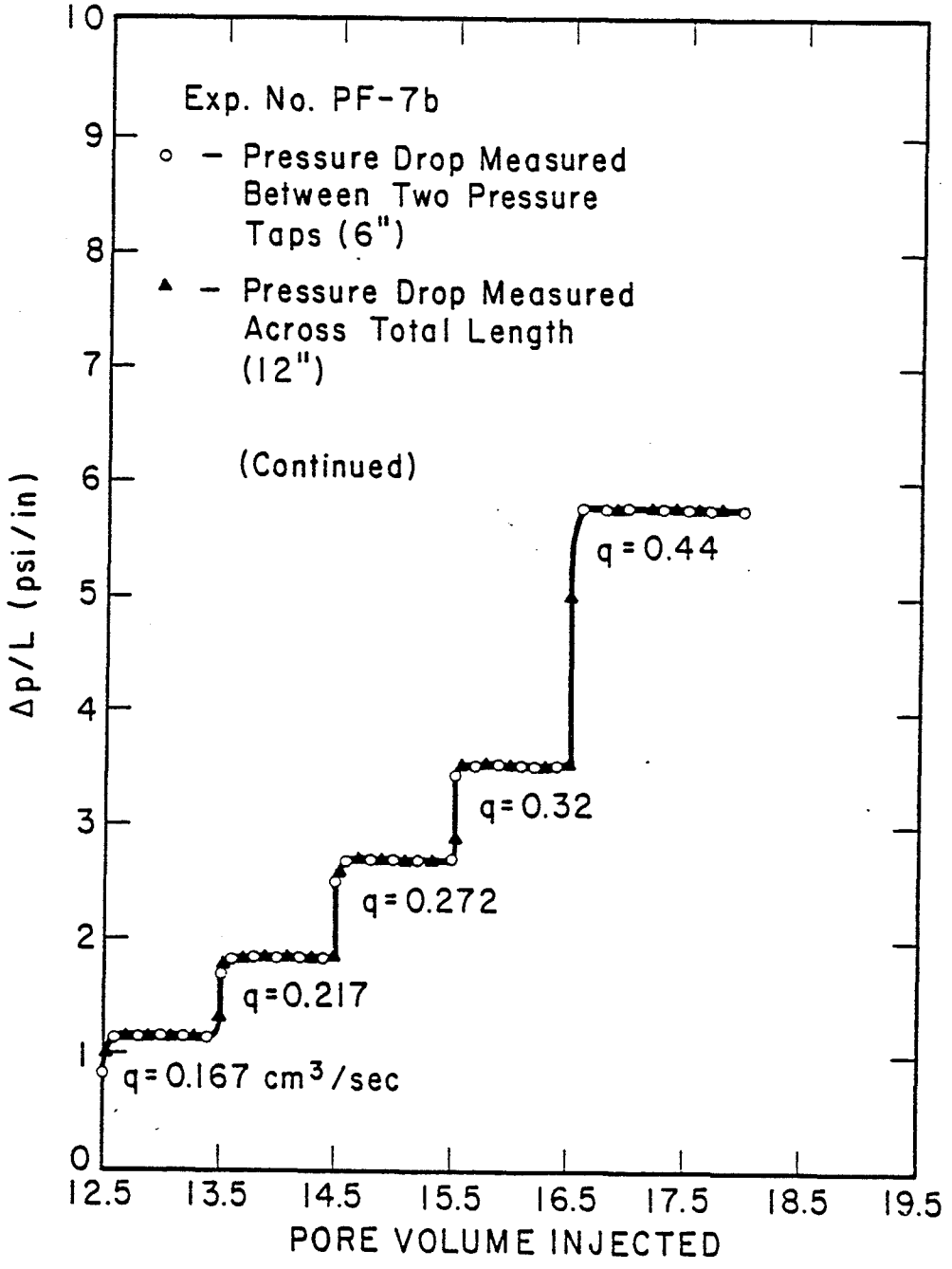

FIGURE 41. Pressure Gradient for Pusher 700 Polymer Solution in Beadpack

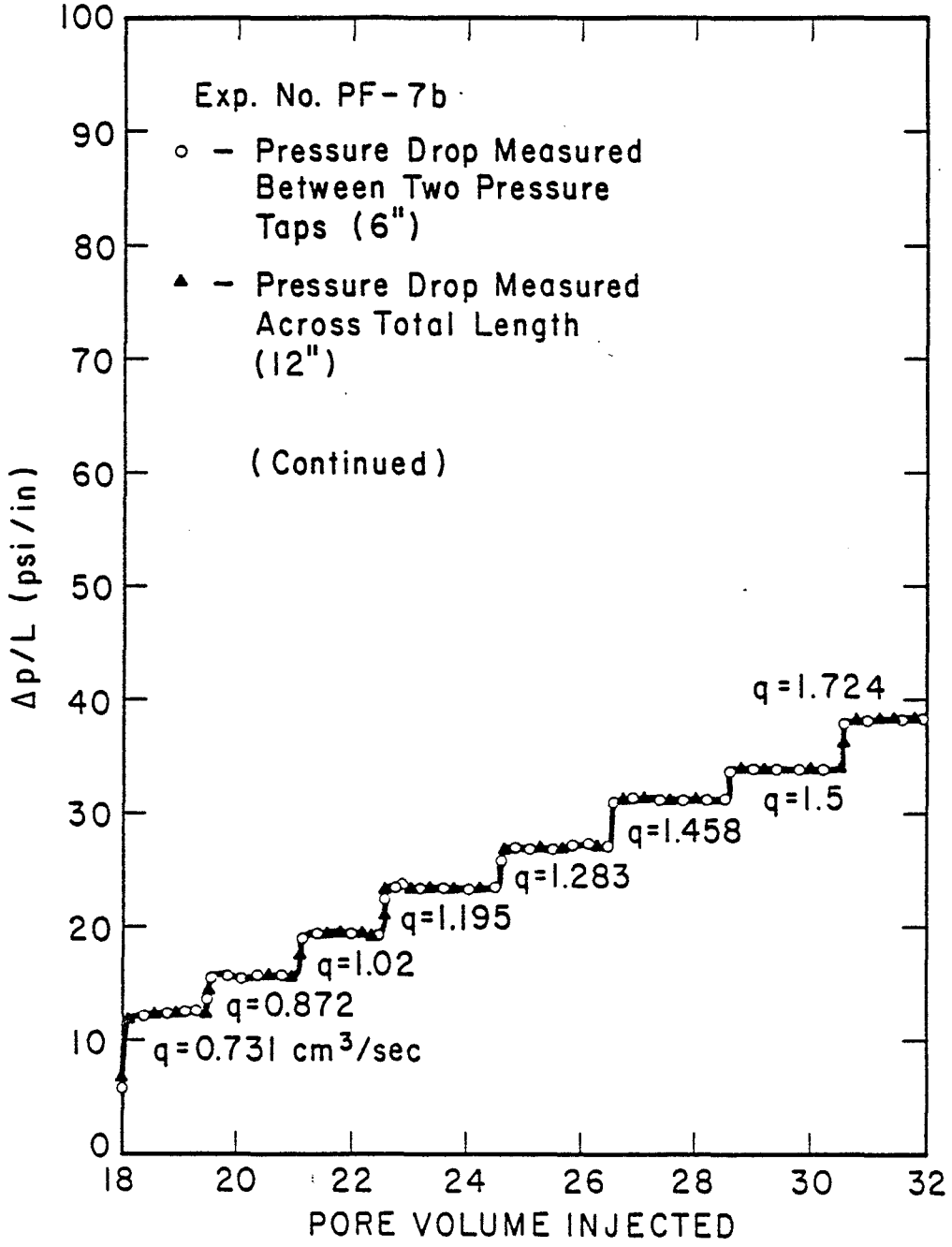

FIGURE 41. Pressure Gradient of Pusher 700 Polymer Solution in Beadpack

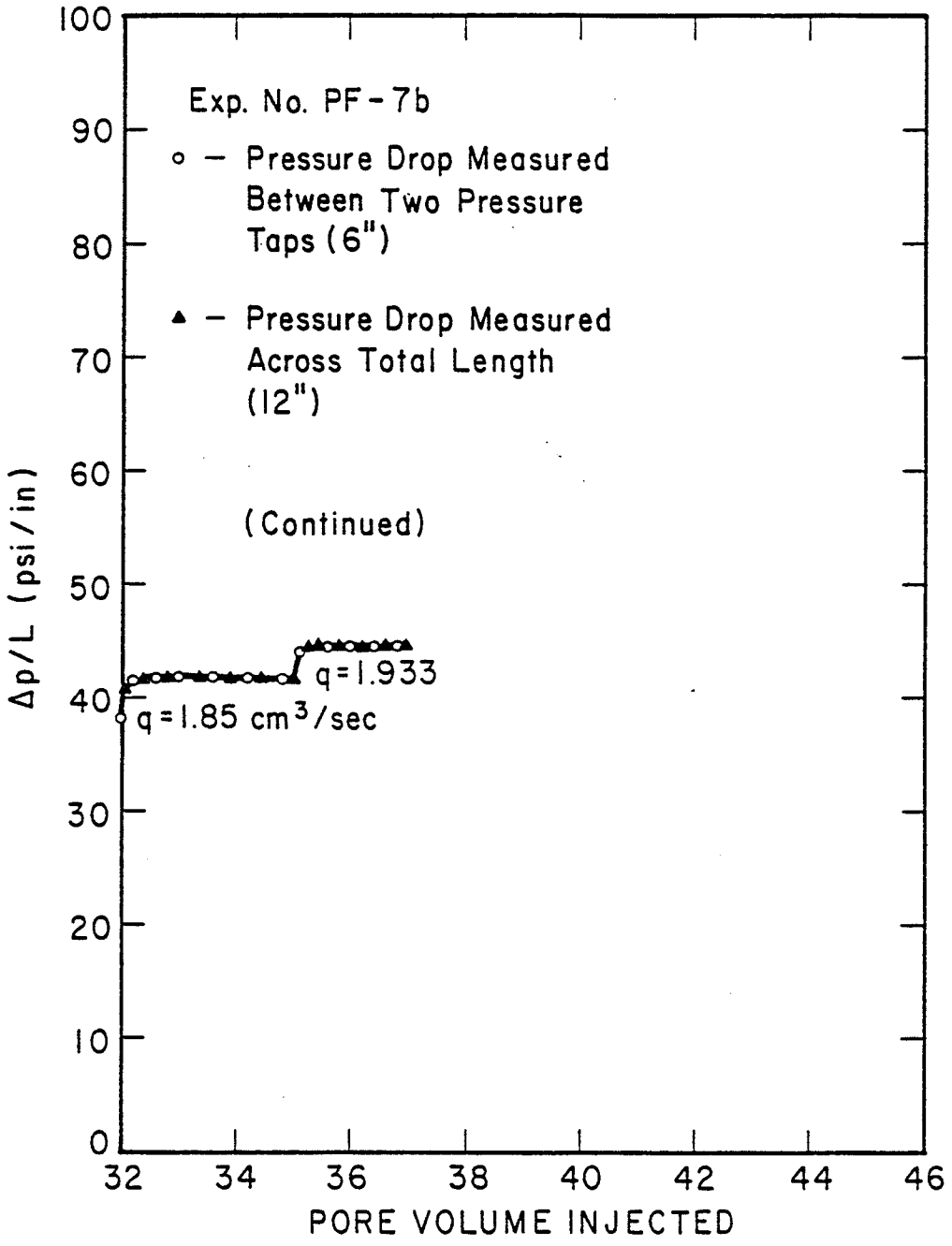

FIGURE 41. Pressure Gradient of Pusher 700 Polymer Solution in Beadpack

FIGURE 42
EXPT PF-7B

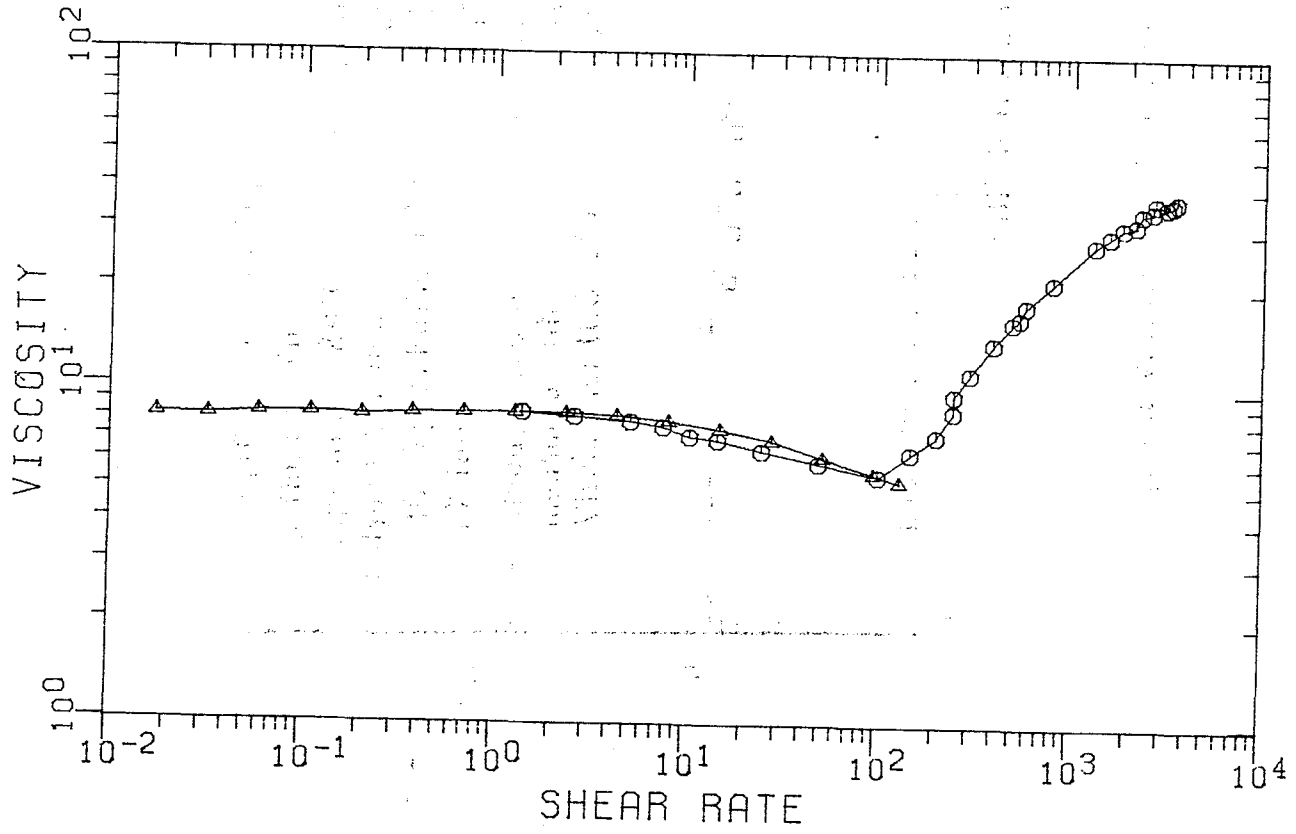

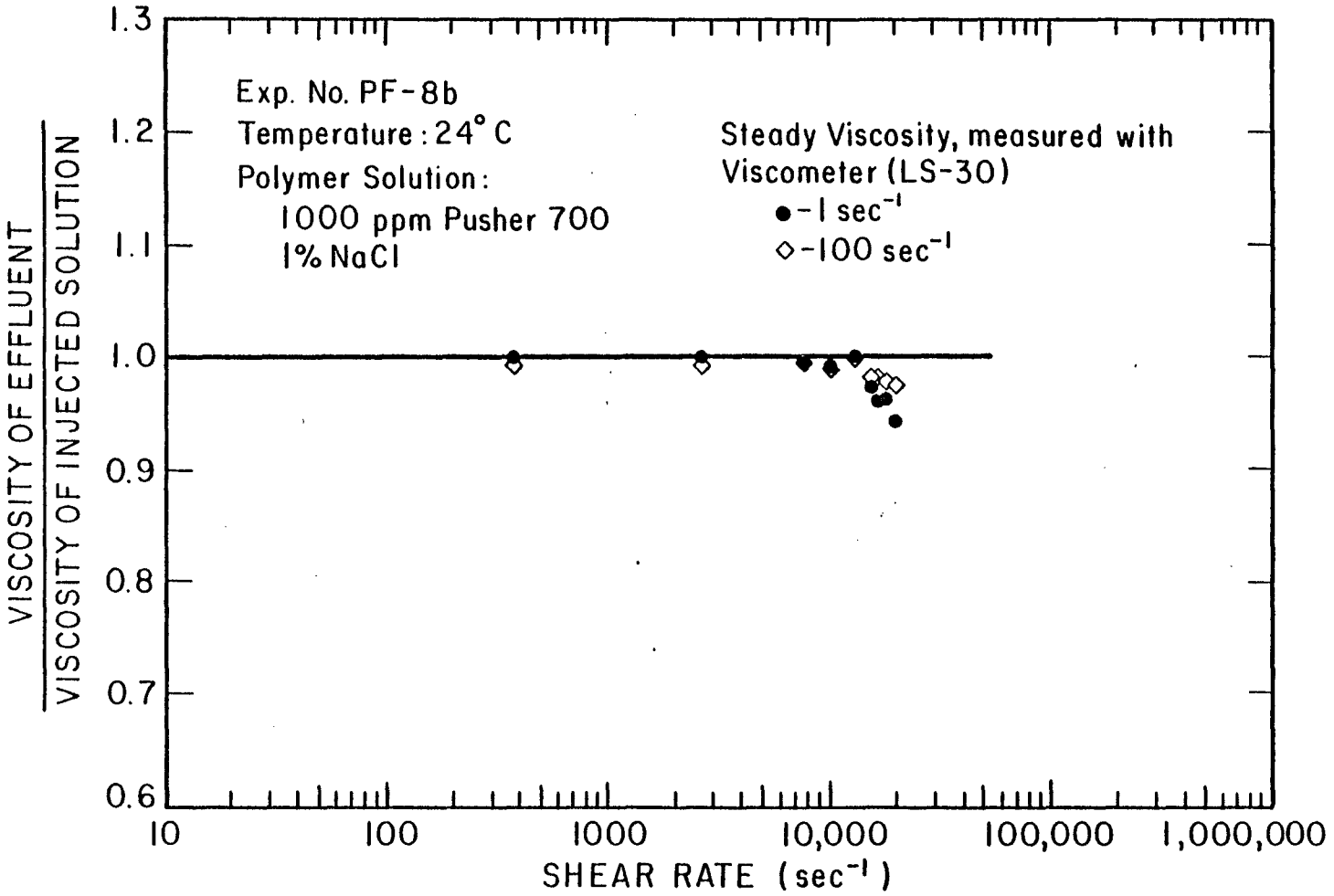

FIGURE 43. Viscosity Loss as Function of Equivalent Shear Rate in Beadpack for Pusher 700 Polymer Solution

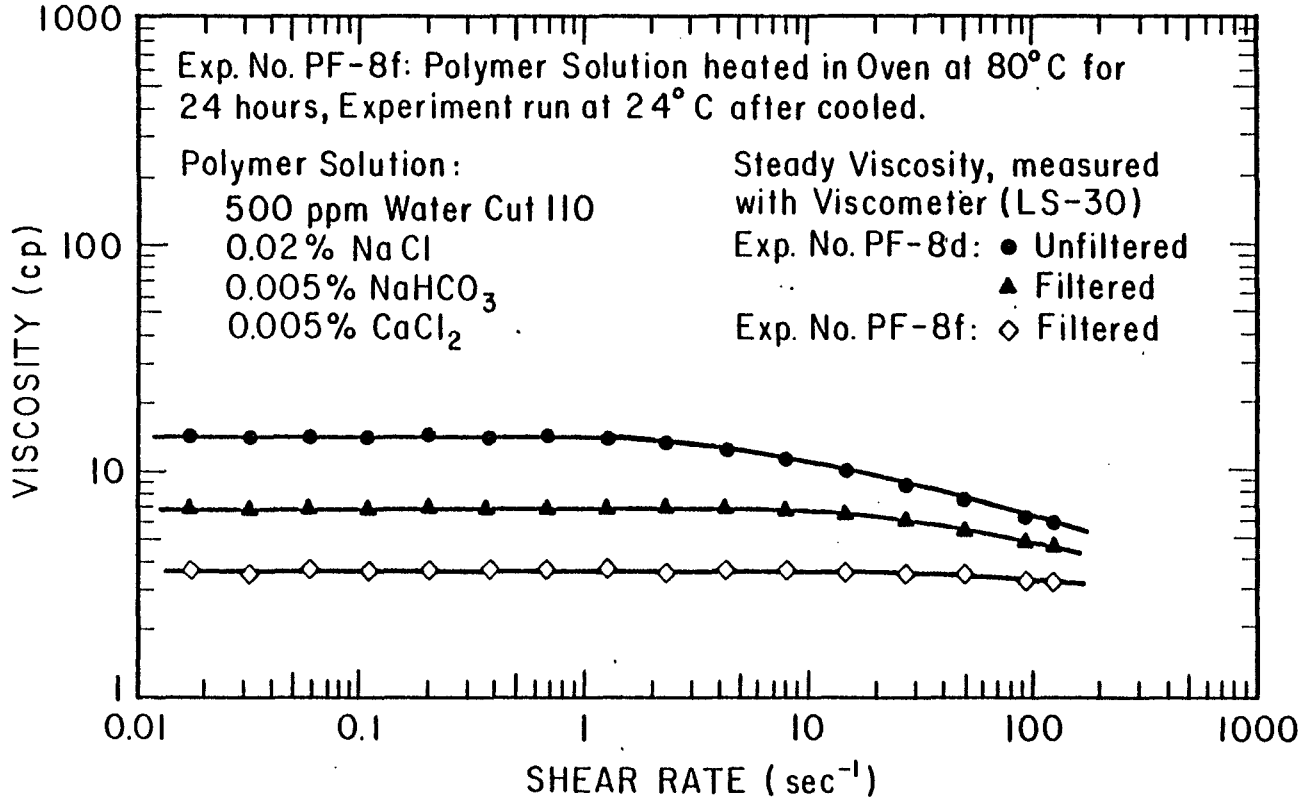

FIGURE 44. Steady Viscosity of Water Cut 110 Polymer Solutions

FIGURE 45B
EXPT PF-8F

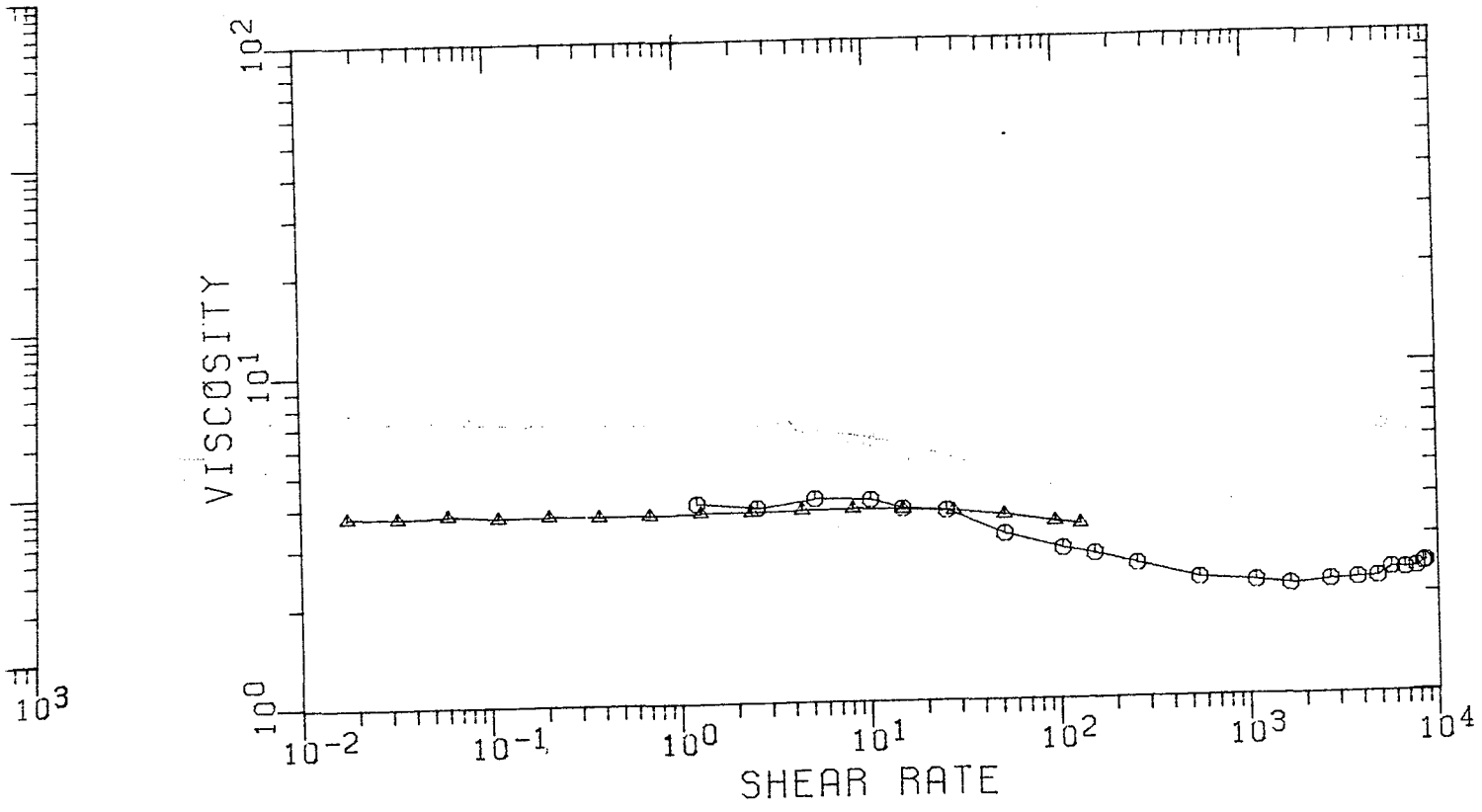

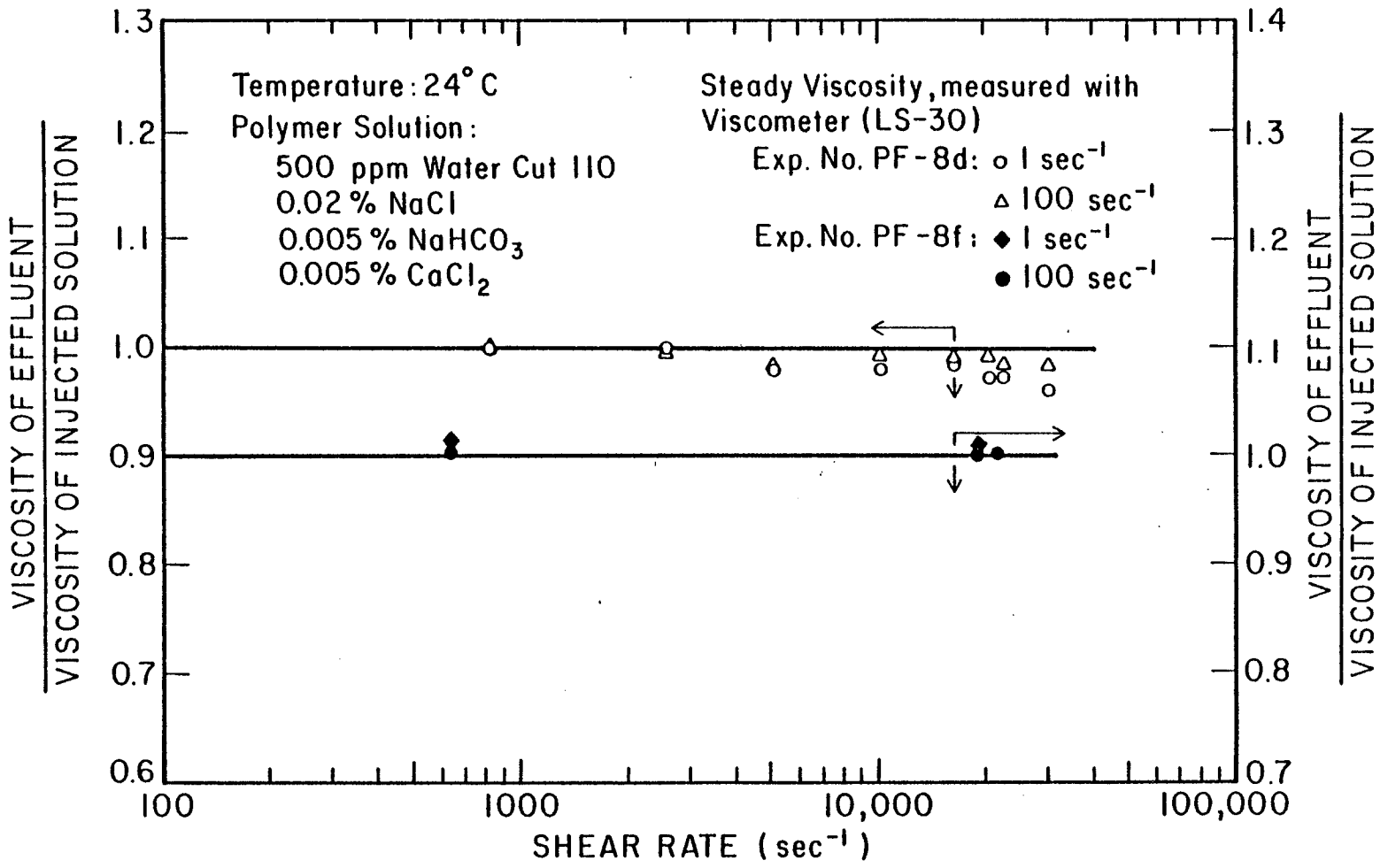

FIGURE 46. Viscosity Loss as Function of Equivalent Shear Rate in Beadpack for Water Cut 110 Polymer Solution

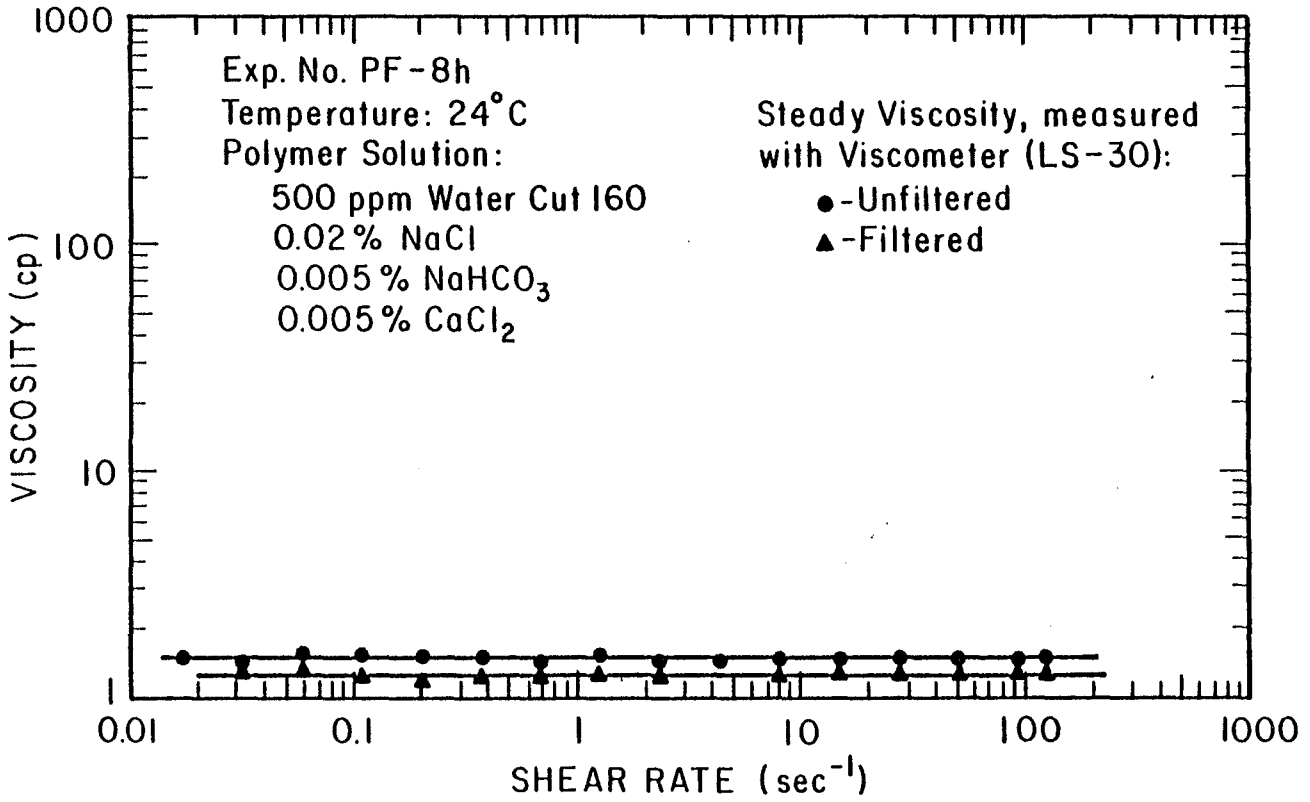

FIGURE 47. Steady Viscosity of Water Cut 160 Polymer Solution

FIGURE 48
EXPT PF-8H

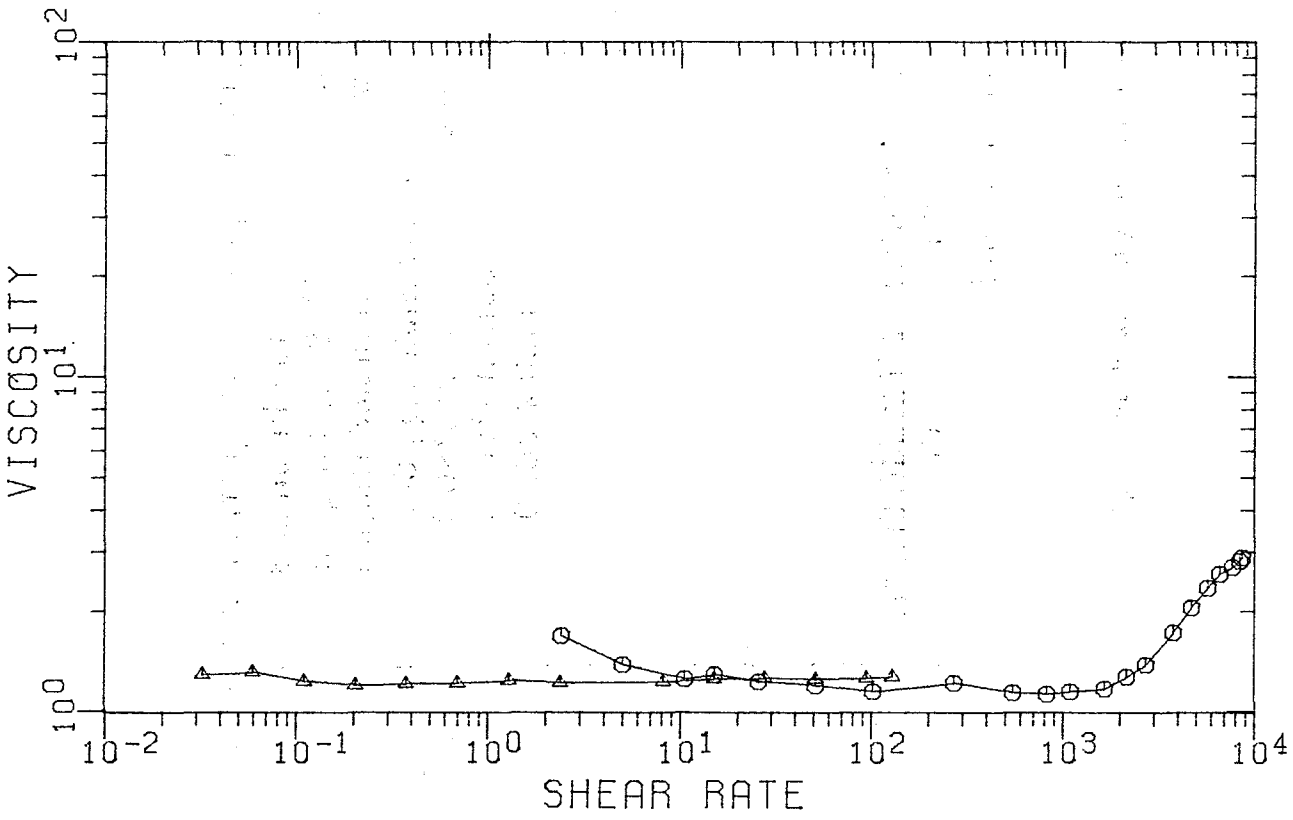

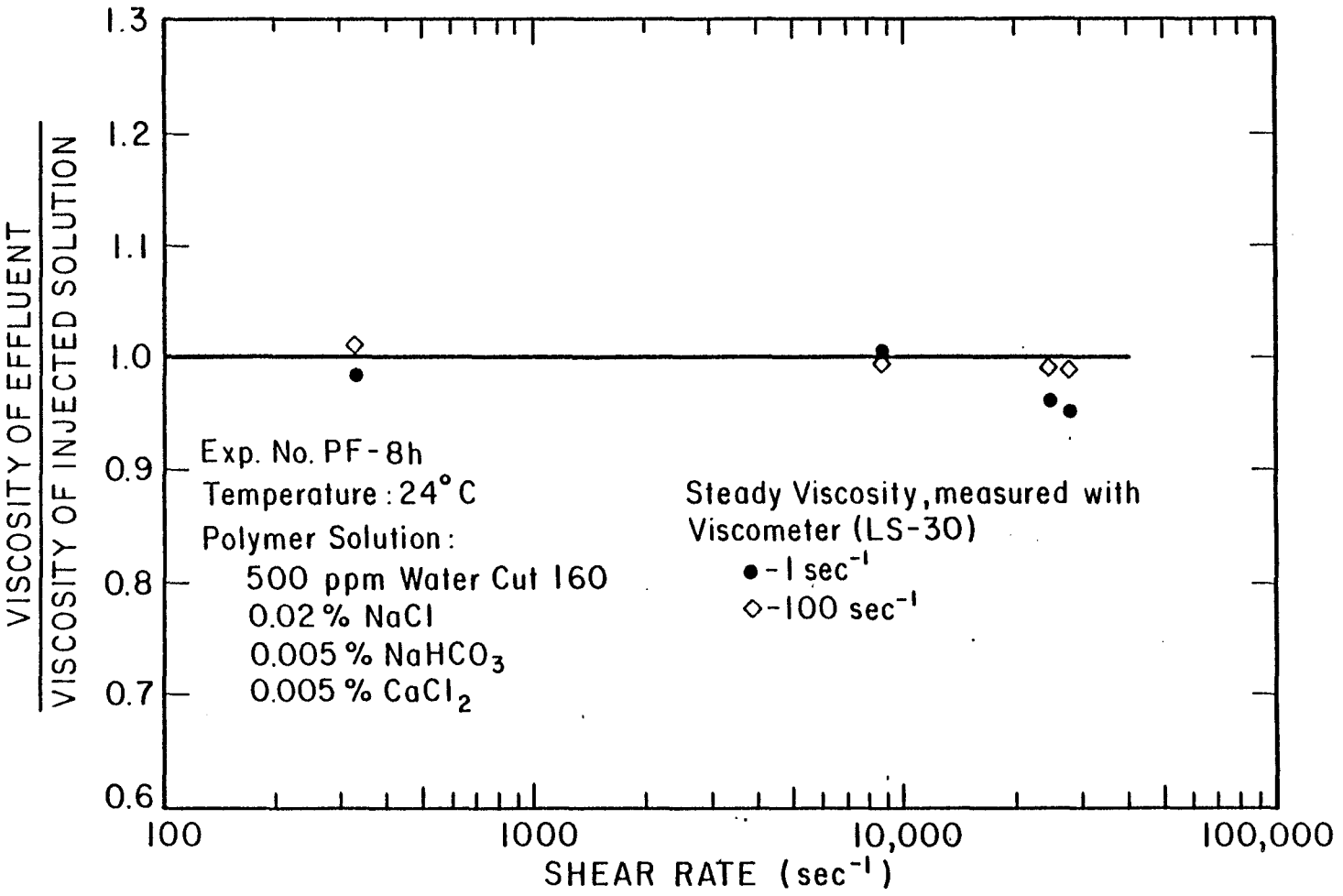

FIGURE 49. Viscosity Loss as Function of Equivalent Shear Rate in Beadpack for Water Cut 160 Polymer Solution

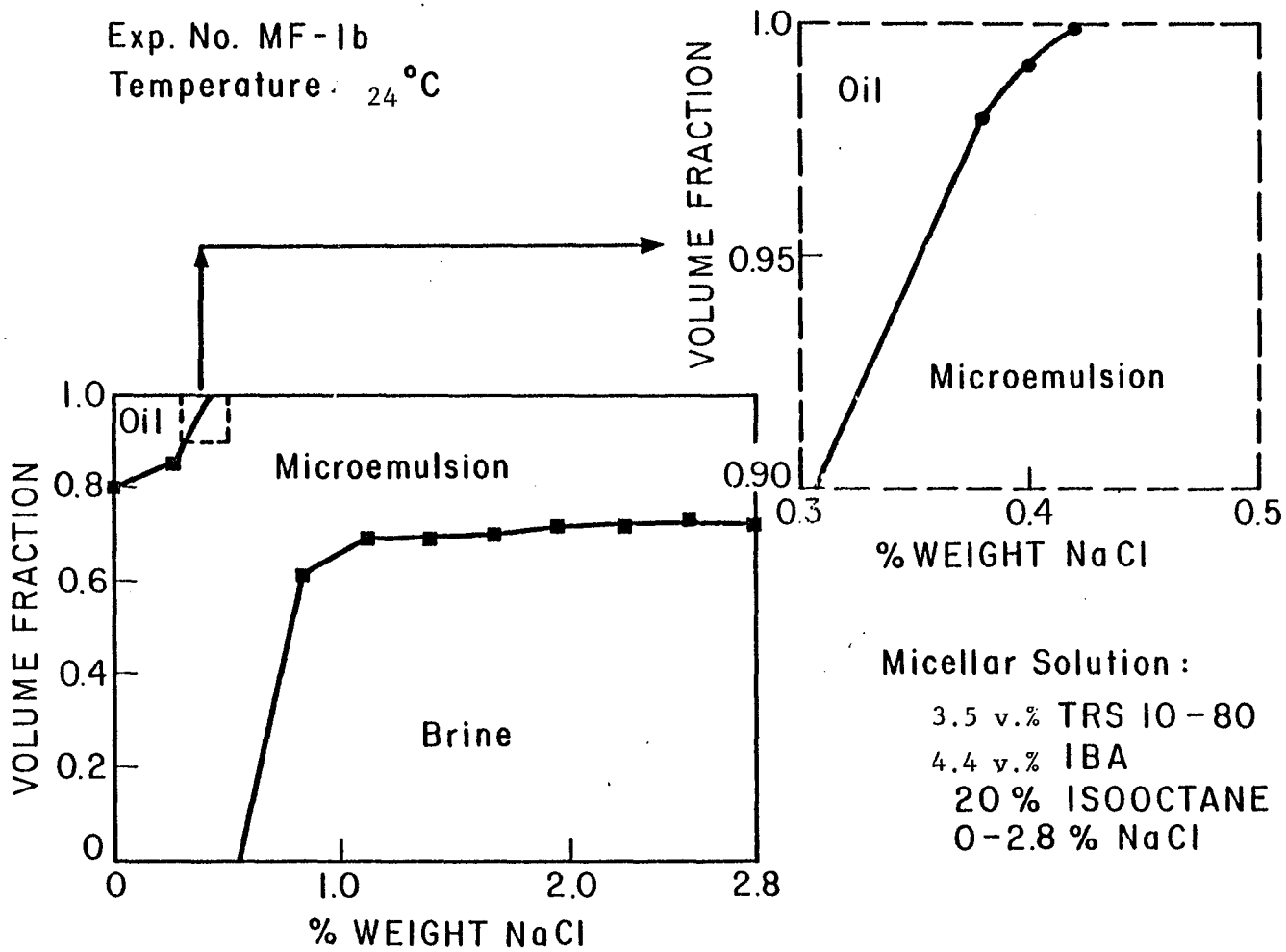

FIGURE 50. Phase Fraction of Micellar Solution as Function of Salinity

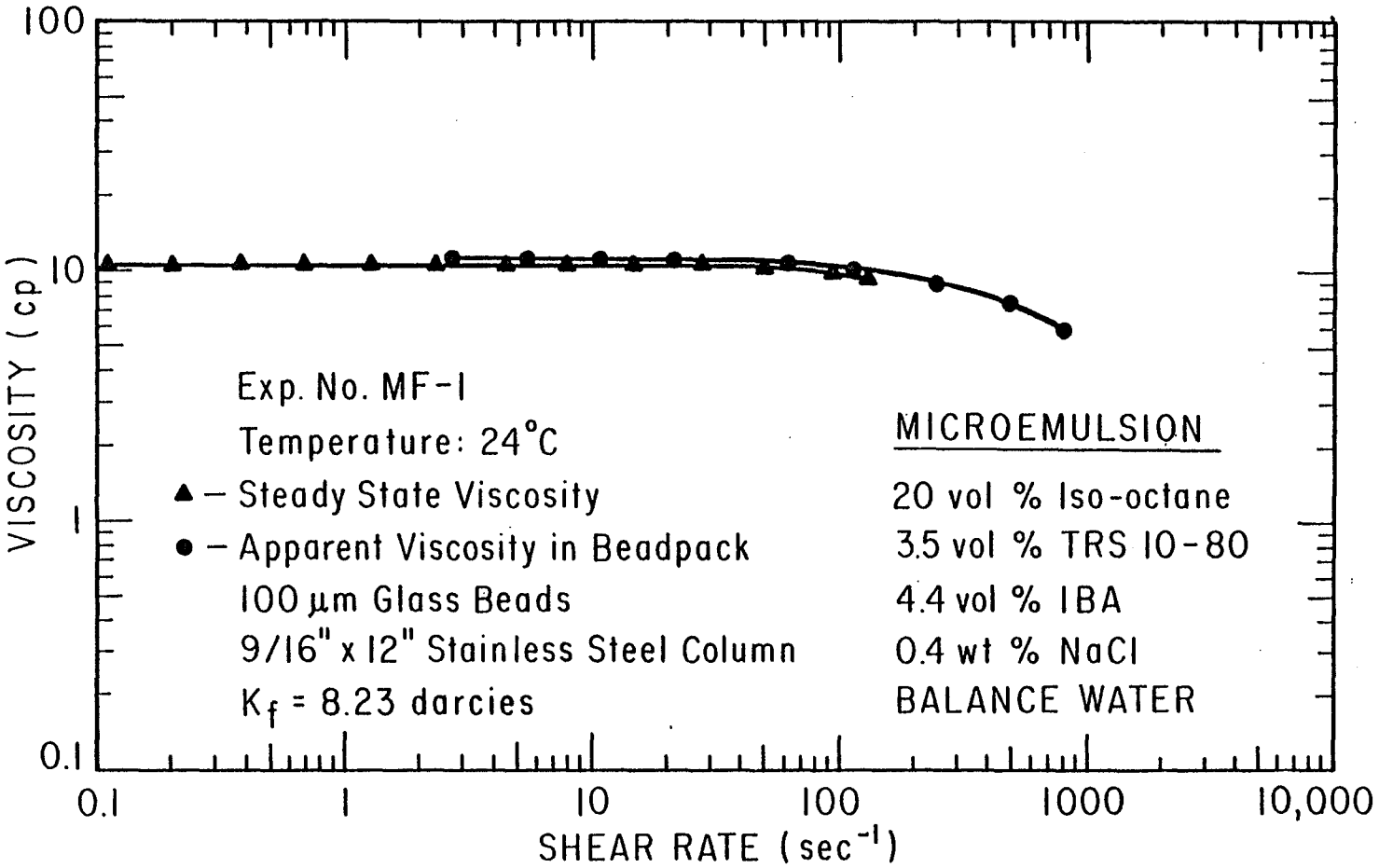

FIGURE 51. Apparent Viscosity of Microemulsion

VITA

MeiKou Yuan was born in Taiwan, Republic of China on June 20, 1951, the son of Mr. and Mrs. Ah-Tai Yuan. In September, 1970, he entered Fu-Jen Catholic University in Taiwan. After obtaining the degree of B.S. in Chemistry in June, 1974, he was commisioned as a secondary lieutenant through the R.O.T.C. for two years. In August 1976, he married Rebecca Hsu in Taiwan. A month later, he enetered the Graduate School of University of Illinois at Chicago Circle, and was awarded an M.S. degree in Chemistry in August, 1978. In September, 1977, he attended the Graduate School of the University of Texas at Austin. His son, Edward Kerjiun, joined the family in Austin, Texas on September 5, 1978.

Permanent address: 1902 Drexel Dr.,
Richardson, Tx. 75081
U. S. A.

This thesis was typed by Rebecca Yuan.